Hydraulic pressure wave bone drilling

A step towards trajectory controlled drilling in the vertebra

T.G. Kaptijn

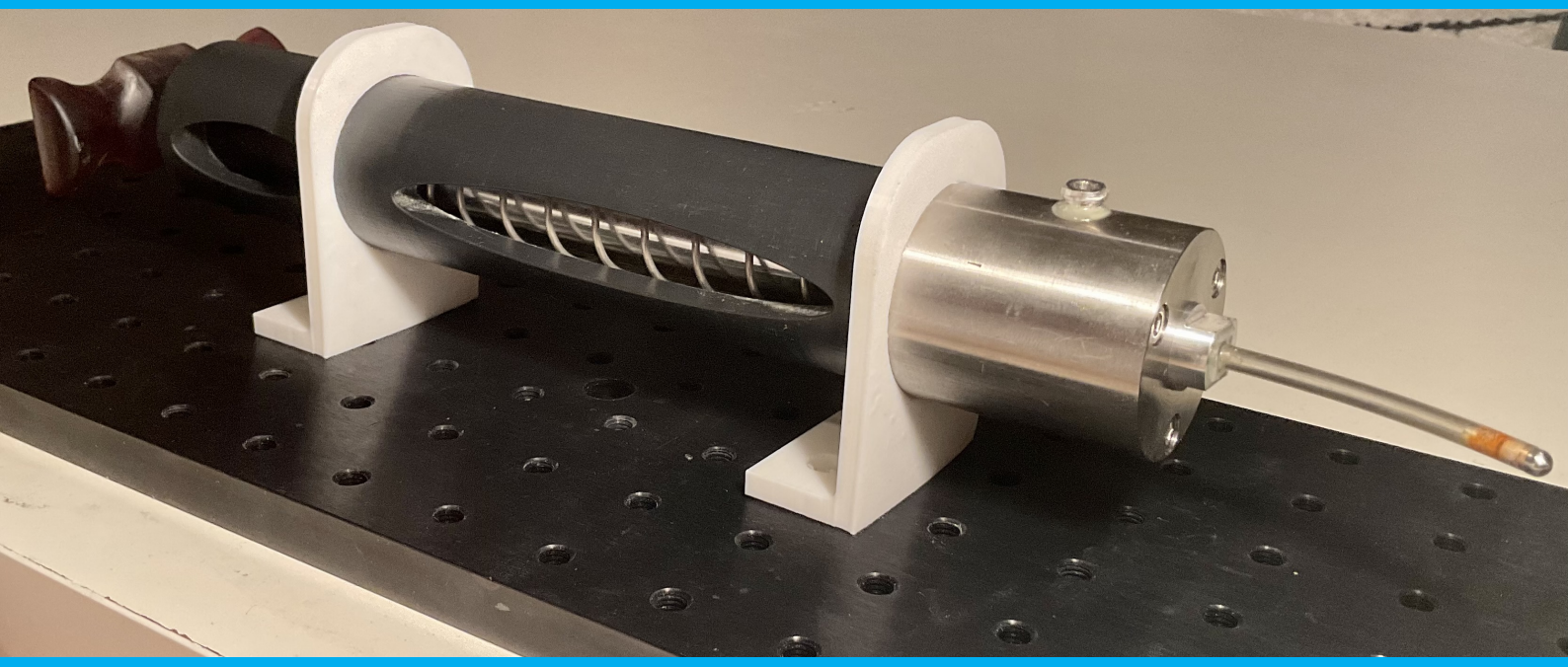

TU Delft

Hydraulic pressure wave bone drilling

A step towards trajectory controlled drilling in the vertebra

by

T.G. Kaptijn

to obtain the degree of Master of Science
at the Delft University of Technology,
to be defended publicly on Thursday February 24, 2022 at 14:00 PM.

Student number:	4475097	
Project duration:	February 1, 2021 – February 24, 2022	
Thesis committee:	ir. E. de Kater,	TU Delft, weekly supervisor
	dr. ir. A. Sakes,	TU Delft, supervisor
	Prof. dr. ir. P. Breedveld,	TU Delft, chair thesis committee

TU Delft

Preface

I started my journey at TU Delft in 2015, keen to learn everything that had to do with technology, purposefully not choosing a medical study as my entire family already did something medical-related. However, when I started my master in BioMechanical Design, I got more and more introduced to the medical side of technology. It ignited a keen interest in medical technology and the human body in me, to my surprise. My interest grew even more when I started my master thesis. During this thesis, I wrote a literature study on ultrasonic surgical bone drills, where after I took the challenge upon myself to design a proof of principle for a new method for steerable drilling in bone, specifically cancellous bone in the vertebra.

I thoroughly enjoyed the project and everything I learned from it. However, due to the pandemic, real face-to-face connections were limited and forced everyone to work from home. Because of this, it was sometimes hard to stay motivated whilst workings day after day at home. Luckily I had my roommates, girlfriend, friends and family to support and motivate me.

I really want to thank Esther de Kater for the weekly support and fruitful discussions concerning this thesis and preliminary literature study. I want to thank Aimée Sakes for providing good criticism, ideas and guidance during our many meetings. Furthermore, I would like to thank Remi van Starkenburg of the DEMO workshop for the incredible help in fabricating the final instrument. Lastly, I would also like to thank Jos van Driel of the Meetshop at the faculty of 3Me for help with setting up the force capturing software for the experiments performed in this thesis. I hope you will enjoy reading this thesis, as I have enjoyed writing it.

T.G. Kaptijn
Delft, February 2022

Abstract

Spinal fusion surgery is applied, amongst other reasons, to correct unwanted curves in a spine hampered by scoliosis. During spinal fusion surgery, holes in the vertebra must be drilled, after which pedicle screws are placed. Traditional drilling only allows for the formation of straight holes. Ill-placed trajectories cannot be course-corrected, leading to repositioning the drill and starting again in the, weakened by the first attempt, vertebra. This thesis aims to develop a drilling method that will allow for the application of trajectory control during operation. This will form the first step towards a new spinal surgical instrument that could be used for course-correcting during spinal drilling or form curved holes applicable for new state-of-the-art alternate bone anchors.

The proof-of-principle instrument designed and fabricated in this thesis consists of an impulse generation part, a bendable tube with a saline medium, and a working head, which will perform the impacts on the bone tissue. The method consists of drilling using the repetitive impact of a solid round tip with a diameter of 4 mm. Through the use of a bendable impulse transmission tube, the instrument allows for the application of steerable drilling. The impulse will be generated by a manual compressed and released compression spring. This impulse will be translated into a hydraulic pressure wave; whereafter it will travel through the liquid medium of the tube, ending at the working head, which translates it into an impact on the target tissue.

The method has been proven to work in every state of curvature of the transmitting tube, ranging from 0 degrees till 90 degrees. Furthermore, almost 20% of the desired impulse output found in this thesis, 0.077 Ns, that would allow for high-speed drilling, 0.3 mm per strike, was reached. A linear increase in impulse output was found, correlating with the linear input increase, suggesting plausible higher impulse output magnitudes could be possible. In the future, the instrument's efficiency should be increased, as a mean efficiency of 3.5% was achieved, caused mainly by leakage of the saline filler and high friction with the mechanisms in the tube. All in all, the method shows great potential to be utilised as a future trajectory controlled bone drilling instrument.

Contents

1

Introduction

1.1. The vertebral column

The spine, or vertebral column, is the body's central structure of support. Your spine helps you walk, sit, stand, bend and twist. It is a vital structure in the human body, as it protects the spinal cord. Around 50,000 species of animals share this feature with us, of having a vertebral column [1]. The human vertebral column is divided into five segments containing a total of 33 vertebrae [2], as seen in Figure 1.1. The cervical is the superior most section of the spinal column, consisting of seven vertebrae. This section is followed by the thoracic section, which has twelve vertebrae. Below that, the lumbar section is found, which consists of five vertebrae. Further down the spine, the sacrum and coccyx sections are found, having five and four vertebrae respectively in their section [2]. The lumbar, thoracic and cervical vertebrae share a similar structure, except for the first and second cervical vertebrae, the atlas and the axis [4]. The other vertebrae in the three mentioned sections are all composed of an anterior cylindrical vertebral body, two lamina, two pedicles, a spinous process, four articular facets and a vertebral foramen, which contains and protects the spinal cord [4], as seen in Figure 1.2. The main axial load bearing structure of the vertebral column is the the anterior cylindrical vertebral body. This structure is mainly composed of cancellous bone, also know as trabecular bone, with a thin outershell of cortical bone encasing the cancellous bone peripherally [6]. Cancellous bone has a porous, inhomogeneous structure, and mostly behaves elastically for a wide range of strain rates. Cancellous bone's strength and the elastic moduli is dependent on the density of the bone to the second power [6]. The surrounding cortical bone on the other hand, has a much higher density and strength compared to the cancellous bone [6]. Each of the lumbar, thoracic and cervical vertebrae are separated by intervertebral discs. These discs allow for flexibility of the vertebral column [2], and are composed of an outer structural, firm fibrous cartilage (annulus fibrosus), with in the centre, the softer, shock absorbing nucleus pulposus [6].

The vertebral column must be strong enough to

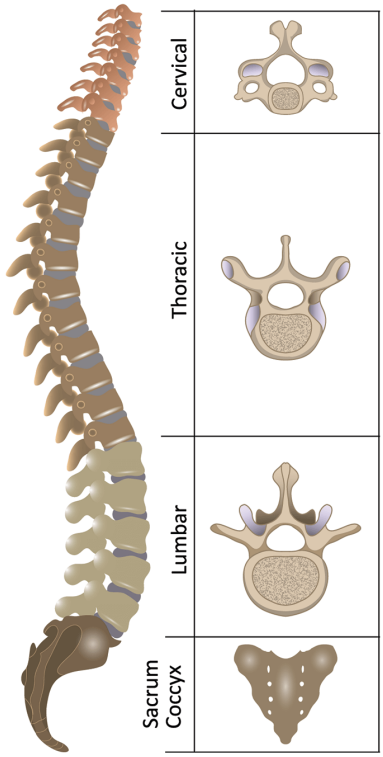

Figure 1.1: A representation of the vertebral column and its five sections: the Cervical, thoracic, lumbar, sacrum and coccyx, with their corresponding vertebrae [3].

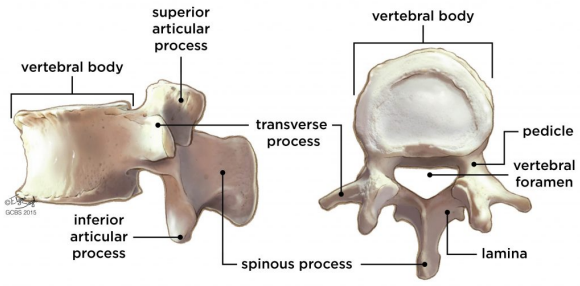

Figure 1.2: Anatomy of the vertebra [5].

protect the cauda equina, nerves that leave the spinal cord between spaces in the bones, and the spinal cord, rigid enough to support the torso, and be able to anchor all the other muscles connecting to the vertebral column for support [4]. Next to this, it must be flexible enough to allow for mobility and twisting of the body in multiple directions. However, these combined properties of mobility and rigidity come at a price, in particular at the lumbar and cervical part of the spine [4]. A well known problem that can occur with the spinal column is scoliosis. Scoliosis is a sideways curvature of the spine. and can occur in patients due to growing irregularities of the vertebral column, osteoporosis, or destruction of joint capsules, facet joints, or discs [7]. Furthermore, ligaments may create segmental instability or spinal stenosis, narrowing of the spaces within the spine, can occur [7].

Spinal fusion surgery can be used to correct the curve in a spine hampered by scoliosis. It works by permanently connecting two or more vertebrae with strategically placed bone grafts, pieces of transplanted bone tissue. The grafts mimic the bodies own healing process of broken bones. By doing this, motion between the fused vertebrae is eliminated, but in return, it can correct the deformity, improve stability or reduce pain the patient might be experiencing [2]. To hold the vertebrae together while it heals into a solid unit, pedicle screws, medical implants, are implanted posteriorly into the spinal vertebrae. The pedicle screws are connected longitudinally to rods or metal plates in order to fixate the vertebral column in place, as can be seen in Figure 1.3. The construct will help correct spinal alignment or promote stabilization [2].

1.2. Current challenges: Pedicle screw placement

Although pedicle screw fixation is claimed to be the state-of-the-art in spinal deformity correction [8], it does come with its challenges and disadvantages. Deepak and Najeeb [9] find that the procedure requires a steep learning curve for the surgeon to master the operation, as it is a very complex and technically demanding operation. Next to this, neural or dural injury can occur as a result of medial or caudal penetration of the pedicle cortex. Furthermore, extensive tissue dissection is required to allow for the optimal screw orientation entry trajectory. On top of that, the pedicle screw fixation procedures demand a very lengthy operative time, as well as, have a high financial cost [9]. Lastly breakage or loosening of the screw can also lead to major complications [2].

Cancellous bone of itself is too weak to achieve sufficient gripping strength on the pedicle screws alone [10]. It is, therefore, crucial that the helical thread of the screw is in direct contact with the outer cortical bone layer, which has a much higher strength than cancellous bone, to ensure enough holding strength of the pedicle screw is achieved [10]. Furthermore, due to the short and bent surface of the cortical bone of the pedicle, where the screws are usually set, only a small contact surface with the screw and the cortical bone is achieved. This decreases the grip strength even more. As mentioned earlier the operation has a very high learning curve. The surgeon has to have a sound understanding of the spine anatomy of the patient, because of limited visibility of spinal anatomical landmarks during operation [11]. Especially, as the operation occurs near vital vascular and neural structures. Next to this, whilst inserting the pedicle screw, the surgeon can not change trajectory. This can lead to mal-positioning of the pedicle screw, resulting in removal and repositioning of the pedicle screw [11]. This compromises gripping strength and incorrect placement of the screw can cause detrimental damage to the vascular and neural structures surrounding the vertebra if the screw were to breach the vertebra wall [11].

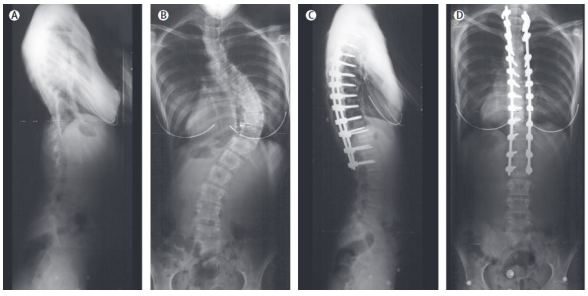

Figure 1.3: Radiographs of a patient with progressive right thoracic adolescent idiopathic scoliosis, with A) preoperative lateral view, B) preoperative anterior view, C) postoperative, after treatment with posterior segmental pedicle screws, lateral view, and D) postoperative anterior view [7].

1.3. State-of-the-art: Spine surgery

The current gold standard of treatment of scoliosis is posterior spinal instrumented fusion [12]. Utilizing pedicle screws is considered to be the best fixation method to achieve spinal fusion in order to treat spinal deformities [2]. Boucher, in 1959, was the first to make use of pedicle screws [13]. He used a longer facet screw across the pedicle in order to fixate it into the vertebra [13]. Tullos and Harrington were the first to insert the pedicle screw through the isthmus, segment of bone connecting the facet joints at the back of the spine [14]. The original method was one were a rod, the Harrington rod system, was used and attached to the spine. This was first done with sublaminar wires, followed by a method that used multiple hooks, which

changed into a hybrid instrumentation of the two, ending in the pedicle screw constructs we see today [12]. The pedicle screw proved to be a powerful anchor, achieving better correction than the previous fixation techniques [12]. As there are numerous varieties in morphology and size of vertebrae and thus of pedicles, a large variety of pedicle screws exist. Each of the pedicle screws having different pitch and screw patterns, thread and pitch sizes, and diameters that vary between the 4.5 mm to 7.0 mm [15]. The pedicle screws further connect to various anchoring devices, such as rods, threads or plates, which fixate the vertebral column. The fixation in combination with the placement of bone grafts result into the current gold standard of spinal fusion surgery.

Minimally invasive spine surgery (MISS), has gotten a lot of attention in the past two decades in the treatment of spinal disorders like scoliosis [16, 17]. This form of spinal surgery is gradually replacing the traditional open spine surgery, with estimates suggesting that in 2020, almost half of the instrumented surgeries were conducted with the use of MISS in the United States [18]. Aided by modern navigation and diagnostic technology, innovative optical and spinal devices, and improved MISS instruments, MISS shows multiple advantages over the traditional open spine surgery, like less trauma to soft tissue, smaller skin incision and reduced blood loss during operation. This all leads to relative faster recovery of the patient [16]. The two main innovations MISS brings are the guidance and imaging techniques, and the robotic aided spine surgery. For guidance and imaging techniques, the use of endoscopic devices is found to have positive results during surgery [19]. Next to this, 3D fluoroscopy is used as well, which reconstructs a 3D image out of multiple 2D fluoroscopic images. This allows for a trajectory for the spinal screw to be set with path-planning software. This trajectory can be projected onto a real-time 3D fluoroscopic image in order to aid the surgeon with navigation [20, 21]. Furthermore, computer-assisted surgery (CAS) is used. This technique uses markers together with software allowing surgeons to monitor and track, in real time, surgical instruments relative to the patient's anatomy. CAS aids in pre-surgical planning and aims to reduce errors to enhance patients outcomes [21].

The robotic aided spine surgery comprises three different categories [17]. The first one is telesurgical robotic systems. These allow for remote control of a surgical robot, with the Da Vinci (Intuitive Surgical Inc., Sunnyvale, CA, USA) robotic system being the first to be introduced to the market [22]. Such teleoperating instruments have the main benefit that a surgeon does not have to be close to the patient to operate on the patient. The second category comprehends Robotic-Assisted Navigation (RAN). RAN employs robotic guidance, using pre- and/or intra-operative real time imaging, to surgeon-operated instruments. Such a robot enabling RAN, is the FDA approved SpineAssist (Mazor Robotics Inc., Caesarea, Israel), which evaluates the position of the pedicles and indicates the correct trajectories of the surgical instruments [17]. The third category is artificial reality (AR). It uses dedicated hard- and software, capable of projecting images directly onto special lenses worn by the surgeon. This allows surgeons to visualize information about the procedure, such as a 3D model of the patients anatomy, in real time [17, 23].

1.4. Goal of this study

There are still a lot of complications that occur with pedicle screw placement and pedicle screw holding strength once a pedicle has been inserted and anchored, as mentioned in Section 1.2. Most of the state-of-the-art is focused on visual and physical guidance innovations for pedicle screw placement, not much is done on actual trajectory control and alteration during the screw insertion procedure. An instrument that can alter trajectory during operation and even drill non-straight holes might come with great advantages. Surgeons, once perforating the vertebra in an ill trajectory could, with such a new instrument, change the trajectory instead of exiting the perforation, repositioning the device and starting again with a new trajectory. The latter will not only increase the operation time, but also weaken the vertebra, due to unnecessary tissue removal. Next to that, creating a curved hole in the vertebra might allow for new pedicle anchor designs, that can have a stronger holding strength in the vertebra, which will reduce complications of pedicle screws not staying in place over time. For this reason, the goal of this study is to develop a new vertebra penetration method that could be used in an instrument that can control and alter its trajectory during penetration of the vertebra. A representation of the possible outcome of this study is presented in Figure 1.4. The focus will be on penetrating the cancellous bone, as that is where the trajectory alteration is required, as well as that, cancellous bone comprehends the lion's share of the total volume that needs to be penetrated.

1.5. Layout of this study

A preliminary investigation will be performed, in Chapter 2, to find a suitable drilling method that can be utilized for the trajectory altering drilling instrument. Following this, in Chapter 3, an experiment will be performed to confirm the validity of the chosen method and prove that it can indeed penetrate cancellous bone. Chapter 4 will showcase the actual instrument prototype design of the instrument that will prove if

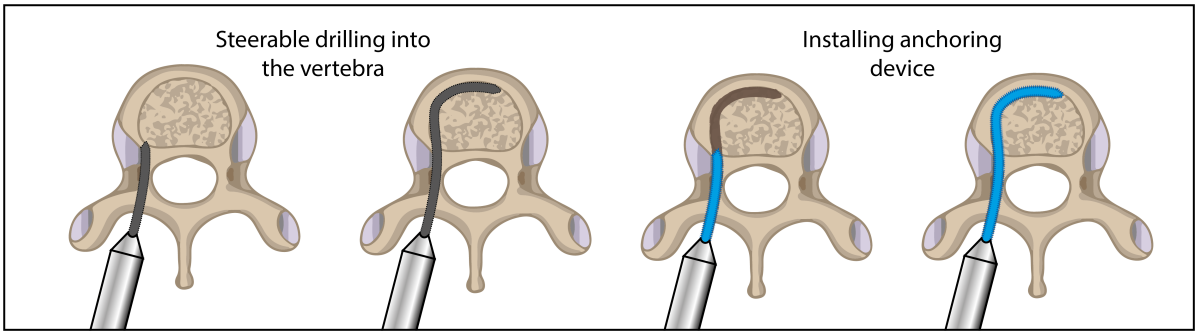

Figure 1.4: Representation of an instrument with steerable drilling capabilities (left two figures) and an instrument that can insert a possible new future anchoring device in the non-straight hole that has been formed (right two figures).

trajectory altering drilling in cancellous bone is possible with the chosen method and design. In Chapter 5, the prototype instrument will be tested to validate the thesis of being a new method for trajectory altering drilling. Following this will be a discussion in Chapter 6 and, lastly, the conclusion, Chapter 7.

2

Preliminary investigation

2.1. Overview: Investigation

To decide on the best method that would allow for drilling a curved hole in the vertebra, different methods of bone machining have to be examined and compared against each other. To compare the different methods, relative to each other, a list that resembles the basic prerequisites for bone osteotomy, surgical cutting of bone, which could also translate to bone penetration, can be used to differentiate between the methods in order to select the best method for the desired goal. The list, compiled by Giraud *et al* [24], contains a number of prerequisites that a surgical tool used for bone osteotomy should abide by. This list is further specified and grouped into either operational prerequisites, fabrication prerequisites and tissue damage prevention prerequisites. Quantification of these prerequisites will be measured by comparing the characteristics of the different methods with each other.

Operational prerequisites

1. **Minimize operation time by rapid cutting of the instrument:** The instrument must allow for quick operation performance, due to that the longer the operation takes, the more postoperative damage the patient will likely have.

2. **Be easy to use:** In order to keep control during the operation of the instrument, the surgeon must be able to perform the operation with much ease in order to reduce complications, which might more easily occur if more actions need to be performed during the procedure.

3. **Allow for cutting in different planes:** To allow for a steerable instrument that will create a 3D curved hole in the vertebra, the method must allow for cutting in different planes.

Fabrication prerequisites

4. **Have a straight forward design:** In the design of the instrument, the eventual benefits an instrument brings must outweigh the complication of the fabrication of the instrument.

Damage prevention prerequisites

5. **Prevent unnecessary removal of bone tissue:** Surrounding bone tissue loss must be kept at a minimum in order to reduce postoperative recovery time [25].

6. **Prevent bone from being destroyed by harmful processes like burning:** Due to many instruments inducing thermal effects, tissue temperature can rise. Bone tissue is very sensitive to heat. Temperatures above 50 degrees Celsius can lead to bone necrosis and neural tissue necrosis can occur at around 43 degrees Celsius [26].

7. **Prevent delay in bone tissue regeneration** Postoperative recovery should be as fast as possible, as prolonged recovery periods increase patients suffering. The surgical method must not induce effects that might prolong the duration of bone tissue regeneration.

8. **Prevent damage to nearby tissue** Tissue in the proximity of the operation site must not be harmed during the operation.

9. **Prevent unwanted biological effects:** The effects of the surgery must not evoke postoperative complications that will delay recovery or become an entire new problem for the patient. In other words, the instrument must not operate in such a way that it might result into damage elsewhere, whilst operating on the target tissue.

There are a lot machining techniques which might be used in an instrument that is able to create a curved hole in the vertebra. An extensive search through literature has resulted in a list of those possible machining methods, as can be seen in Figure 2.1. It provides an overview of the possible machining methods.

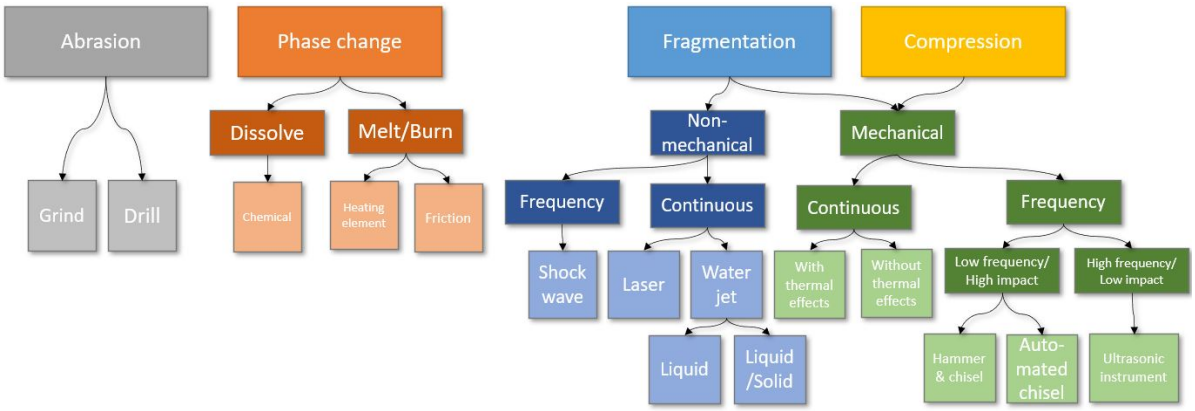

Figure 2.1: Categorisation of different machining methods. The overview is divided into four different sections based on the method the bone tissue is affected whilst performing the penetration of the bone. These four ways of bone alteration are: compression, fragmentation, phase change, and abrasion. These are further divided into different sub-categories.

The overview is divided into four different sections based on the method the bone tissue is affected whilst performing the penetration of the bone. These four ways of bone alteration are: compression, fragmentation, phase change, and abrasion. These are further divided into different sub-categories. In Figure 2.1, it can be seen that 'mechanical' falls under both fragmentation and compression, as it is believed to be a hybrid, as the bone initially get fragmented and then gets compressed to the side. Further research and experimentation, performed during this thesis, will investigate if this is truly the case, as the literature is unclear on this concept in relation to cancellous bone of the vertebra. The possible methods will be further analysed and compared with each other in order to find the most suitable method to use in the steerable drill design. It must be noted that a systematic literature review could have been performed on the different methods of penetrating bone from where, possibly, an alternate result would show the best method for creating a multidirectional hole in bone. However, due to this not being the main scope of the thesis, certain assumptions were made in order to choose a promising technique that would allow for sufficient achievement of the goal, very interesting results and allow for innovation instead of repeating the golden standard. In the next section a structured overview of the methods has been applied that corresponds with the structural overview of Figure 2.1.

2.2. Machining method analysis

2.2.1. Abrasion

Drilling

Two methods use abrasion as a means of bone removal. These two methods are drilling and grinding. Abrasion uses the process of wearing or scraping bone away, as seen in Figure 2.2.

The most common method for penetrating bone is drilling bone [24]. The instrument creates a rotary movement of the drill head. This drill head than penetrates the bone, due to the high speed rotation of the drill head, which abrades away the bone. Advantages are that drills can provide very rapid execution in penetrating the bone, with one of the main advantages of drilling being that it is relatively simple to design [24]. Hence, this method already has a lot of literature and patents that showcase a steerable drill with the ability to drill through bone with an adjustable or set curve, as seen in the patent review of Sendrowicz *et al* [27]. However, only six of the 41 examined patents were commercially available [27] indicating that there still might be some difficulty in creating a drill that can drill a curved hole. Disadvantages of drilling consist of possible accidental damage to surrounding tissue as tools tend to slip. Next to this, drilling generates a lot of heat, which is detrimental to the surrounding tissue [24]. In the study of Gupta *et al* [28], two drills were compared to each other. The first one being an ordinary bone drill and the second having an additional

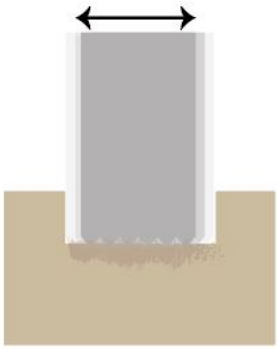

Figure 2.2: Abrasion is performed by repetitive scraping or grinding of the bone.

ultrasonic vibration added to the rotary motion of the drill bit. The study concluded that using additional ultrasonic vibration minimized the torque and cutting force required, and had a lower temperature increase than the conventional method [28].

Grinding

The second abrasion method is grinding. Bone grinding is done with high-speed abrasive tool grinds [26]. The bone is scrubbed away by the abrasive surface of the instrument's working head. The tool can grind through rotary movement or lateral movement of the grinding surface. The design of the rotary version is similar to the previous mentioned drill, just that the working head consists of an abrasive surface instead of a drill head, indicating that this instrument has a relative simple design as well. However, the problem with bone grinding is that it produces much more energy compared to other cutting processes, which leads to an increase in temperature [26], which can again lead to bone necrosis [26]. This results into a big disadvantage for bone grinding, as one of the most essential points in bone osteotomy is the minimization of high thermal effects [24].

2.2.2. Phase change

Heat

Bone can be machined by changing the phase of the tissue, as seen in Figure 2.3. This can be achieved in two ways with the first method being burning or melting of the tissue due to friction. This can also be done in a rotational manner which melts or burns the bone due to friction of the working head against the bone. As has been explained in the previous method, that generating a lot of energy is very disadvantage in bone osteotomy, this method is believed not to be relevant for further analysis in finding an optimal method for creating a curved hole in bone.

Chemical

The second method to change the phase of bone is with the use of chemicals. The process of dissolving a structure is known as chemolysis or dissolution [29]. As no literature is found on the use of this method on bone, chemical lithotripsy, where kidney stones are destroyed with chemicals, was investigated to try and draw a comparison to bone machining of cancellous bone. It must be noted that calculi, kidney stones, are a free floating structure and cancellous bone is not. In this form of lithotripsy, the chemical solvent is transported through a catheter to the kidney stone, where it will be applied to kidney stones in order to dissolve it [30]. However, it would be very hard to control the solvent into creating the desired hole and not spread through the bone uncontrollably, dissolving the surrounding cancellous bone tissue. Spreading of the solvent must be avoided as it could have catastrophic consequences for the patient. For this reason, it is concluded that other machining methods are more favourable than chemolysis for creating the desired hole in the vertebra and further analysis is disregarded.

2.2.3. Fragmentation

Water jet

Another method for removing bone is done by fragmenting. With this method bone gets fragmented into small pieces in order to remove the bone, as seen in Figure 2.4. This can be done either by mechanical machining or non-mechanical. A non-mechanical continuous machining method is with the use of a water jet. In this method fluid impacts the material with a high kinetic energy in order to remove and cut material [31]. Cutting cortical bone with a water jet requires pressures of more than 80 MPa to efficiently and sufficiently cut through the bone tissue. If a water jet beam gets reflected, at those pressure levels, on the bone, the beam might hit another tissue and damage it. Therefore, this method is undesirable due to safety reasons [31]. For this reason solid particles have been

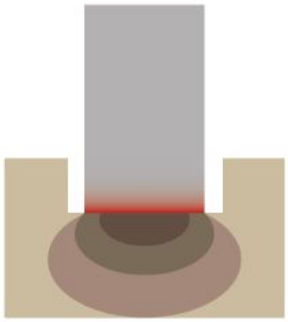

Figure 2.3: Bone can be removed by changing the phase of the bone by either burning or using chemicals. This will alter the bone so it can be removed.

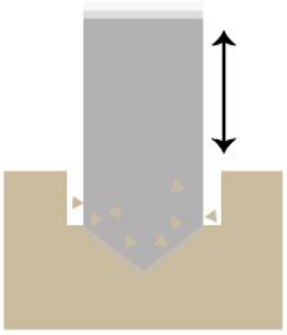

Figure 2.4: Bone can be removed by fragmenting the bone into small pieces by using a repetitive impact mechanism. It is similar to a jackhammer mechanism.

added to the fluid creating a variation called abrasive waterjet machining, which increases the cutting efficiency significantly [31]. In the study of Schwieger *et al* [31], an abrasive waterjet, with water pressure ranging between 35 MPa to 70 MPa, is investigated. The nozzle diameter, were the waterjet exits the instrument, is around 0.2 mm. The study shows success in the cutting of cancellous bone without any thermal effects, however, because of the high porosity of cancellous bone, the jet will be bent due to the numerous material transitions. Next to this, the abrasive waterjet cutting stream only has a diameter of 0.2 mm, which for cutting through bone would be sufficient, but drilling a relatively larger hole in bone would result into certain complications of a drastic increase in operation time. Next to this, if a larger waterjet diameter is utilized, a lot more force would be needed to create the same pressure, which might result into an unsafe operation.

Laser

Lasers could also be used as a continuous machining method, however, pulsed laser is utilized as well [32]. A state-of-the-art bone cutting tool is the Er:YAG [32]. The radiation of the laser is absorbed by water surrounding the target tissue. This water explodes and evaporates, generating well circumscribed and sharp superficial incisions in the target tissue. The laser has options to change the energy settings and power frequency. The laser can also operate in a pulsed or even super pulsed mode [32]. In the study of Umberto *et al* [32], two laser groups were used. One 30Hz, 3W, 100mJ and 35J/cm2, the other with the same wattage and double the remaining parameters. They used this with a 600μm diameter fibre tip [32]. With these applied parameters they found that no bone fragments or sharp edges and a standardised depth was achieved [32]. Next, it is also mentioned that utilizing laser is a reliable stone fragmentation method, regardless of the hardness of the composition [33]. Laser seemed also to be more precise than piezosurgery, using ultrasonic vibrating instrument to resect bone, and standard bone drilling using a rotational drill, although it lacked speed [32]. Another disadvantage of laser is the complete lack of depth control [34], which is a critical point in creating a hole in bone. Especially in the vertebra, as going too deep might result in penetration of the neurons in the spinal cord, which would be detrimental. The last problem with laser, might be if you want to drill a relatively large hole big enough for a pedicle screw, the beam size needs to increase, which will require a lot of energy. A different option is an additional rotational head that aims the laser beam at multiple locations in order to further penetrate the bone, which would increase the operation time. A final option would be to penetrate the hole multiple times with a smaller beam to get the desired hole diameter, which would also increases the operation time. It hereby has the same problem the water jet has, that the benefit of an increased beam size might not outweigh the negative effects it would bring with it.

Shockwave

The use of shockwaves is another non-mechanical method of machining. As no literature again has been found on this method in relation to bone machining, a comparison is made with a lithotripsy method using shockwaves [35]. Electrohydraulic lithotripsy is a method that works by generating a spark discharge, which leads to plasma formation that expands the surrounding water rapidly, generating a hydraulic shock wave. This shockwave fragments solid objects in its path [35]. It is an effective, safe and cost effective way of lithotripsy compared to other methods [36]. This method might generate a new method of bone machining, as bone machining with laser almost works on the same basis as mentioned before in the paragraph on laser. The two methods are quite similar and share, apart from the price, their advantages and disadvantages [35].

In the field of lithotripsy, extracorporeal shockwaves are also utilized. The method works on the basis of sending a targeted shockwave towards the kidney stone with the means to fragment it [37]. This, however, might not work for generating a hole in bone as such a method could easily harm surrounding bone tissue, which is not the case for kidney stones as they are free floating in soft tissue.

2.2.4. Compression

Continuous load

Both compression and fragmentation have been linked to the mechanical machining method section. This is because it is still unclear how the methods effect the cancellous bone of the vertebra. For now it is believed the cancellous bone will fragment and be compressed towards the sides, indicating that the mechanical section is a hybrid version of both compression and fragmentation. Compression is achieved by applying a force onto the bone in order to penetrate it, as seen in Figure 2.5. One of the machining methods in this section is applying continuous pressure to penetrate bone. Possible applications utilizing this method are surgical knifes, wedges or bone awls. The idea is to apply a large enough load on the target tissue with the surgical instrument such that the tissue will give way and break in order to penetrate or cut the tissue. However, applying an excessive force, that is generated by a surgical tool, might lead to micro-cracks and fracture formation which could ultimately lead, in the adjacent area, to permanent damage, which in turn may lead to a delay in the postoperative recovery of patients [38].

This, however, was analysed on cortical bone as there was no relevant literature to be found on the penetration mechanics of cancellous bone, which might act in a different way because of its high porosity [39].

A study done by Mulligan *et al* [40] showed that an increased force was needed to penetrate the cancellous bone when larger depths were reached. The study used a gauge-8 (4-mm diameter) biopsy needle. Penetration speeds were used between 1 mm/s to 5 mm/s. For 1 mm/s the force required at a depth of 25 mm was found to be 1000 N. For 5 mm/s at 10 mm the required force stayed around 500 N no matter the depth that followed [40]. When comparing applying a constant load to a repeated impact method, the constant load might be at an disadvantage, as sudden stress might require less force to break a material than the same force applied slower to a material. The material has no time to react in a ductile way [41], indicating that less force is needed for the repeated impact mechanism. However, an instrument that just applies a single load has, most likely, a less complicated design than one that generates repeating impacts.

This concept can also be applied with an addition of a thermal tip, with the idea of having a continuous load combined with a high temperature, which might be beneficial for some materials. But as already mentioned, thermal damage to the surrounding tissue is a critical point to consider.

Repeated impact

Repeated impact to the target material is another method of mechanical machining working with a frequency. For bone osteotomy, this can be done in numerous ways, with the most basic method being a hammer and chisel. More advanced methods might make use of a pneumatically driven oscillating working head [42], that strikes the bone, chipping bone fragments off the bone. This working head could have numerous tips depending on the surgical operation that needs to be done. Cokkeser *et al* [43], find that using a hammer and chisel provides an inexpensive technique that provides practical and fast bone removal. Next to this, they claim that it is a controllable and very simple procedure compared to drilling [43]. However, from the research of Çukurova *et al* [44], it is concluded that piezosurgery, osteotomy by using ultrasonic vibrations, apart from the increase in price, out performs the hammer and chisel method. The results show a shorter operation time, a decrease in pain and less recurrence compared to the traditional hammer and chisel method [44]. In the study of Edward and Gallo [42] a traditional hammer and chisel is compared to a pneumatically driven one. They conclude that the pneumatically driven one out performs the traditional one. It is found that the pneumatic osteotome provides more ease of use, and allows for more accuracy and visibility whilst performing the operation [42]. Next to this, it provides for a relatively safe machining method as it does not cut into soft tissue [42]. There is, however, a scarce amount of literature on the subject of using impact to fragment bone, in particular cancellous bone. For this reason, pneumatic lithotripsy, which is already a successful application in the field of removing kidney stones through high speed impact fragmentation [33] and therefore might indicate a possible application in the field of penetrating bone, has been analysed as well. In the study of Abedi *et al* [33], laser lithotripsy is compared to pneumatic lithotripsy. From this study, it is concluded that pneumatic lithotripsy is less expensive, yet laser lithotripsy is the safest, most effective, and most adaptable method. It fragments the target tissue into smaller pieces and has less pushback compared to its pneumatic counterpart [33]. This pushback might become a problem when creating curved holes, as the curved part of the instrument might buckle. Another problem from repeated impact might come from crack forming, as bone is a very brittle material. Repeated impact might cause crack propagation in the surrounding bone tissue. Presumably, due to the scarce amount of literature on penetrating bone by means of using repeated impact, no definitive forces or frequencies were found indicating the right parameters to penetrate the bone with this method.

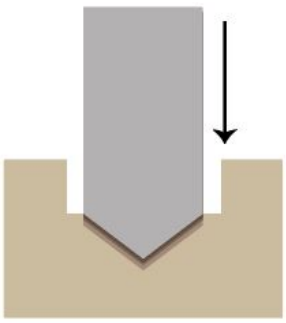

Figure 2.5: Bone can be penetrated with the use of compression. By applying a large enough load onto the bone with an instrument suitable for this operation, the bone will give way in order to form a hole.

Ultrasonic vibration

The last mechanical machining method uses the principle of ultrasonic vibration. For medical applications it is usually called piezosurgery, as briefly mentioned earlier. Piezosurgery uses the principle of making incisions in bone with piezoelectric induced micrometric ultrasonic vibrations [45]. When the instrument is in operation, contact with the target bone tissue causes the bone to break down into smaller pieces due to the repetitive impact mechanics of the ultrasonic instrument [46]. Piezosurgery can be used for a large variety

of osteotomy, and proves especially important in cases where soft tissue is adjacent to bones which results in limited access for the surgeon. Its primary benefit is namely that peizosurgery devices are harmless to soft tissue, as the ultrasonic vibration only effects the target tissue it was designed for [45].

In Umberto *et al* [32] and Troedhan *et al* [34], a comparison is made in cutting bone between drills, lasers and piezotomes (ultrasonic surgical instruments). Umberto *et al* [32] finds that the laser produces the most precise bone cuts compared to the other two techniques, especially compared to traditional bone drilling techniques. However, laser cutting does provide a longer operation time and learning curve than the other methods. The laser also does not produce any bone fragments, which makes it better for healing. Piezosurgery showed less precise cuts, but showed no thermal damage on the surrounding bone tissue. Troedhan *et al* [34] find that laser osteotomy still has a long way to go and has lack of depth control [34], which might make it less viable candidate for using it for creating the desired multidirectional hole. Backed by clinical and experimental studies, Troedhan *et al* [34] state that piezotomes improve bone-healing, provide a smooth bone cut surface, have the least amount of thermal side effects on the surrounding tissue, and have precise osteotomy design, protection of soft-tissue and excellent depth-control. Compared to rotary instruments, piezotomes reduce the postsurgical morbidity [34].

2.3. Machining method selection

In this section, the main reasons are given for the selection or deselection of a method. To select the best bone machining method, that will be utilized for a steerable drilling device that can create a multidirectional hole in the vertebra so pedicle screws can be placed in the vertebra, the list of prerequisites given in the overview section is cross analysed in relation with the methods presented in the previous section. Additionally, with the disadvantages and advantages of every method a selection will be made to identify the most promising method for creating a curved hole with a steerable drill in the vertebra. It must be noted that many of the previous methods had little to no literature on the method utilization on cancellous bone. Especially, almost no literature was found on actually penetrating cancellous bone with the found methods. Therefore, comparison is made between the methods based on how the methods compare in bone tissue osteotomy mentioned in the literature and logical reasoning.

Many methods can already be discarded as they are already proven less plausible to be a viable candidate in the method analysis section. For rotation, this is the grinding and melting method, as drilling is the better method, due to having the least amount of thermal effects on the surrounding tissue. Next to this, in the case of multidirectional drilling both grinding and melting will most likely have the same transition mechanism. Therefore, only drilling will be further compared to the other methods. The method of applying continuous pressure with and without additional heat is also discarded. The reasons for this are that it is believed that microfractures will occur in the surrounding bone tissue, which will delay patients healing [38], when pressure is applied to the bone in order to penetrate the bone. Another reason is at some point the hole will be perpendicular to the force applied by the surgeon to penetrate the bone, which results in variable force needed to generate curved holes in bone. This can lead to high forces that need to be applied in order to penetrate the bone, if the surgeons applied force will be perpendicular to the direction of the hole. The last reason, is that when comparing applying a constant load to a repeated impact method, the constant load might be at a disadvantage, as sudden stress might require less force to break a material than the same force applied slower to a material. The material has no time to react in a ductile way [41], indicating that less force is needed for the repeated impact mechanism.

The method with the additional heated tip is also discarded as, again, the thermal effects are a big disadvantage. For the waterjet method, the abrasive waterjet is more preferable than the waterjet that utilizes liquid without additional particles, as that method requires more pressure to penetrate bone [31]. Chemolysis is also regarded as an undesirable method for creating a curved hole in the vertebra. Namely, because it is assumed controlling the solvent will be difficult and risk of the solvent spreading uncontrollably can have detrimental effects, especially if it breaches the spinal canal and harms the neurons.

The laser and the (abrasive) waterjet methods are both great tools for bone osteotomy, but when it comes to generating a relative large hole for a pedicle screw to be inserted it might take too long, which is in conflict with one of the prerequisites of minimizing operation time by rapid cutting. Next to this, due to the lack of depth control as mentioned in the previous section, there is an increased risk of penetrating the spinal canal and harming the neurons. Even if the beams were bigger for the abrasive waterjet the force needed to generate the required 35 MPa to 70 MPa [31] is assumed to be too high for safe operation. For the laser method creating a larger beam would require more energy [32] and will result in more thermal build up, which is in contradiction with a the prerequisite of preventing bone from being destroyed by harmful processes like burning.

Comparing the traditional drilling method to ultrasonic vibration method, both studies of Umberto *et al* [32] and Troedhan *et al* [34] conclude that the use of ultrasonic vibration in the form of a piezotome is better than the traditional drilling method, on the basis of more precision, less thermal heat build-up and quicker recovery for the patients [32, 34]. When looking at generating multidirectional holes in the vertebra there is no clear indication of which technique will be more beneficial, thus based in the previous advantages of piezotomes over traditional drilling, the ultrasonic vibration method is considered the better method. The combination of ultrasonic vibration with traditional drilling method is considered better than just the traditional drilling method [28], however, it will still retain some of the disadvantages of drilling compared to an instrument using pure ultrasonic vibration as their means to penetrate the bone.

The method of generating shockwaves seems to be a likely candidate due to its effective, safe and cost effective way it performs lithotripsy compared to other methods [36]. Such a method could possibly be translated to an instrument that will penetrate the cancellous bone. This method will also suffice in creating curved holes as there are no stiff long components required in the part that enters the body, hence, its use in lithotripsy [35]. One drawback of this method is that regulating the shockwave intensity to allow for high precision penetration in the cancellous bone can be quite difficult, due to the heterogenous nature of cancellous bone [39]. The shockwaves can be either too large or too small due to the cancellous bone not having the same density and strength through the entire vertebra [39]. Next to this, depth control might be an issue as the device is not in contact with the bone in the drill direction [35]. This might make it hard for the surgeon to estimate its position in the vertebra. But it is still believed the hydraulic shockwave method might be a plausible candidate, due to the possibility of an easy design for curved drilling, as an easy design is favoured by the prerequisites.

The usage of ultrasonic vibration and repeated impact might be a better alternative for reaching the goal, as these methods might have more control over generating a multidirectional hole in the cancellous bone of the vertebra, than the hydraulic shockwave method, but they lack in simplicity of design. Ultrasonic and repeated impact both have the same characteristics of using mechanical impact to penetrate bone. One using high frequency, low impact drilling, the other using low frequency, high impact drilling. As already explained in the method analysis, they allow for fast, safe and relatively cost effective bone machining. It is, therefore, believed, the three remaining methods, ultrasonic vibration, repeated impact, and hydraulic shockwave seem to be plausible candidates that are believed to be able to sufficiently generate a multidirectional hole in the cancellous bone of the vertebra in order to insert pedicle screws for spinal fusion.

To better understand all three methods and make an eventual choice as to which method will be utilized for the continuation of this thesis, the methods are further analysed into their specifics. Next to this, solution proposals of steerable instruments utilizing the three different methods are proposed.

2.4. Bone machining method solution proposals

2.4.1. Overview: Proposals

The three identified possible options to further investigate, ultrasonic vibration, repeated impact and hydraulic shockwave, will be examined in more detail below. The exact workings of bone removal and the required parameters needed in order to achieve its bone machining capability will be explained. Next to this, a general instrument solution proposal has been made, based on current understanding of the techniques and addressed literature. These solution proposals propose a possible way of achieving the desired goal with one of the three selected methods. It is hypothesized that the technique used in the instruments will be able to penetrate the cancellous bone. Next to this, it is important that the technique must allow for bending to allow for steerable drilling. Creating an instrument with the ability to allow for steerable drilling through the vertebra, requires a transitional medium to translate the required input to the output, which is the working head. This transitional medium must be able to bend in order to allow for the steerable drilling. The three solution proposals give a general overview of the possible parts which together will form the end result. These parts are general descriptions with specifications left out, as this will only become relevant in the actual design phase after a certain solution proposal has been chosen. The following three solution proposals show general interpretations of what an instrument utilizing a certain method might look like. It must be noted that there are many different ways the following instruments could be designed, with a variety of mechanics. The following proposals are just for illustrative purposes and to show that there are possibilities in creating a relevant instrument utilizing the different methods.

2.4.2. Ultrasonic surgical instrument

As explained in the previous section, ultrasonic instruments cut bone through ultrasonic vibration of the instrument. The fundamental design concept of ultrasonic surgical instruments is resonance. It allows for minimum external energy input resulting in, at the op-

erative end, maximum possible excursion. The entire instrument is constructed with the half-wave resonant condition in mind, with the goal of creating maximum excursion at the working end [46]. It is found that ultrasonic instruments usually operate around 25-35 kHz [47, 48, 49] for hard tissue and frequencies above 50 kHz for soft tissues, and an amplitude of the working end that can reach in between 100μm to 300μm [47, 49]. Due to the mechanical waves induced by the ultrasonic transducer, a phenomenon called agitation occurs. Agitation induces fragmentation and disorganization in the different bodies the instrument comes into contact with [50].

An instrument using ultrasonic vibration can cut material by utilizing three different methods, with 1) segmentation occurs through ultrasonic vibration by solid to solid interfaces by means of distinct vibration, 2) solid to liquid segmentation occurs by means of cavitation, and 3) due to high energy, ultrasonic vibration makes it also possible to burn through soft tissue [50]. Because of the last method, one can see irrigation or other cooling methods are needed in order to keep the instrument cool if thermal effects are not wanted [50]. Four parameters characterize the ultrasonic surgical tool from conventional tools. These are the insert's weight, the form, hardness and the induced frequency of the instrument [50]. Next to this, the working pressure, tip characteristics as shape and size, alloy and sharpness, and the bone density influences the cutting power of the instrument [49].

For the ultrasonic vibration method a solution proposal has been made using a waveguide wire, for the transitional part. These wires can translate ultrasonic vibration generated as input and be translated to the working head, which will vibrate as output [51]. These wires have the ability to bend, making curved drilling plausible, as seen in Figure 2.6. It further has an ultrasonic transducer in the handle to induce the ultrasonic vibration, an amplifier between the transitional part and the handle, the transitional part, and at the end of the instrument the working head. The controls will be built into the hand piece, allowing the surgeon to activate the drill and to steer it. As ultrasonic vibration causes thermal build up, the transitional tube also functions as an irrigation channel.

2.4.3. Repeated impact

Penetrating bone through repeated impact can be done in various ways. The most basic form being the chisel and mallet, and more advanced forms, using automation, being a pneumatic chisel or other automatically driven chisels. The chisel can also be replaced with different working heads to achieve the required penetration application. The chisel and mallet work by striking the chisel with the mallet in order to cut or fragment the target tissue. For the automated version, the surgeon only has to turn on the device and the chisel starts oscillating, resembling a jackhammer effect. Due to repeated impact of the working head on the bone, the bone will fragment.

Parameters effecting the cutting speed of the instrument are similar to those of the ultrasonic surgical instrument. The parameters are the form of the working head, the frequency of the repetitive strikes of the instrument on the target bone tissue, the material hardness of the working head, the weight of the working head and the speed of which the working head strikes the bone. The difference between ultrasonic vibration and repeated impact mainly is that the first focusses on high repetitive frequency wearing down the target tissue, whilst the latter uses a stronger impact at lower frequency to break down the target tissue. For the repeated impact, the solution proposal has been made using a tube filled with liquid as transitional medium, that will translate a generated impact in the handpiece to the working head, allowing the working head to repeatedly strike the target bone. This is believed to be a good candidate for this application as a liquid filled tube allows for bending, thus for steerability, as can be seen in Figure 2.7. Such a method of translating impact through a liquid medium in order to activate a working head has already been described by Sakes *et al* [52] for the use of lithotripsy. In this study, an impact, generated at the start of the tube, was translated through the liquid to a working head giving it an impulse, which would result in the striking of a calcified occlusions in order to remove it. Possible ways of generating a repeating impact might be with the use of a jackhammer mechanism, a solenoid, or by using repeated liquid shockwaves generated by a spark generator. The working head will have a mechanism that will pull the working head back after receiving its initial impulse in order to achieve the repeated impact effect.

2.4.4. Electrohydraulic shockwave

Electrohydraulic shockwaves induce a phenomenon called bubble cavitation. It works by generating a plasma in a liquid medium. This can be done by either a spark discharge or an optical breakdown [35]. With supersonic speed, the plasma will initially expand, which will cause the hydraulic shockwave and impact the target material. Following the plasma, is a cavitation bubble. This bubble can be in the range of several millimetres. This is dependent on the amount of energy is applied. Around 100 microseconds later the bubble will collapse, which will cause another pressure pulse. The collapse might induce high-speed microjets of liquid, which are capable of even pitting metal surfaces [35]. Therefore, they may also provide a valid option for stone fragmentation [35]. The bubble cavitation can be calculated with the Rayleigh–Plesset

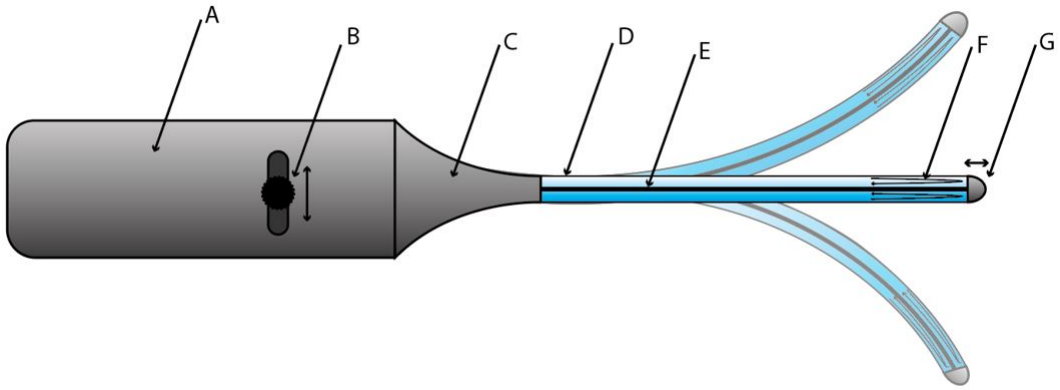

Figure 2.6: A possible representation of a steerable ultrasonic drill with A) handpiece, housing the ultrasonic transducer, B) steering mechanics, allowing the surgeon to steer the drill, C) ultrasonic horn, amplifying the ultrasonic vibration of the transducer and translating it to the waveguide wire, D) the transition tube containing the waveguide wire, the liquid and the steering mechanics, E) the waveguide wire, translating the ultrasonic vibration to the working head, F) the irrigation fluid flowing past the working head in order to cool it down while operating, G) the working head, which will make contact with the target tissue in order to fragment it.

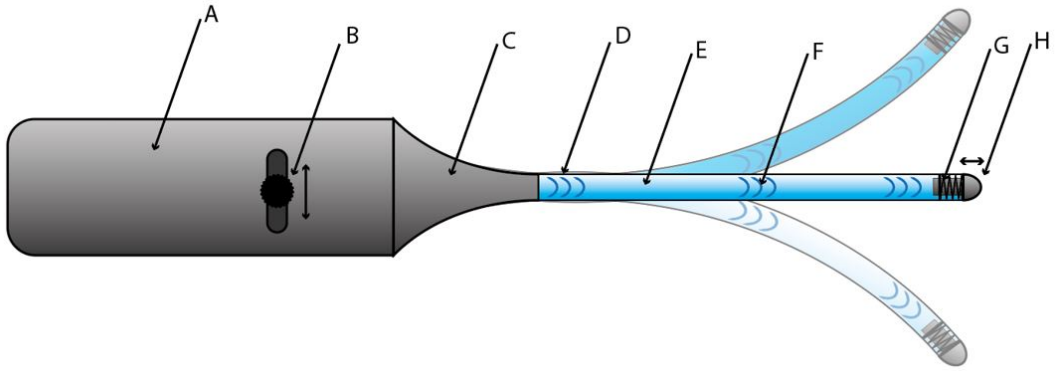

Figure 2.7: A possible representation of a steerable drill utilizing repeated impact with A) the handpiece, housing the mechanism that will generate repeated impacts, B) steering mechanics, allowing the surgeon to steer the drill, C) the translational part, connecting the handpiece to the transition tube, D) the transition tube, housing the liquid, the steering mechanics and connecting the handpiece to the working head, E) the liquid, were the impulses will travel through, F) A representation of a repeating impact pattern, G) the mechanism that will return the working head to its initial position after it has received an impulse, H) the working head that will strike the target tissue through repeated impact received by the generator in the handpiece.

equation (Equation 2.1), or with an approach of this equation, were tension and viscosity are neglected, called the Young-Laplace equation (Equation 2.2) [53].

$$R\frac{d^2R}{dt^2}+\frac{3}{2}\left(\frac{dR}{dt}\right)^2+\frac{4\nu_L}{R}\frac{dR}{dt}+\frac{2\gamma}{\rho_L R}+\frac{\Delta P(t)}{\rho_L}=0 \quad (2.1)$$

$$P_B-P_\infty=\frac{2\gamma}{R} \quad (2.2)$$

In the research of Vorreuther *et al* [53], cavitation bubbles were generated with a spark generator. Energies from 50mJ to 1300mJ and above were used. With these inputs cavitation bubbles were reached of 4 to 6 mm for energy inputs of 400mJ and cavitation bubbles reaching 15mm diameter with the use of energies up to 1300mJ [53]. In order to design an instrument that uses the method of electrohydraulic shockwaves to penetrate bone, again a transitional tube containing liquid has been used with the ability to bent, to allow for steerability. Through this tube, a flexible wire runs, that transports electrical charge towards the end piece, as seen in Figure 2.8. The end piece, or the working head, in this case is a spark generator. Around the spark generator, a constant flow of liquid will be supplied. This spark generator will generate a spark, that will cause the surrounding liquid to superheat and to form cavitation bubbles, which will enable the instrument to penetrate the bone.

2.5. Continuation of the research

For the continuation of this thesis, a choice must be made for a particular method. As there is already a lot

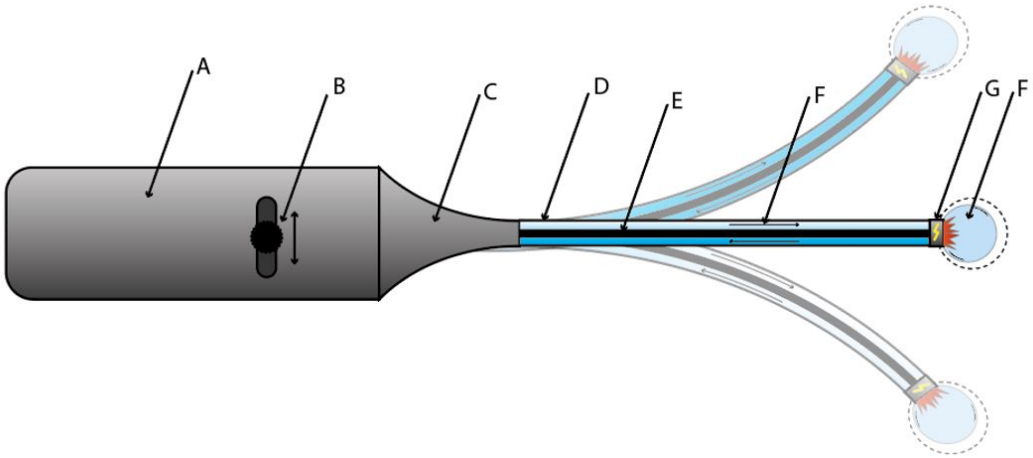

Figure 2.8: A possible representation of a steerable drill utilizing hydraulic shockwaves with A) the handpiece, housing the mechanism and electronics that will enable the instrument to function, , B) steering mechanics, allowing the surgeon to steer the drill, C) the translational part, connecting the handpiece to the transition tube, D) the transition tube, housing the liquid, the steering mechanics and connecting the handpiece to the working head, E) the flexible electronic wire that will transport the electrical charge towards the end piece, F) the irrigation channel that will provide fluid to the end piece in order to create cavitation bubbles, G) the spark generator, that is connected to the electric wire and will create a spark which will generate a cavitation bubble, F) a representation of an increasing cavitation bubble with its surrounding shockwave, that will be used to penetrate the cancellous bone.

of literature on bone osteotomy with the use of ultrasonic vibrations and the benefits of using such a method compared to other methods [46], the ultrasonic vibration method is a highly likely candidate for the utilization in the further research towards the end goal. Because of the lack of literature on the impact method, but with the believe such a method might make a viable solution for drilling a multidirectional hole in cancellous bone, due to reasons explained in the previous section like no heat generation, ease of use and simplicity of design, the repeated impact method will also be a valid choice. Together with hydraulic shockwave, these methods all utilize a form of impact in order to resect bone. As again there seems to be little relevant literature on the effect of impact on cancellous bone, it will be interesting to perform experiments that will shine a light on the effect of impact on cancellous bone and what parameters will need to be utilized in order to achieve relevant penetration of the tissue through impact. For initial impact experiments, the repeated impact method has been chosen. It is believed, the experiment will require the least elaborate setup, as the other two methods require either an ultrasonic transducer or a electric pulse generator, which are not easily obtained. Further research, for this reason, will be done on the repeated impact method, as it is believed that with the acquired data from the research, educated guesses can be made that might predict the usefulness of the other two methods in penetrating cancellous bone, as they too use impact.

3

Proof-of-principle experiment: Repeated impact

3.1. Overview: Repeated impact

An experiment is performed to prove if penetration of cancellous bone by means of repeated impact is possible and if so, which variation of impact would be most suitable for further research. To validate this, a setup will be made. This setup consists of a system that can generate an impact, that will consist of a mechanical impulse, S [Ns], which is the integral of force, F [N], over a time interval, dt [s], and a target tissue that will receive the impact. However, the target tissue, in this case being cancellous bone of a vertebra, is difficult to acquire. Therefore, an alternative must be found which has characteristics in the range of this particular bone. To imitate the cancellous bone, a substitute, polyurethane foam, is used. The substitute often used in literature [54, 55], with a density mostly in the range of 0.16–0.64 g.cm-3 [55]. This material is less complicated to acquire than actual cancellous bone and has thermal and mechanical properties in the documented ranges of human cancellous bone [54]. Certain companies, like Sawbones, offer a variety of specialized bone models and replica material with the same properties as the actual bone. However, the products they offer are relatively more expensive than polyurethane foam and have a a long delivery time. Therefore, an extra test was performed in order to establish that polyurethane foam is an adequate substitute for cancellous bone found in the vertebra. This was done with a compressive strength test, which resulted in the continuation of using polyurethane foam as a sufficient substitute for the initial, as can be examined in Appendix A.

To come to a meaningful conclusion, the repeated impact experiment must validate a number of aspects. This experiment will, foremostly, validate if it is feasible to penetrate cancellous bone by means of repeated impact. Next, what the effect of different variations of impact would be on the target tissue, by using different geometries of the target tissue striking part and a range of different impulse magnitudes. Finally, the impact tests will be cross examined with a previous experiment that applied a pure continuous pressure on the target tissue, found in Appendix B. This is done, to see if repeated impact requires less input force than applying a continuous force, and if this is significant enough to claim a more beneficial status of penetrating cancellous bone than just applying a continuous load.

By analysing the previous aspects, results as which magnitude of input force is needed to show visible fragmentation effects, target tissue penetration rate [mm/strike] and most efficient impulse variation can be found. For simplification of the experiment and to save valuable time, the repeated impact test will be done with single impacts performed manually. This is done, because it is hypothesized that at the probable frequencies of operation, around 5 Hz to 15 Hz, the results will not vary much if those same 5 to 15 impacts per second are done over a longer period of time, instead of a second.

3.1.1. Requirements

The requirements will provide a guideline from which a design for test setup can be designed. The following list showcases the requirements:

- **Generate impulse:** The instrument must be able to generate an impulse through an input force that will impact the target tissue.
- **An energy input in the range of 0 to 0.282 Joule:** The impact must be generated from a compressed spring, which can deliver an energy output of at least 0.282 Joule according Appendix B. The spring must, at least, be able to compress over a distance of 30 mm, to allow for sufficient variation in the impact magnitudes. The spring must have a spring constant of at least 0.63 newton per millimetre, as was found in Appendix B.
- **Consistent impact:** The generated impulse must be consistent in order to achieve valid results.

- **Variable impact:** The impulse must be variable in order to measure different impacts and the effects on the target tissue.
- **Visible force input:** The input force, the impact will have, must be visible each test cycle.
- **Adjustable distance between the tip and the target tissue:** The distance between the tip and the target tissue must be accurately adjustable with a 1 millimetre margin of error, in order to strike the target tissue with the same travel distance each time.
- **Interchangeable working heads:** The working heads must be interchangeable, in order to test the effect of different tips on the target tissue.
- **Resilient test setup:** The test setup must be strong enough to resist the forces of the input and output of the experiment.
- **Measurable output:** The impulse that the impact of the working head on the target tissue will make must be measurable.
- **Measurable penetration depth:** It must be possible to measure the depth of penetration in the target tissue.
- **Interchangeable target tissue:** Test tissue must be easily exchanged for new test tissue to allow for a large number of tests.
- **Durable working heads:** The working heads must be of a hard metal in order to not wear down after multiple uses, as well as inelastic, in order to decrease the elastic collision effect.

3.1.2. Experiment proposal

Through application of these requirements, a test setup is proposed that will use compression springs that will allow for the generation of a mechanical impulse, S [Ns], as seen in Figure 3.1. In order to initiate the impulse, the compression springs are compressed over a certain distance d [mm] by means of a input force F_{input} [N] and then rapidly released. The springs are connected to a medium, the linear slider, that will translate the mechanical impulse of the springs. At the distal end, closest to the target tissue, of the linear slider, different working heads are positioned in the form of cylinders from hard material with different shaped tips, and with a variation of different diameters, as seen in Figure 3.2. These will strike the target tissue with the generated impact made by the compression spring. With a force loadcell, this impact will be measured, as S_{output} [Ns].

3.2. Method: Repeated impact

3.2.1. Research goal

The goal of this experiment is to prove if penetration of cancellous bone by means of repeated impact is possible and if so, which variation of impact would be most suitable for further research.

3.2.2. Research variables

Independent variables

Impact shape

The working head that will strike the target tissue will consist of cylinder shaped working heads, with a variation of different tips, as seen in Figure 3.2. Seven different tip shape variations will be utilized. They range from sharp tips all the way to blunt tips. This is done to see which shape of tip seems to be most efficient at penetrating the target tissue through repeated impact. Next to this, a range of different diameters is chosen for the working heads. Different working head diameters will be examined to see, what effect a larger diameter has on penetration of the target tissue. Through testing with alternate diameters, an optimal diameter could be established, that will require relatively low impact pressure, whilst maintaining good penetration capabilities, compared to the rest.

Straight pedicle screws typically have a diameter around 5 mm to 8 mm in the lumbar region [56], although thoracic pedicle screw diameters are more in the range of 4.0 mm to 4.5 mm [57]. By using curved holes in the lumbar region, a thinner curved pedicle screw might possibly be used, as a thinner curved pedicle screw might show the same holding strength as a straight thicker pedicle screw. Therefore, the range of the working head diameters will be set from 4 mm to 8 mm to accommodate for the possibility of having thinner pedicle screws. Three different working head diameters will be analysed (4 mm, 6 mm and 8 mm). Three are chosen to see if linearity in the results, found by performing the repeated impacts, occurs when increasing in size or not. This will allow for consideration of the best diameter size for the working head. With the three different diameters of the working heads and the seven different tip forms, a total of twenty one different working heads will be analysed.

Input impulse

Through the use of a compression spring and compressing the spring over alternate distances, a range of impulses can be generated. This will allow for a range of impulses in relation to different working heads to be analysed, to find the most efficient combination. The amount of maximum energy the spring needs to deliver to generate the right impulses, was found in Appendix B, which resulted in 0.282 Joule. By conservation of energy, the spring potential energy can,

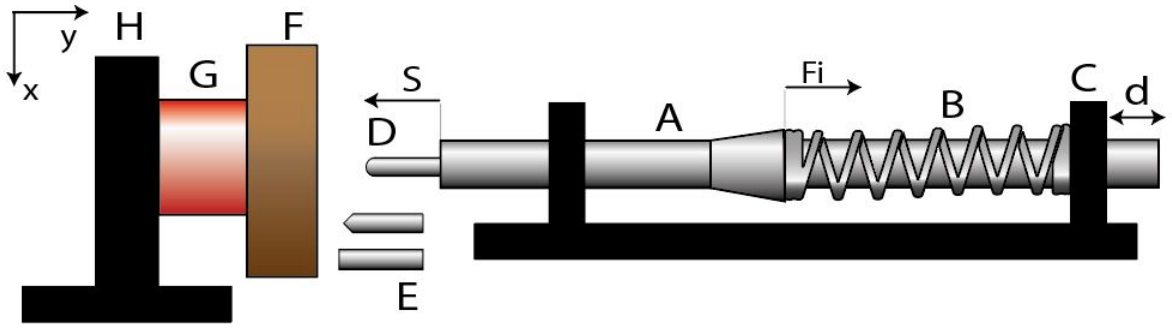

Figure 3.1: Schematic representation of the mechanical impulse generating device, that will generate a mechanical impulse, S, by compressing a spring with a force, Fi, over a distance, d, on a target tissue that is connected to a loadcell, in order to, capture the required data with A) the linear slider, that can slide horizontally and holds the compression spring, B) the compression spring, which will generate the impulse when compressed and released, C) the linear slider mount, which allows for the linear slider to rapidly move in one direction, D) the working head that will strike the target tissue, E) different variations of those working heads that can be interchanged with each other, F) the target tissue that will receive the impact, G) the loadcell that will capture the data of every impact that is generated on the target tissue, H) the loadcell mount that holds the loadcell in place, so it will not move when receiving the impact.

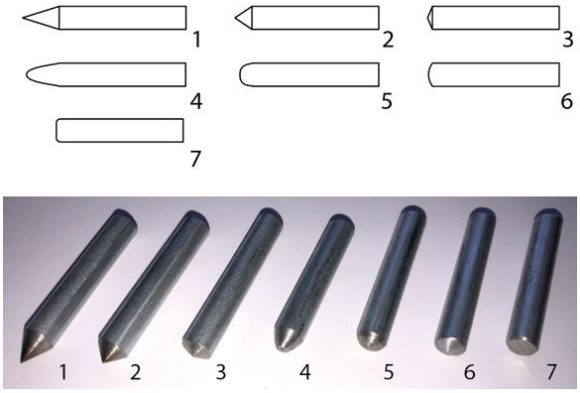

Figure 3.2: Seven tip variations, with top a schematic representation and bottom the actual working heads (8 millimetre diameter variation). Tip variation 1 to 3) has a sharp point, tip variation 4 to 6) has a blunt point, and tip variation 7) only has a flat surface as working head tip.

theoretically, be fully translated to kinetic energy, K [J], as shown in Appendix B. By rewriting the kinetic energy equation (Equation 3.1), and with the known mass , M [kg], of the translating medium, the velocity of the impact can be calculated (Equation 3.2).

$$K = \frac{1}{2} M v^2 \tag{3.1}$$

$$v = \sqrt{\frac{2 * K}{M}} \tag{3.2}$$

With the same mass of the translating medium, M [kg], and the newly found impact velocity, v [m/s], the impulse, S [Ns], is found using Equation 3.3.

$$S = M * v \tag{3.3}$$

This impulse will be varied in magnitude by using a range of different spring compression distances.

Dependent variables

Output impulse

The output impulse, S [Ns], will be measured by a loadcell directly behind the target tissue. The loadcell will provide the force, F [N], over a period of time, t [s]. With this data, the impulse, S [Ns], is calculated by the integral of time over the force, given by Equation 3.4, that the target tissue receives, can be analysed.

$$S = \int_t F dt \tag{3.4}$$

Theoretically this should equal the input impulse, but in reality this is not the case. There will be several losses that will decrease the magnitude of impulse that will be measured by the loadcell. These losses consist of friction from the linear slider with the setup, air resistance, damping caused by elasticity of the polyurethane foam (Appendix A) and potential heat loss. With the impulse output data, the magnitude of the impulse can be compared to the penetration rate for the different working heads, in order to find the most efficient way of penetrating the target tissue with the repeated impact method.

Penetration rate

The penetration rate, millimetres per strike [mm/strike], will be found by measuring the depth of a hole, that is formed due to a number of repetitive strikes of the working head on a particular spot on the block of polyurethane foam. The depth of the hole will be divided by the amount of strikes it took to reach that particular depth, which results in the average penetration depth of that particular working head. With this data, comparison between the different working heads can be done, to see which working head performs the best.

3.2.3. Experimental facility

For this experiment, an experimental facility is used, illustrated in Figure 3.3. With this setup, an impulse can be generated by a compression spring (ø24.4 mm, spring constant k=0.78 N mm^{-1}) over a set distance and then releasing the spring to generate an impulse. The spring is chosen, as compressing the spring over a distance of 30 millimetres would give more than enough energy, theoretically, to perform relevant impacts with the working head that needed the largest force to penetrate the polyurethane foam, variation 7 with a 8 mm diameter, as is established by the experiment in Appendix B. This spring was placed on a linear slider that could be pulled back over a set distance and then be released to propel the linear slider towards the target tissue. The linear slider could be pulled back accurately, manually by the operator, in order to provide the right amount of impulse. This was done by pulling the linear slider back till the end was in contact with a stop, that was positioned at a precise distance, to allow for precise and accurate impact inputs. The stop can be altered to allow for different distances, to perform different magnitudes of impact. This is done by sliding the screw up or down the slot and fixating it at the right distance.

The working heads, were positioned at the distal end of the linear slider, closest to the target tissue. They could be interchanged and secured with the use of an Allen screw located at the side of the linear slider.

To move the linear slider mechanism up and down, a linear stage is utilized. The linear stage is a custom made linear stage, found in the MISIT lab of the TU Delft, that allows for vertical displacement of 1 mm per step, with a maximum load resistance of 100 N. The working head tip is positioned, with the linear stage, in such a way that it rests on the target tissue without compressing the spring. Any further movement down would initiate compression of the spring. This is done so that the tip of the working head will always strike the target tissue with the same travel distance, allowing for a more accurate impulse result.

The impact of the working heads was delivered upon a polyurethane foam block (100 mm x 100 mm x 30 mm), which was positioned on top of a platform connected to the loadcell. This way, the entire impulse can be measured, as the working head strikes the target tissue. The foam block was generated by using polyurethane foam, made from a ratio of 1:1 from the substances Polyol and Iso, and using a mould to achieve the required form.

The data analysis and acquisition of the output impulse was done with a data acquisition system (NI USB-6002: 12-Bit, 10kS/s Low-Cost Multifunction DAQ) and an analogue signal conditioner (CPJ RAIL, SCAIME, S.N.: 001436), all connected to a loadcell (PST, S-Type Load Cell) with a capacity of 150 kg. The loadcell was controlled with a software programme (NI LabVIEW 2018). The programme registered a change in force on the loadcell and provided a data sample of the force over time change during a 3 second window.

3.2.4. Experimental protocol

Before the experiment an initial test was performed to see if the loadcell could capture the maximum peak forces generated by the impact. The spring was compressed over a range of distances ranging from 10 mm to 30 mm with incremental steps of 5 mm in between. The spring was then released, generating an impact with a blunt tip at the distal end striking the loadcell platform without the polyurethane foam block. These same steps were repeated with the polyurethane foam block. After confirmation that no peak force was outside the bounds of the loadcell with a maximum load of 150 kg, the main tests could be initiated.

Different impacts for each working head were performed, by compressing the spring over a set distance, in a range of 10 mm to 30 mm with 5 mm incremental steps, starting at the smallest compression distance and then working up to larger distances with steps of 5 mm. After 5 strikes of the working head on the polyurethane foam, the sample was examined to see if any relevant hole, further penetration of the working head than just the tip, has been made. If no relevant hole appeared, five more strikes were performed to validate if this working head, with its current impact magnitude was too small to allow for drilling into the polyurethane foam, by seeing if the hole would become deeper after the additional 5 strikes. If this was not the case, the working head was registered at not being able to penetrate the hole with that particular impact magnitude. If after the additional 5 strikes, the working head had penetrated the material further than its tip, the 5 strikes were performed again at a new spot on the surface of the material. The penetration depth of the newly formed hole was then registered. These steps were performed for every working head, for every compression distance of the spring, in the chosen range.

For each working head with a certain compression distance, the test was performed 3 times, in order to, provide a more accurate penetration distance by taking the average of the three. If a penetration depth of 12 mm with 5 strikes was reached by a certain working head, higher magnitude impacts were not further performed for that working head, as such high penetration rates would not be relevant in real life surgery, because they would lack control if a surgeon were to penetrate the cancellous bone with such a fast rate.

3.2.5. Data analysis

For each test, the penetration depth after 5 strikes was registered in an excel table. The depth of the hole

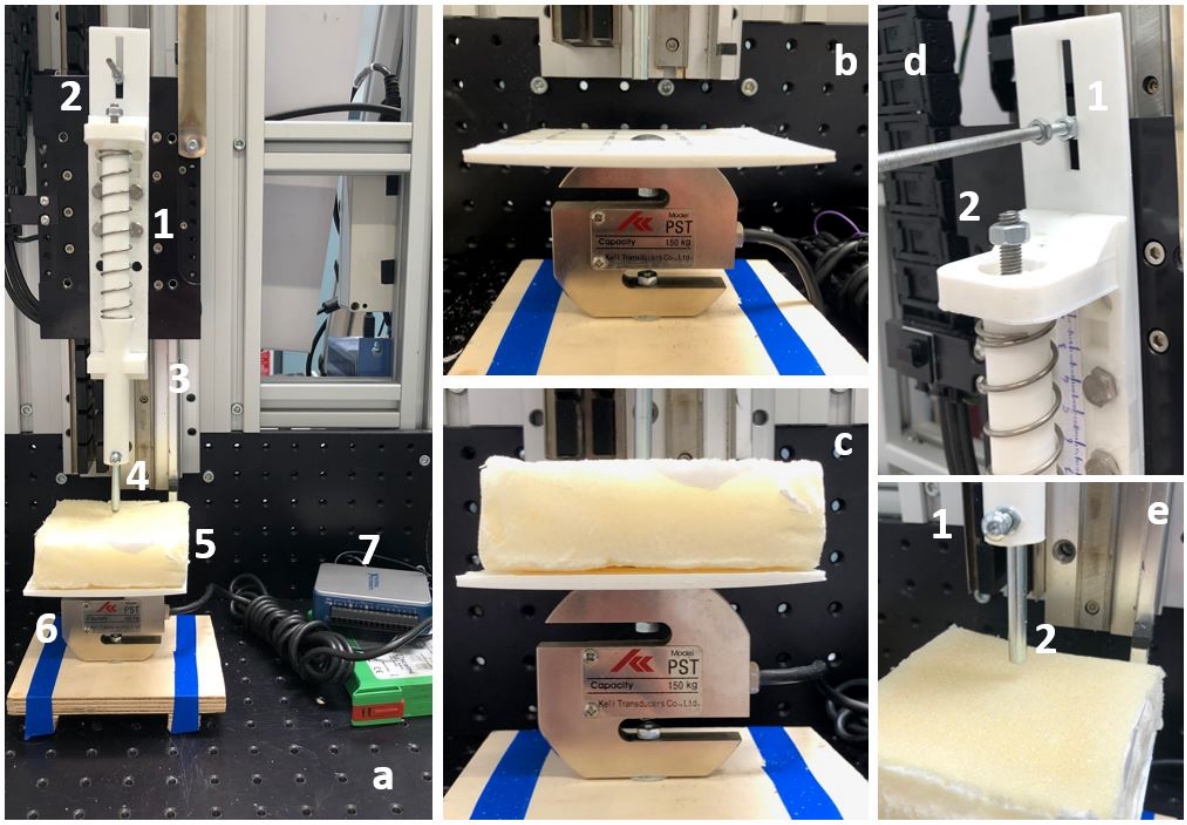

Figure 3.3: Experimental test setup used to analyse different forms of impact on a polyurethane foam block with a1) the linear slider, containing the compression spring that will generate the impact when the linear slider is pulled up and released, mounted to a linear stage, a2) the stop, a3) the linear stage used to translate the linear slider up and down, a4) the distal end of the linear slider, where the working head is fixed, a5) a block of polyurethane foam (100 mm x 100 mm x 30 mm), a6) the loadcell, a7) data analysis and acquisition equipment connected to the loadcell, b) the loadcell with a platform attached to it, c) the loadcell with a polyurethane foam block resting on the platform, d1) the stop, which can alter in position in order to provide the right pullback distance of the compression spring, d2) the handle which allows for manual pullback of the linear slider, compressing the spring, e1) the Allen screw that fixates the working heads onto the linear slider, e2) a working head, that will strike the target tissue below.

was measured with the help of a calliper with an accuracy of 0.1 mm. For each test the mean penetration depth was taken and from that, the average penetration rate, millimetre per strike, was calculated. The data of the output of the loadcell, captured with the help of LabVIEW, was processed with MATLAB R2020a, to generate force over time graphs. These force over time graphs were used to find the impulse generated for every single impact of the working head on the target tissue.

3.3. Results: Repeated impact

In this experiment, impact through striking a block of polyurethane foam with different working heads was tested. Figure 3.4 shows for different compression distances of the spring, together with different working head variations, the corresponding penetration rate that was achieved. Every working head test of 5 strikes was performed 3 times to minimize the chance of outliers. All working head impact tests were first performed at 10 mm. From there, with steps of 5 mm, the compression distance of the spring was increased. Would a working head after the initial 5 strikes not show relevant penetration depth, were only part of the tip would have penetrated the target tissue, as seen in Figure 3.5, 5 more strikes would be performed. If after those final strikes, still no increase in depth was seen, the working head with that spring compression distance, would be registered as not enough impact with current spring compression. If the working head showed that after 5 strikes, a penetration depth of 12 mm (penetration rate of 2.4 mm per strike) or more was reached, no further tests with increased compression distance of the spring, were performed for that diameter working head. This was done, as having such a large penetration rate would not be beneficial during actual penetration in the vertebra, were delicacy and control is required in such a vital structure.

Taking the previous aspects into account, Figure 3.4 shows 6 different working head diameter and compression distance variations. For the working heads having a diameter of 6 mm and the spring compressed

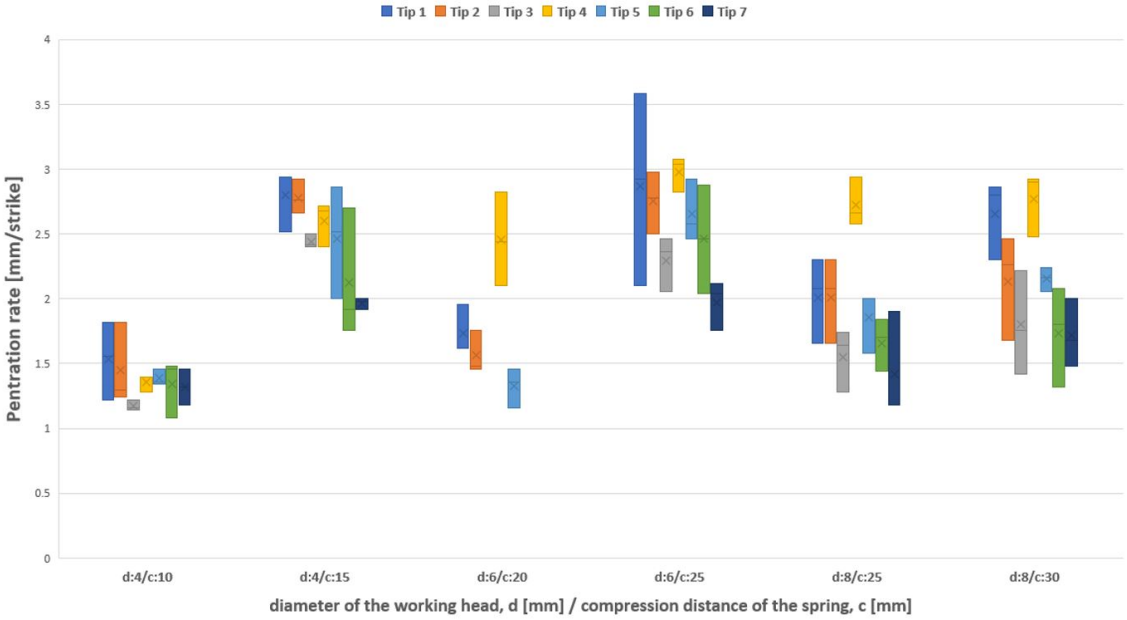

Figure 3.4: Standard deviation of penetration rate [mm/strike] of tip variations at different spring compression distances, with the cross being the mean and the horizontal line being the median, found in the coloured bars. Figure 3.2 presents the tip variation numbering.

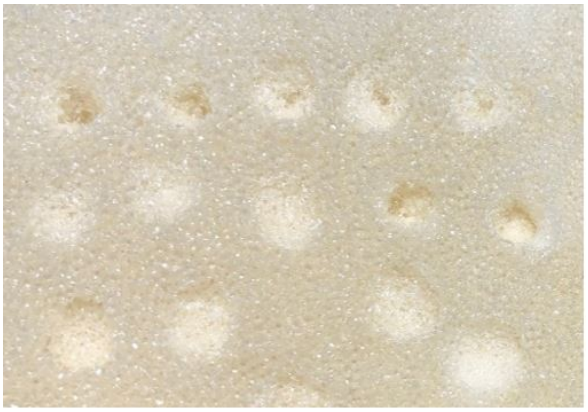

Figure 3.5: Indentation of the working heads, without further penetration into the polyurethane foam block.

to 20 mm, tip variation 3, 6 and 7 were excluded as they did not show relevant penetration depth. All working head diameter variations showed relevant penetration depth at an initial spring compression and exceeded the maximum relevant penetration depth after just an increase of 5 mm from the initial spring compression. For this reason, the graph presents six different working head and spring compression distance variations.

The impulse, the working heads generated on the target tissue, was measured as well with the loadcell. The loadcell data was analysed with MATLAB. With Equation 3.4, the measured mean impulse with standard deviation was found. This impulse is shown and compared with the theoretical impulse, that those same tip variations with the same compression distances of the spring would give, in Table 3.1. The table also shows the impulse that was measured when no target tissue was present, where the working head hit a metal screw attached to the loadcell directly. Figure 3.6 presents a comparison between the two variations of measured impulse, one with the target tissue and the other without.

3.4. Discussion: Repeated impact

3.4.1. Main findings

The feasibility of the penetration by repeated impact on polyurethane foam has been proven by this ex-

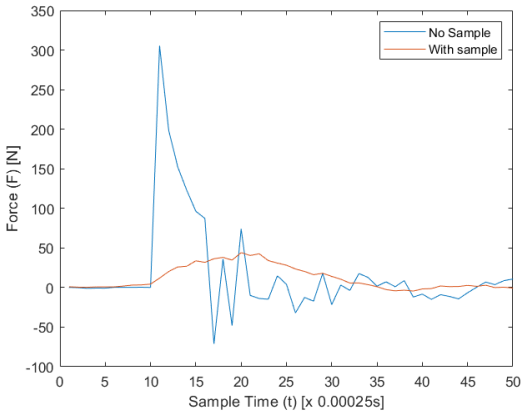

Figure 3.6: Comparison of the impulse of tip variation 7 with a diameter of 6 mm, striking loadcell with the target tissue (orange) and without the target tissue (blue). Figure 3.2 presents the tip variation numbering.

2*	Impulse at different compression lengths [Ns]									
	Theoretical					Measured				
Tip diamter [mm]	**10**	**15**	**20**	**25**	**30**	**10**	**15**	**20**	**25**	**30**
4 mm	0.0707	0.1015	0.1317	0.1615	0.1910	0.087 ± 0.0105	0.08955 ± 0.145			
6 mm	0.077	0.1102	0.1428	0.1749	0.2067			0.09465 ± 0.0247	0.1324 ± 0.0247	
6 mm*	0.077	0.1102	0.1428	0.1749	0.2067	0.0671 ± 0.011	0.0967 ± 0.020	0.1417 ± 0.020	0.1739 ± 0.034	0.2136 ± 0.014
8 mm	0.899	0.1281	0.1654	0.2023	0.2387				01735 ± 0.0311	0.1948 ± 0.0076

Table 3.1: Overview of experimental results for the theoretical impulse and the impulse measured by the loadcell for the different tests. The values are indicated as mean ± standard deviation (n=7). * impulse values for the 6 mm diameter working head striking the loadcell without the polyurethane foam block sample.

periment. It is possible to penetrate a block of polyurethane foam, representing cancellous bone, with all the different working head variations. The accuracy of the penetration rate, however, has shown to have a rather large range, as can be seen in Figure 3.4. This is most likely due to the inhomogeneity of the polyurethane foam, causing different penetration depths after each strike. This same figure also shows that, just like in the working head compression experiment (Appendix B), that Tip 1 and 4 perform the best. For each diameter and compression distance of the spring, they have the largest penetration rate, with Tip 4 performing slightly better than Tip 1. It can also be noted that for the 4 mm tip variations, not a lot of difference in the penetration rate between the seven variations was observed. This is probably caused by the diameter of the working head being very slim by itself, resembling almost a point already.

The phenomena of the material accumulating in front of the more blunt tips, as was observed in the working head compression test (Appendix B), was found in this experiment as well. Figure 3.7 shows holes formed by the same working head diameter. The larger holes are formed by the more blunt tip variations, and the smaller ones are formed by the pointier. It can be observed that the blunt tip variation pushes the material in front of it, whilst the pointier variations pushes it to the side, hence, the slightly smaller hole. This all proves that having a sharper tip, is more beneficial when using an impact method to penetrate a material like polyurethane foam, and so also, most likely be more efficient when penetrating actual cancellous bone.

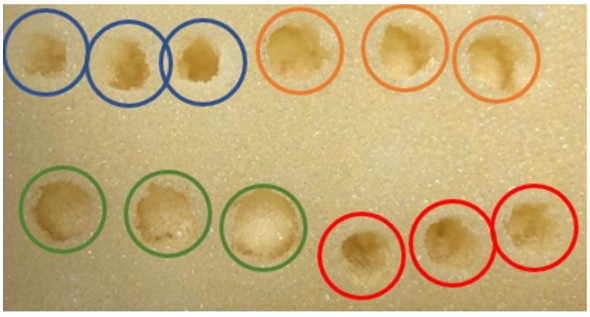

Figure 3.7: Block of polyurethane foam with penetration holes generated by different tip variations, with a 6 mm diameter, striking the material, with blue) tip variation 1, orange) tip variation 6, green) tip variation 7, and red) tip variation 4. Figure 3.2 presents the tip variation numbering.

When examining the impulses (Table 3.1), it is clear that the measured impulses are lower than the theoretical impulses. This is logical, as the system, whilst performing the impact, experiences multiple losses in the form of friction between moving parts and air, possible heat losses, and losses caused by damping of the impact by the material. This can be observed as in Table 3.1, the impulse measured while striking the loadcell without the target tissue showed a higher output than striking the loadcell with the target tissue on it. The measured values for the output impulses measured without a sample gave an almost identical value to the theoretical impulses. For the measurements of the impulse with the sample, the values were slightly lower than the theoretical ones. This is most likely caused by the damping effect of the polyurethane foam, which is not present at the measurement without the sample.

The hypothesis mentioned earlier in Section 3.1, stating that performing the repeated impact method with single manual impacts, with multiple seconds between each strike, would have no consequence on the end results found, then if these same impacts were performed at a rate of 10 Hz, has been proven true. Figure 3.6, shows that after a single strike, the block of polyurethane foam only takes around 0.0125 seconds to return to its rest state, as can be observed by the force over time curve returning to a stable line around zero Newton after the mentioned time period. This means that scaling the frequency of impacts to a frequency of 10 Hz will have no effect on the penetration rate of the working heads. This means that higher frequency impacts can be tested by performing single strikes over a longer period, which makes experimentation with this method have less complications, which could possibly result in better data.

3.4.2. Limitations

Due to the inhomogeneity of the polyurethane foam, less accurate measurements were found, as there was a large range of penetration rates for each working head variation. This is, however, a problem that will also be experienced when eventually, real human can-

cellous bone is utilized. The inhomogeneity is greater in human cancellous bone than that of polyurethane foam. Real bone has a unique internal viscoelastic and architecture properties, whilst polyurethane foam is more consistent in shape, size and density [58]. Furthermore, the polyurethane foam used for these experiments had a lower compressive strength than that of real cancellous bone, as mentioned in Appendix A. However, due to its similar mechanical behaviour and the enormous amounts of samples needed to perform all the tests, the current polyurethane foam was a good alternative. It allowed for easy sample fabrication and was cheap to use at large scale. It must be noted that, if this method will be utilized on actual cancellous bone, higher impulses must be performed in order to penetrate the cancellous bone at the same rate.

3.5. Final method choice

For further research, continuation of the repeated impact method has been chosen. Reason for this is that, with relative small input forces, penetration through target tissue can be performed, as has been proven by the impact experiment. For the continuation of this thesis, Tip 4 will be utilized. It has proven, in both the impact experiment and the working head compression experiment (Appendix B), to be the most efficient and effective working head tip. It had the relative best penetration rate, compared to other tip variations, for every tip diameter and compression distance of the spring. The additional perk of pushing the resected material to the side, instead of accumulating it in front of the tip adds to the effectiveness of this tip.

Tip 1, performed almost as well, but the choice was made for Tip 4. This was because having a sharp tip might lead to detrimental complications when working in the vertebra. If by accident the spinal column would be pierced by the sharp tip, which characterizes Tip 1, during operation, Tip 1 might cause more harm to the patient then Tip 4, as Tip 4 has a more rounded tip, which might be less damaging if it comes in contact with nerves. Sharper objects could cause rupture of the nerves, whereas, a more blunt object could avoid that, as the area pressure of blunt object is smaller than that of sharper objects.

As the polyurethane foam used in this experiment had a lower compressive strength than cancellous bone in the vertebra, as earlier mentioned, a final impact test will be performed on a new sample of polyurethane foam, in the range of actual cancellous bone. The results of these tests will decide the parameters that will be used for designing the actual instrument, that can penetrate human cancellous bone with repeated impact. These results are found in Appendix C.

4

Instrument design

4.1. Design direction

In order to establish a new method of steerable drilling in the vertebra, a proof of principle test must be performed. This will validate if the method actually works and if it shows promise of actual usefulness for the use of a future surgical instrument. As the previous experiment has verified, Tip 4 which has the conical shape with a blunt tip (Figure 3.2), performed the best. This tip variation will be utilized as tip for the working head. It required the least amount of energy input to penetrate the target tissue. Furthermore, accumulation of material in front of the tip was kept at a minimum.

To allow for an instrument that can perform steerable drilling, a bendable transmission part must be utilized. This bendable part will connect the part that will generate the impulse, to the part that will convert the impulse to an impact on the target tissue. In the study of Sakes *et al* [52], a bendable tube with liquid is utilized to transmit a generated impulse from one end, as a hydraulic pressure wave, to the other end were it translates into an impact used for breaking highly calcified occlusions in blood vessels. It is believed such a method can be utilized, as it portraits the same capabilities that are needed for this proof of principle test as well, with proven positive results [52]. These results, however, were achieved by using a thinner tube with a lower magnitude hydraulic pressure wave, than is needed for the proof of principle test being researched in this thesis. Therefore, it is still unknown if the method will work for larger impact situations. A detailed explanation of the theoretical principles of this method is presented in Appendix D.

The parameters of the proof of principle will conform to the requirements of performing spinal drilling in the thoracic vertebra. The thoracic vertebra has been chosen as it requires a much lower margin of error than the lumbar spine, due to the pedicle shape. The lumbar spine has pedicles that are thicker and the trajectories that need to be drilled tend to not skirt important neural or vascular structures. Therefore, drilling through the lumbar vertebrae is less complicated [59]. The thoracic spine, on the other hand, has a smaller error margin, as errant screws can more easily injure the spinal cord or other close by vital structures, which are more present around the thoracic spine [59]. Next to this, the thoracic vertebrae tends to be more anatomically varied, more variation in shape, than their lumbar counterparts [59]. For these reasons, it is believed that having a steerable drill is more beneficial in the thoracic vertebrae than in the lumbar vertebrae. Therefore, the focus of this proof of principle will be on the thoracic vertebrae.

The average pedicle screw size in the thoracic vertebrae is 4.0 mm to 4.5 mm [57]. As testing was already performed with the 4 mm diameter working head, continuation of the tests will be performed with that working head diameter. This will allow for a 4 mm diameter wide hole to be formed. The probable point of entry into the vertebra will be located at the posterior entry point of the pedicle, as seen in Figure 4.1. In the paper of Roop *et al* [60], it is found that the dis-

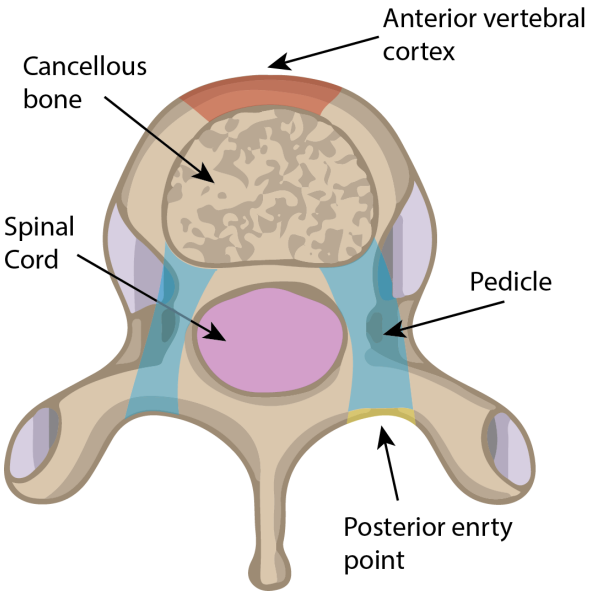

Figure 4.1: Representation of a thoracic vertebra showing, in yellow) the posterior entry point of the pedicle, in red) the anterior vertebral cortex, in purple) the spinal cord, in blue) the pedicles, and in brown) the cancellous bone of the vertebra.

tance from that point to the anterior vertebral cortex for the largest thoracic vertebra, T12, is 22 mm. Therefore, a length of 40 mm is chosen for the bendable part that will enter the target tissue to perform the drilling. This distance is believed to allow for sufficient penetration depth capabilities taking into account that curved holes will be formed.

The goal of this experiment will be to create a proof-of-principle in the form of a prototype instrument that will validate that it is possible to penetrate a cancellous bone substitute through repeated impact with a transmission part that can bend. This will prove whether it is possible to utilize this method for a future instrument that can penetrate the cancellous bone of the thoracic vertebra through repeated impact forming curved holes. Future research can then be performed on adding additional steering mechanisms, automated higher frequency impulse generation and a guidance system. Combining everything will result into a new way of performing steerable drilling in the thoracic vertebra to allow for new state-of-the-art curved spinal screws, that could enable a higher holding strength. Next to that, it will allow for a safer way to penetrate the vertebra, as the penetration direction can be altered during operation, which is much harder with a drill that can only penetrate in a straight path.

The general form of the instrument will consist of three parts, which combined will perform the required function, as seen in Figure 4.2. The first, is the transmitting part of the drill, which the pressure wave (impulse) will travel through to activate the working head. The second, consists of the working head of the drill, which is the part that gets activated by the pressure wave in order to drill the bone. Lastly, is the impulse generator. This part will generate the impulse input, the impact, which will be translated through the transmission medium to the working head.

4.2. Design requirements

Transmitting part

The requirements consist of the three main parts, which correspond to the marked sections in Figure 4.2. The transmitting part allows a liquid medium to be sustained in it. As explained in the previous section, it will have the shape of a tube. The material of this part must have certain characteristics in order to allow for a hydraulic pressure wave to travel through it. For this to happen the tube must be able to:

1. **Not expand:** If it were to expand, it might damage the surrounding area, by building up pressure in the radial direction. This might alter the diameter of the hole that is being generated, by the tube expanding outward compressing the cancellous bone, which will cause problems with screw placement. Next tot this, expanding the tube in the radial direction will decrease the output delivered to the working head, as energy gets lost by expanding the tube. This will make the process less efficient.

2. **Transition the impulse through the tube with minimal friction:** Friction will result into a decrease of the impulse, as stated by Sakes *et al* [52]. More energy is needed to reach the desired output. Friction can be caused by the inner wall of the tube having a rough surface which slows the flow of liquid near the surface of the tube, taking energy away from the hydraulic pressure wave.

3. **Be bendable:** The tube must present bending capabilities in both directions on a xy-plane, without requiring much force to bend the part. This is required to make the instrument have multiple options in steering, when drilling a curved hole in the target tissue. A curve of 90 degrees over the entire tube would be sufficient in proving operation under bended conditions.

4. **Have a maximum diameter of 4 mm:** Spinal fusion surgery allows for a certain range of diameter of the tube to perform the surgery in the previous section it has been decided that the hole that will be drilled will be 4 mm. For this reason, a tube larger than 4 mm will not be effective.

5. **Have a minimum length of 40 mm:** A certain minimum depth is needed to allow for a successful anchoring of a pedicle screw. In the previous section, it has been decided that the instrument must allow for a minimum depth of 40 mm to be reached inside the vertebra to allow for a sufficient depth for a pedicle screw to be placed.

6. **Have a minimum inner diameter between 2 mm and 3 mm:** To allow the hydraulic pressure wave, with sufficient impulse, to travel through the tube, a certain inner diameter is needed to transmit the impulse most efficiently. Due to the no-slip boundary condition, friction formed between the fluid and the solid tube wall causes the fluid to come to rest at the boundary. This is because all surfaces are rough when examining them on a microscopic level [61]. This decreases efficiency in translating the impulse through the tube. Sakes *et al* [52] finds that this effect is especially large in a smaller diameter tube were the boundary layer between the fluid and the tube is relatively larger than if a larger inner diameter was used. Next to this, a thinner outer wall will allow for better bendability of the tube, which will enhance the steerability of the instrument.

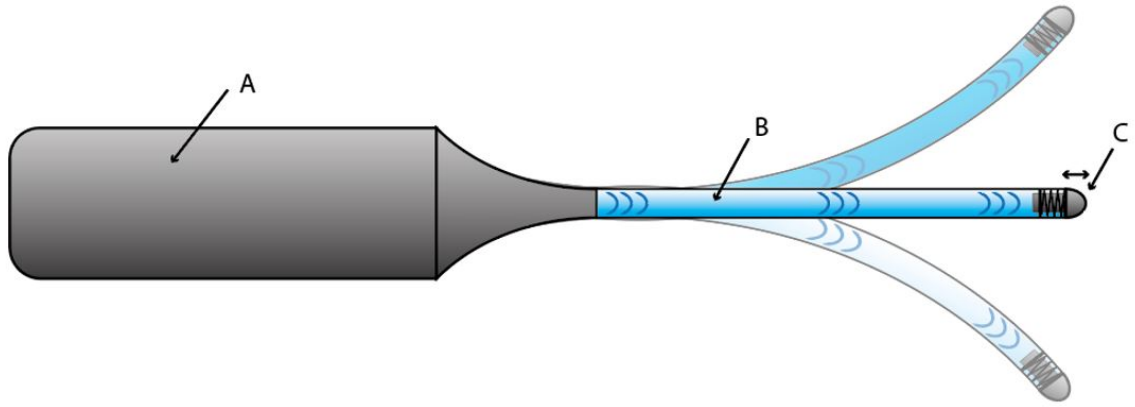

Figure 4.2: General solution direction representation of the proof of principle design with A) the impulse generation part, B) the bendable pressure wave transmission part, and C) the output impact working head part.

A larger inner diameter allows for additional sensors and a steering mechanism to be inserted through the tube as well in possible future versions of the instrument. It must, however, be noted that having a too large inner diameter will decrease the compression strength of the tube, which might cause compression at the end of the tube. This can be caused by the working head striking the target tissue, or buckling of the tube caused by the operator applying pressure on the instrument. Both points are explained further in the following points. As there are a lot of factors that come in to play for deciding which inner diameter would be most beneficial, a choice is made to have the inner diameter between 2 mm to 3 mm, as a larger inner diameter is most likely better than a smaller one.

7. **Have resistance to buckling:** The tube must not buckle in any way. This might be caused by recoil from the impulse, or pressure caused by the operator pushing the instrument. For this reason a certain stiffness is required. Buckling will most likely only occur outside the hole that will be drilled, as inside, the tube will not buckle as it is in contact with the inner wall of the hole, formed in the vertebra, on all sides.
8. **Resistance to compression:** Striking the target tissue with the required impulse causes a lot of recoil. Therefore, the tube must have high compression strength. If it does not, the working head would just push of the target tissue and compress the tube instead of penetrating the target tissue. Less compression strength will therefore dampen the impact the working head will produce.
9. **Allow integration of the working head:** A working head with its mechanics must be able to be integrated with the tube.
10. **Have minimal fluid leakage:** Leaking fluid might cause complications if the fluid that will be utilized for the instrument causes harmful effects on the human tissue. Next to that, leaking fluid will cause malfunction of the device, as the impulse might not be able to be transmitted efficiently anymore through the tube. Therefore a constant fluid pressure and volume must be sustained whilst leaking harmless fluid or no fluid must be leaked at all when utilizing the instrument.

Working head

This part will have the end effector of the drill which will be able to drill the bone with the use of the impulses generated by the hydraulic pressure waves. The working head must be able to:

1. **Be activated by the hydraulic pressure wave:** The pressure wave, traveling through the transmitting part, must activate the working head so it can perform its output of penetrating the target tissue through repeated impact.
2. **Be hard, durable, enough to not break when it is drilling the target tissue:** The instrument must be utilized at least a few hundred times to undergo thorough testing of its capabilities. For this reason the working head must be durable.
3. **Create only the desired path through the bone and keep damage to the surrounding area at a minimum:** The working head must not cause any other damage to the surrounding tissue, while penetrating the target tissue. If it does, it will have negative consequences on the recovery of the patient or the screw placement, after a hole has been formed.

4. **Drill a hole with a diameter of 4 mm:** The working head must be capable of drilling a hole with a diameter of 4 mm, as stated earlier. For the desired operation a hole of 4 mm is required.

5. **Have a travel distance between 1 mm to 2 mm:** The working head, when receiving the impulse must perform a travel distance between 1 mm to 2 mm. This distance is chosen to allow for visible confirmation that the working head receives the impulse and performs the impact. Next to this, in the paper by Sakes *et al* [52] it is found that a larger travel distance results into higher peak forces. This might be beneficial in order to penetrate the target tissue with more efficiency. This travel distance is chosen for the proof of principle application, but in reality, the method will require the operator to apply a certain force on the instrument. This causes the working head to be always in contact with the end of the hole, resulting in a travel distance of 0 mm.

Impulse generator

This part must generate the required impulse that will be transmitted through the tube towards the working head to activate it and allow for the required impulses to be applied on the target tissue. To achieve this, the impulse generator part must be able to:

1. **Generate an impulse of at least 0.2 Ns:** This part must be able to generate an impulse of at least 0.198 ± 0.022 in order to achieve a penetration rate of almost 1 mm per strike, as was found in Appendix C. This penetration rate has been chosen to be the benchmark rate. If the instrument can achieve this high penetration rate, it will prove its viability as a method for drilling into the vertebra. In reality a much lower penetration rate will be utilized as the previous mentioned rate will be too fast for a controlled and delicate operation on the vertebra.

2. **Must have a variable impulse input:** The input impulse must be variable, in order to allow for different testing to see what is most efficient for drilling.

4.3. Mechanism analysis

Transmitting part

The transmitting part or tube will be used to transport the impulse generated in the impulse generator in the handpiece to the working head in the form of a hydraulic pressure wave. This must be done as efficiently as possible, as losing to much impulse might make the device not operatable. To select the right tube, with the capabilities of translating the required impulse through it, whilst allowing for bendability and without causing complications, a good combination of strength and bendability must be selected.

The inside and outside of the tube must be smooth to minimize friction for both the impulse traveling through the tube and the tube traveling through the bone. The tube must also be strong enough to withstand the pushback from the working head striking the target tissue. The tube must not compress, as that would dampen the impact, which might cause failure for the working head to penetrate the target tissue. Next to this, the tube must not plastically deform. This will generate unevenness in the tube which might decrease the efficiency of the impulse, due to an increase in friction for the traveling impulse. The material the tube consists of must not be harmful for the human body, although this point has lower importance, as the instrument, that will be designed, is just a proof-of-principle for a possible later actual device and will not be used on real human tissue.

To select a strong enough tube, Barlow's formula can be utilized (Equation 4.1). It is used to determine the bursting pressure of the tube, P [MPa].

$$P = \frac{2 * S * T}{O.D.} \tag{4.1}$$

With S being the ultimate tensile strength [MPa], T, the tube wall thickness [m], and O.D., the outer diameter of the tube [m]. When performing the impact drilling, the part of the tube that is outside the formed hole is prone to buckling as the operator must apply a certain pressure on the instrument. This must be done, otherwise the instrument will push off from the target tissue every time an impact is formed. This is disadvantageous as no drilling can be performed in this case. Therefore, initial pressure applied by the operator must be applied. To combat the buckling of the tube, a telescope or sleeve, that fits exactly around the tube with high strength and bending resistance, can be applied. This sleeve reaches from the handpiece all the way to the entry point of the formed hole. This sleeve will retract the further the tube enters into the formed hole. Through this application the tube can be retained from buckling and therefore minimize impulse loss.

Choosing a suitable tube will rely on a combination of the previous mentioned aspects. For this proof-of-principle no other possibilities of steerable parts that could translate an impulse through its system is regarded, as this is the method of impulse translation that this experiment is trying to prove. All tube possibilities will have the same general shape, a circular form with a certain inner and outer diameter, and a certain length. Variance in selecting the right impulse translating part will only be done through choosing between different materials and inner diameter sizes.

Working head
The working head end will resemble a kind of conical shape with a blunt tip. The maximum diameter of the working head will be 4 mm. The working head will translate the impulse received through the tube to an impact on the target tissue. Next to this, it must be strong enough to withstand the repeated impacts it will receive, both from the liquid impulse that activates it and the impact with the target tissue. The working head will travel a certain distance when it is activated before it strikes its target. After this, the working head must return to its initial position rapidly, in order for the next impulse that will activate it. Besides this, it must be tightly integrated into the end of the tube to minimize leakage. Every part must have an exact fitting and refrain from plastic deformation. Plastic deformation causes parts to jam or rub against each other, which will drastically decrease the efficiency of the device.

Besides the tip shape of the working head, which has already been explained, there are a few options the design of the working head can have, as seen in Figure 4.3. Figure 4.3A shows a mechanism that uses a compression spring. When the working head gets activated, the spring gets compressed. After the initial impulse has diminished, the spring will push the working head back to its initial position. Figure 4.3B shows the same concept but then with the use of magnets. After activation of the working head, the working head will be pushed back to its initial position by the two magnetic rings due to the same polar sides facing each other. Figure 4.3C shows the last possibility. This option uses vacuum or pressure difference to return the working head to its initial state after the impulse has passed. The idea is that after the initial impulse has receded the inside volume of the tube is increased resulting in the outside pressure being higher than the inside pressure of the tube. This causes the working head to be pushed back into the tube to return the inside of the tube to its initial volume.

The challenges of fabricating the working head will lie in the exact dimensions of every part. Every part has to fit exactly in order for no jamming to occur. This will require very precise fabrication. Especially for the last method which uses the pressure difference. The whole system must be airtight in order for it to work, otherwise air will be sucked in through gaps between the parts, due to the pressure difference inside and outside the tube, with a result that the working head will not return to its initial position. However, it does have the smallest working head length. This is beneficial in the case that the tube is curved. Having a smaller length allows for a larger curve, which will improve the eventual steerability application for a device that might utilize this method. This is because when the tube is curved the working head will push against the inside of the tube as the working head does not curve with the tube. For a larger length of the working head, this will happen more quickly when the tube curves. That is why having a as small as possible working head length is the most beneficial when applying this method to curved drilling.

It is believed the first option using the compression springs will have the largest length of the working head. This will be a downside to this option. However, this option is, most likely, the easiest to fabricate, as it can be fabricated with a little less precision and the parts are easily obtained. For the second option this might be a problem, as obtaining ring magnets having the exact size that is required for the fabrication is quite challenging. Next to this, a non-magnetic material must be used as working head. Otherwise, friction can occur between the working head and the rings which will decrease the efficiency of the device. Besides this, using magnetic devices in the body can call for complications as the devices can for instance interfere with a pacemaker, which can have negative consequences. It is believed the second option will have a length that is in between the first and the third option.

Impulse generator
The impulse generator will produce the required impulse that will be translated through the tube and will activate the working head to perform the impact. To find the right amount of impact needed to efficiently penetrate the target tissue, the impulse generator must have an option to alter the impulse magnitude. The impulse generator must connect with an exact fit to the tube, to minimize leakage of the system. There are multiple options for the mechanism that can be used in the impulse generation part. The first option utilizes a solenoid. This device can generate a highspeed impulse with a variable impulse magnitude. This solenoid could for instance strike a piston, pushing it forward, that is partly in the tube which will generate the impulse that will travel through the liquid of the tube. It must be noted that a return mechanism of this piston must also be designed. The second option uses a compression spring. This spring can be compressed at various distances to allow for a variable impulse. This method resembles the instrument used for testing the different kind of tip variances described in the previous chapter, Chapter 3. The third option works by using a pressure difference. By enlarging the volume in an airtight cylinder, pressure will decrease. If this enlarging mechanism is than released, it will shoot back to its original volume due to pressure differences outside and inside the mechanism. This can be used to create some kind of striking mechanism, that can generate the required impulse. The fourth option uses electrohydraulic shockwave to produce the

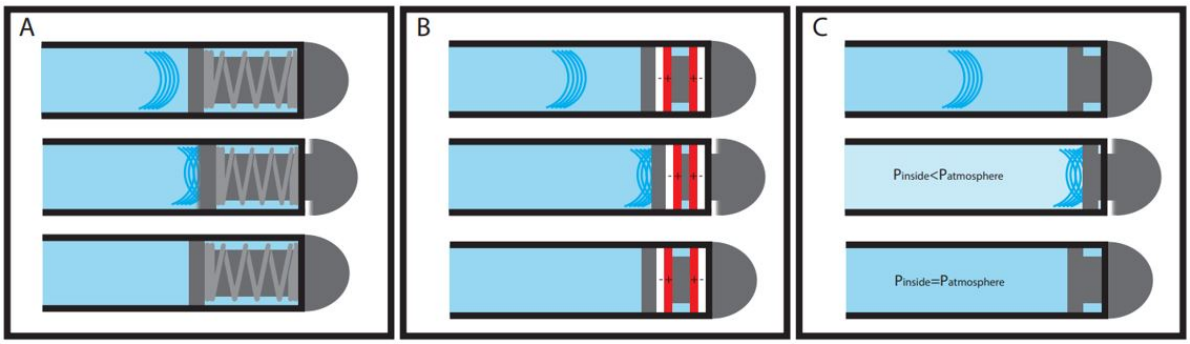

Figure 4.3: Three different options for the initial position return mechanism in three different stages. The first stage shows an incoming impulse, stage two shows the moment of impact of the impulse and the working head shooting forward (to the left of the figure), and the last stage shows return to the initial position with the impulse having receded. The different options show A) using a compression spring, B) using same polar side magnets facing each other, and C) using pressure difference to return the working head to its initial position.

impulse. This method has been analysed in Section 2.4.4. It produces a hydraulic shockwave with the use of a spark generator. This shockwave will become the impulse that will travel through the tube to activate the working head. The last option uses compressed gas. Compressed gas can be released in a chamber, which causes a rapid expansion of that chamber. This can activate, for instance, the earlier mentioned piston in the tube to generate an impulse.

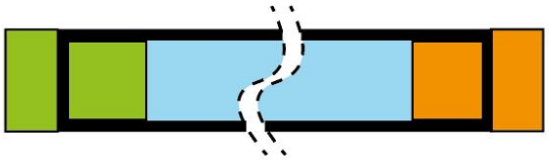

Figure 4.4: Representation of the tube with on the left the impulse input (green) and on the right the impulse output (orange). The impulse input will receive the impulse from the impulse generator and translate it to an impulse that will be transmitted through the tube, in the form of a hydraulic pressure wave, towards the impulse output, which will translate the impulse to an impact on the target tissue.

4.4. Mechanism selection

Transmitting part

The choice for the impulse translation is by using a circular tube. This tube will have a burst resistance of at least 5 bar to allow for the right impulse to be transmitted through the tube without damaging or deforming it. This minimum burst pressure is selected, because of the earlier experiments done that analysed the impact of different magnitude impulses on a piece of cancellous bone replica. The pressure such impacts, as seen in Appendix C, will generate are far below the minimum burst pressure chosen. Next to this, an inner diameter of 2.5 mm is desired, as it is believed such an inner diameter will allow for a sufficient size for an impulse input mechanism at the proximal end of the tube. Besides this, it will also allow for an impulse output mechanism to be installed at the distal end of the tube, which would more easily break if it were smaller due to the high impulse magnitude it receives. These impulse input and output mechanisms translate the impulse generated by the impulse generator to the tube at the proximal end, which transmits the impulse to the distal end of the tube through a hydraulic pressure wave, were the impulse translates to an impact formed by the working head on the target tissue, as seen in Figure 4.4. Having a 2.5 mm inner diameter will allow for enough size to fabricate these mechanisms so they work properly and do not break after a couple of tests. The tube must also allow for at least a 90 degrees bend over the entire length of the tube. Such a bend will be sufficient in proving operation of the instrument under bended conditions. The outer diameter will remain 4.0 mm, as has been stated by the requirements.

Working head

For the working head, the compression spring mechanism has been chosen. This mechanism was chosen because it was the least complicated to fabricate and the parts needed were easily obtainable. For the magnetic working head option, the ring magnet sizes that were required were very hard to obtain. Next to this, the working head itself would bring extra complications with it, as it needed to be non-magnetic, yet extremely strong because of its small size. The vacuum option seemed difficult as well. This was because a relative large magnitude impulse would be used. Having a system that would seal of every possible gap, would most likely require a lot of force to remain together and not let any liquid or air escape out of the system. This will most likely increase friction in between the parts, which would decrease the efficiency of the device.

The compression spring method will work in a way that it will receive the impulse that is transmitted

through the tube. This impulse will contact the proximal part of the working head, which will fully capture the impulse. The working head will shoot forward through the tube, were the end of the working head, containing the tip, will make contact with the target tissue to deliver the impact. Through recoil and the compression spring the working head will be pushed back to its initial position, ready to receive a new input. The mechanism resembles Figure 3.1.

Impulse generator
For the impulse generator, again, a compression spring method has been selected. This method is selected as experience has already been obtained in this method through the previous impact experiment. It has proven to be a relatively simple and robust method for generating an impulse. Compared to the other methods, not much complications are used with this method which would increase the chance of failure during the experiments. Next to this, it allows for a variable impulse magnitude by altering the compression distance of the spring. Different springs can also be inserted, which allows for a whole range of impulses to be tested with relative ease compared to the other methods. The parts are also easily obtainable and relatively cheap. This is in contrast with the solenoid. Obtaining a solenoid which has the right parameters, impulse, size and frequency, has been found to be very expensive. However, in a future instrument, using a solenoid would be the better option. It can deliver high frequency high magnitude impulses, which eventually would be needed if this method will be utilized for an actual device used for drilling in the vertebra. Besides that, it removes the manual activation of the impulse and automates it. But, for a proof of principle, using such a solenoid would not be necessary.

The pressure difference method, again, seemed more complicated than the compression spring system. Parameters and experience with this method were also unknown, as no use was made of this method during this thesis. For this reason no continuation was done with this method. The same was the case with the electrohydraulic shockwave. Uncertainty of it actually working and finding the right parameters to generate the right impulse would be another study on its own, which timewise would not be beneficial for this thesis. However, it is still believed this method might show interesting results, as the spark generator could be inserted all the way at the distal end of the tube, removing the part were the shockwave has to travel through the tube, as has been hypothesized in Section 2.4.4. The compressed air method could be utilized, but performing a lot of different tests would require a lot of compressed air. This might not be extremely useful compared to the compression spring which does not require an additional exhaustible input. For these reasons continuation of the proof of principle design will be performed with the compression spring mechanism.

4.5. Final design

4.5.1. Operational steps

Figure 4.5 shows the 2D concept of the proof of principle device in four different states. This system contains an impulse generator, a tube for transmitting the generated impulse and a working head that will translate the impulse received through the liquid of the tube, to an impact that will strike the target tissue. State A represents the rest state of the instrument. By applying a pulling force on the handle mechanism on the left side of the figure, the compression spring can be compressed over a certain distance depending on the pullback distance of the operator. The distance will be measurable to allow for a variable magnitude input of the impulse that will be generated, as seen in State B.

State C showcases the state were the pullback mechanism is released by the operator, the middle beam, which is connected to the spring, will shoot back in the opposite direction, due to build up of the spring energy. This part will strike a piston which is partly inserted into the tube, indicated by State D. This piston will receive the impulse and shoot forward. As part of the piston is in the tube, it will push the liquid inside the tube forward (to the right side of the figure), forming a hydraulic pressure wave. This hydraulic pressure wave will travel through the tube till it reaches the proximal end of the working head at the distal end of the tube. The hydraulic pressure wave will form an impact with the working head. The working head will shoot forward as well (to the right side of the figure), till it strikes the target tissue, in order to break the tissue down.

After the impulse has travelled through the system, all parts will return to their initial position due to spring placement, pushing the parts back, till State A is once again achieved. Furthermore, the tube will be able to bend in all directions for at least 90 degrees. With this concept, the proof of principle could be achieved that will prove the possibility of using the method of hydraulic shockwaves, in order to drill through cancellous bone with the application of potential steerability. The 2D concept will be actualized into a 3D model, which will then be fabricated. The three segments of the concept will be discussed individually in the following sections.

4.5.2. Segment design

Transmitting part
For the design of the transmitting part a circular tube has been selected. This circular shape has been cho-

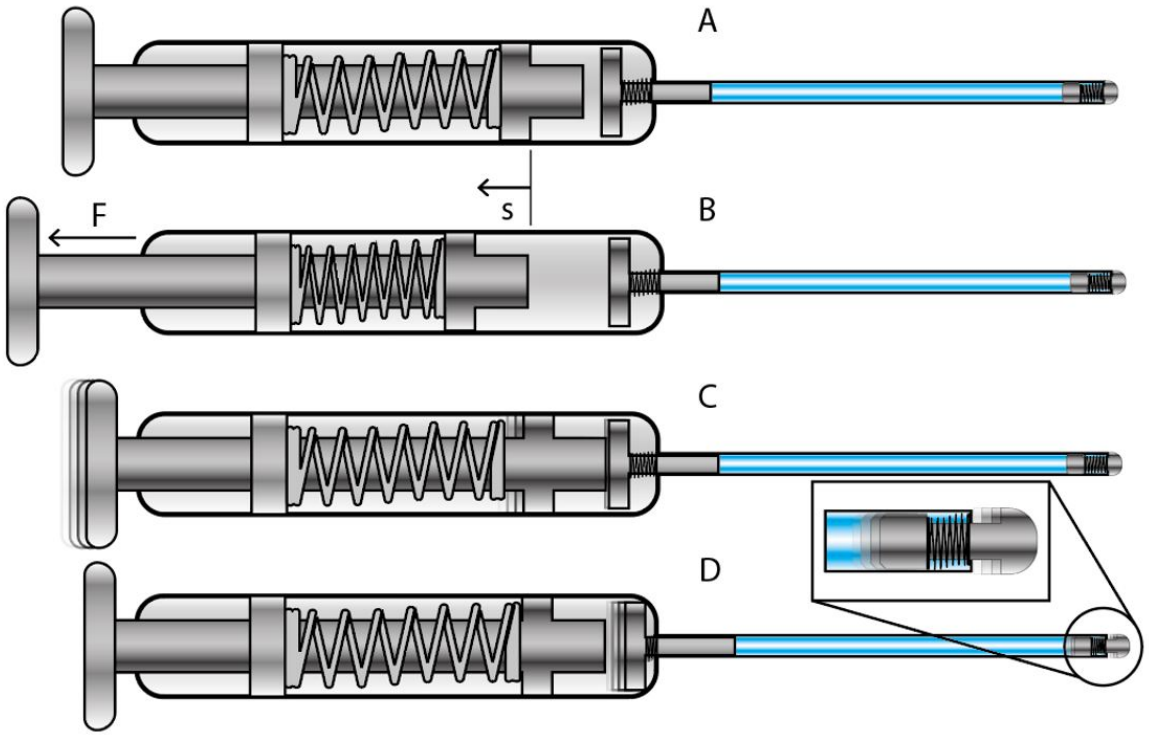

Figure 4.5: 2D concept of the proof of principle instrument, in four different states, used to test the method of steerable drilling with the use of repeated impact. (A) The initial position of the instrument. (B) Compressing the spring through pulling back the handle with a force, F, over a distance, s. This will allow for a variable magnitude of the impulse to be generated. The amount of distance the spring is compressed will determine the impulse the device will generate. (C) Release of the pullback mechanism will cause it to shoot forward, till contact occurs with the piston. This piston is located partly in the tube and can be activated by striking the piston head (most left part of the piston). (D) The piston is activated by the strike and shoots forward, pushing the liquid inside the tube. This forms a hydraulic pressure wave, which travels all the way through the tube towards the distal end of the tube activating the working head. The working head will receive the hydraulic pressure wave on the proximal end of the working head. This will cause the working head to shoot forward rapidly till it will strike the target tissue. After the impact is performed the device returns to its initial position represented by situation A.

sen, as it is the most efficient shape. This is because it has the lowest volume to surface area ratio, which is beneficial for translating a hydraulic pressure wave through the tube, as is found in Appendix D. The reason for this has to do with friction loss between the inner wall of the tube and the transmission liquid in the tube. Decreasing the friction loss, will increase the efficiency of the translation of the hydraulic pressure wave through the tube. Appendix D also shows that having a larger inner diameter is beneficial, because it increases the volume to surface area ratio of the tube. The 3D design and visualisation of the linear tube with a certain inner and outer diameter speaks rather for itself and does not require anymore thorough explanation. The fabrication and characteristics of the tube do require some explanation, and are found in the Section 4.5.3.

Working head

Figure 4.6 shows a 3D visualisation of the exploded view, and the side view of the initial position and activated position of the working head. With Part (a) being the piston, which will be fully inserted into the tube at the distal end of the tube. The segment with the larger diameter is the proximal side of the working head (seen on the left of Figure 4.6). This will receive the hydraulic pressure wave that is transmitted through the tube, shooting the entire working head forward in the distal direction. The impulse receiving part will have a diameter around -0.1 mm of the tube's inner diameter, in order to fully receive the impulse, whilst still move forward without too much friction. The smaller diameter part of the piston allows for placement of the compression spring, Part (b). The compression spring will fit exactly around the piston, with an outer diameter smaller than the inner diameter of the tube. This part will compress against the stop, Part (c), if the working head is activated. The stop is fixed at the distal end of the tube, enclosing the tube. The centre hole through the part allows for only the piston to slide through it. Part (d), is the tip of the working head. This part will strike the target tissue. It can be fixated to the distal end of the piston, Part (a), through a threaded section. The entire mech-

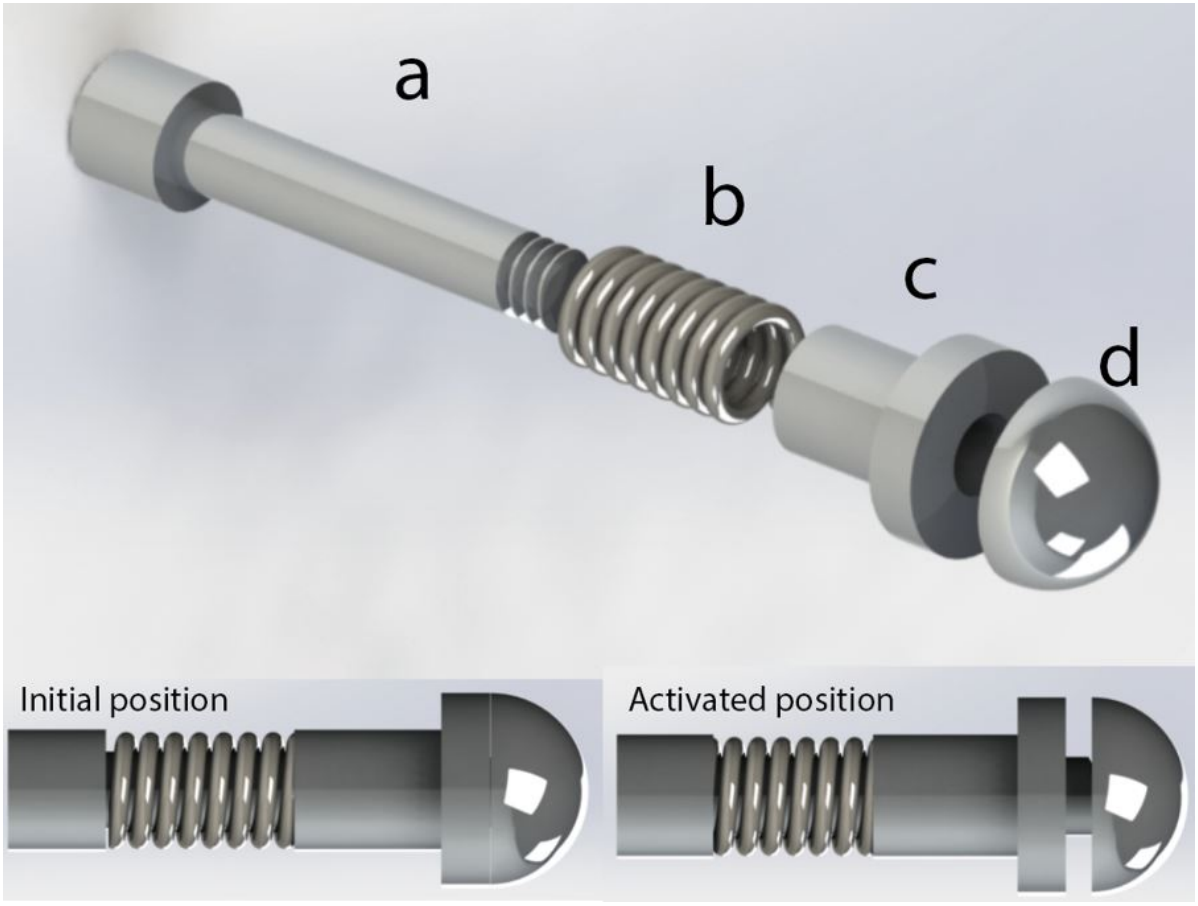

Figure 4.6: Exploded view (top) of the working head, with the initial position (bottom left) and activated position (bottom right). The proximal side is to the right of the mechanism, the distal end to the left of the mechanism, with a) The piston, which will receive the hydraulic pressure wave at the proximal end, b) the compression spring, c) the stop, which will withhold the working head from shooting out of the tube, and d) the tip, which will strike the target tissue.

anism was constructed in this way to fit precisely in the tube. A minimal amount of parts were utilized in order to keep fabrication time to a minimum and with less complications, less unwanted situations can occur.

Impulse generator

The impulse generator is divided into two segments. The first segment is the part were the operator can generate a variable impulse, as seen in Figure 4.7. The second segment will translate the impulse into the tube, as seen in Figure 4.8, but this will be discussed later in this section. The first segment contains a compression spring placed around a beam, located in a protective housing. This beam also connects to a handle that is used to compress the spring over a certain distance, by pulling it. The handle is connected via a threaded section to the beam. By rotating the handle, Part (a), clockwise or counterclockwise, the beam, Part (e), will be inserted respectively more or less into the handle, depending on the direction of rotation of the handle. This allows for adjustment of the pullback distance of the compression spring.

The handle has a stop (Part (c)) on the end of the handle, which will prevent the handle from being pulled further than a certain distance, by coming into contact with the housing. Depending on how far the handle is rotated along the thread of the beam, will determine how fast the stop will come into contact with the protective housing and prevent further pullback of the handle. For instance, a handle rotated further along the thread of the beam will allow for a further pullback distance till the stop comes into contact with the protective housing, resulting in a larger compression distance of the spring. If the handle is released the entire system in the protective housing will shoot forward due to the spring energy being released. The beam will strike a piston located in the second segment.

The second segment is the impulse translation part, which translates the impulse, generated by the compression spring, to the tube, as seen in Figure 4.8. It does this by receiving the impulse from the beam of the first segment, which will strike the piston in the

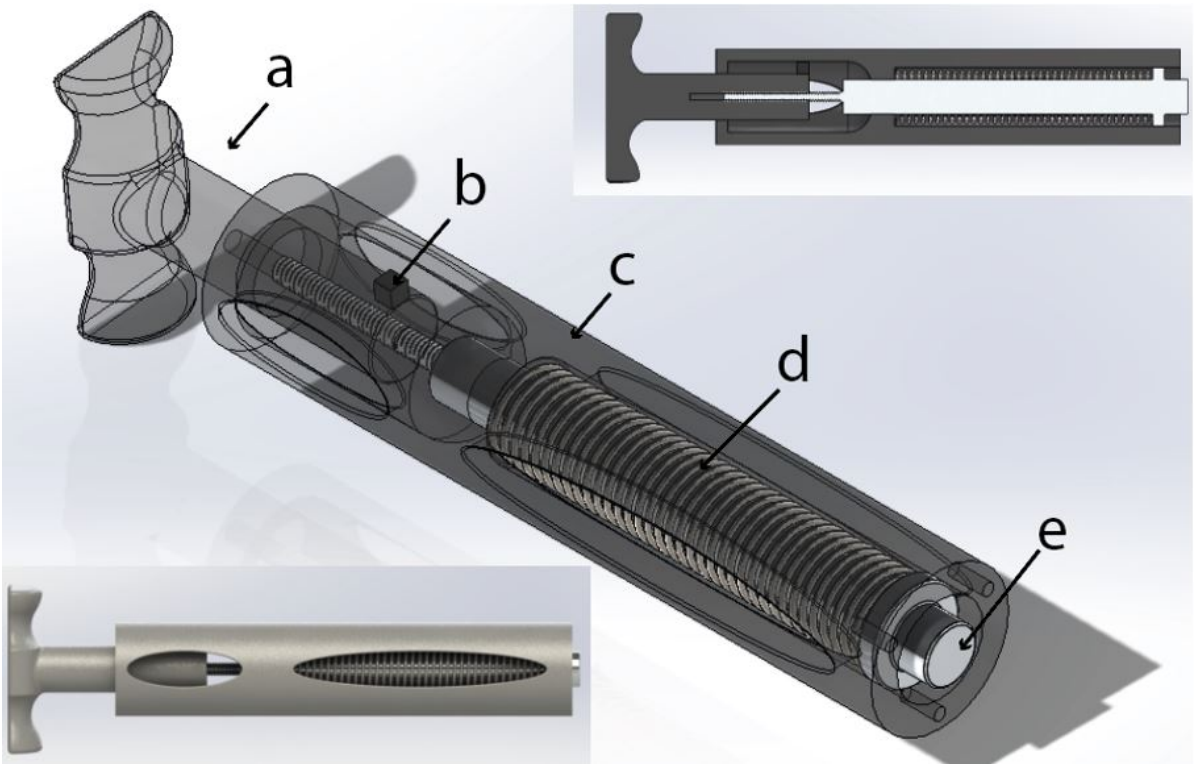

Figure 4.7: 3D visualisation (middle), side view (bottom left) and section view (top right) of the first segment of the impulse generator, were the operator can generate a variable impulse by pulling the handle, with a) the handle, used for pulling back the mechanism resulting in compression of the spring, b) the stop, which prevents further pullback after a certain distance, c) the protective housing of the mechanism, d) the compression spring, which will produce the impulse by being compressed and then released e) the beam, connected to the spring and the handle, which will strike the piston located in the second segment. The beam can be rotated into the handle, to alter the pullback distance of the mechanism.

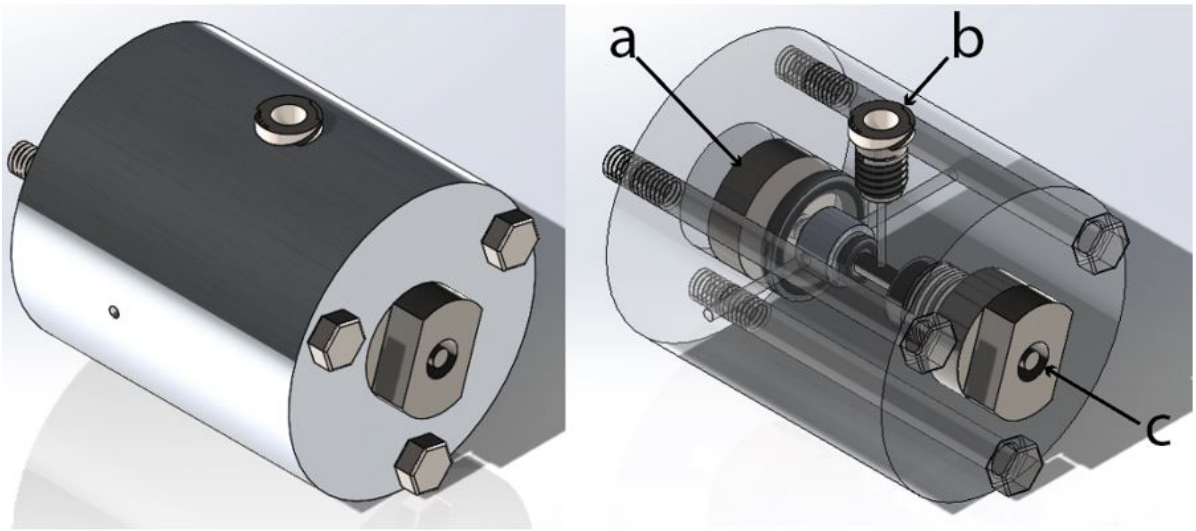

Figure 4.8: 3D-visualisation (left) and an x-ray visualisation (right) of the second segment of the impulse generation part, which will translate the impulse generated in the first segment to the tube, with a) the piston, which will receive the impulse from the beam of the first segment and translate it to the tube to form a hydraulic pressure wave, b) the Luer-Lock, which will allow for a liquid supply to be attached, which will allow for additional liquid to be added to the tube, in order to keep the right volume and pressure, and c) the front insert, which will connect the tube to the impulse generator part.

second segment. This piston is partly located inside the tube. So if the piston gets shot forward, due to the impulse, the piston will generate a hydraulic pressure wave inside the tube, by a sudden pressure increase at the proximal end of the tube. This segment has a secondary function as well. It connects the liquid

supply to the tube. The liquid supply, which will be attached at the Luer-Lock, will be used to keep the pressure and liquid volume constant in the tube. This is done to optimize the efficiency of the system and eliminate the problem of leakage in the tube.

Figure 4.9 shows a section view of the second segment. The beam of the first segment (Figure 4.7 Part (e)) will strike the piston, at the proximal end, in the second segment (Figure 4.8 Part (a)). The piston reaches all the way through the segment to the tube, which will be inserted on the distal side of the segment (Figure 4.8 Part (c)). The piston has a compression spring around it. This compression spring is used to return the piston to its initial position after it has translated the impulse to the tube. An O-ring is used to dampen the piston, to minimize damage to the piston, and refrain it from shooting too far forward. Another O-ring is positioned around the piston more towards the distal end. This O-ring is used to stop the liquid from leaking out. This liquid comes from the liquid supply channel. The channel transports the liquid from the Luer-Lock, were the liquid supply is attached, towards the tube. The tube is connected to the second segment with the use of the front insert. This front insert has a centre hole were the tube can be glued into. The front insert can be screwed tightly into the front of the second segment. Furthermore, the second segment is fixed to the first segment, with the use of three screws.

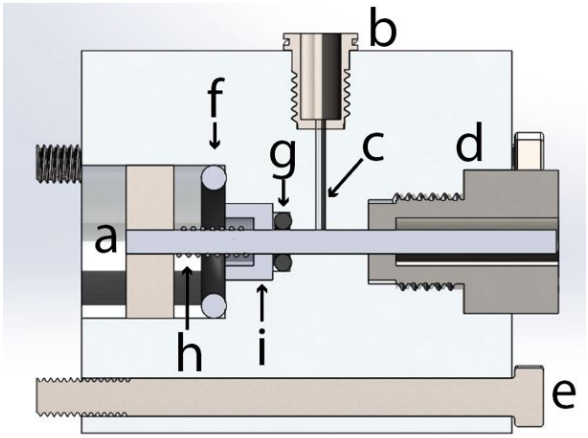

Figure 4.9: Cut-through visualisation of the second segment of the impulse generation part, which will translate the impulse generated in the first segment to the tube, with a) the piston, which will receive the impulse from the beam of the first segment and translate it to the tube to form a hydraulic pressure wave, b) the Luer-Lock, which will allow for a liquid supply to be attached, which will allow for additional liquid to be added to the tube, in order to keep the right volume and pressure, and c) a hole through which water will flow to the tube, d) the front insert, which will connect the tube to the impulse generator part, e) a bolt, that will connect the first segment to the second, f) an O-ring that will cushion the impact of the piston, g) another O-ring that will stop water flowing to the left of the image, h) a spring that will return the piston to its original position after the impact has occurred, i) an insert that stops the O-ring from falling out.

4.5.3. Segment fabrication & assembly

Transmitting part

For the tube that connects the impulse generator with the working head, a 4.0 mm O.D x 2.5 mm I.D Metric Nylon PA12 tube (Advanced Fluid Solutions, United Kingdom) has been selected. The manufacture states that the tube is extremely stable in high moisture environments and has a maximum working pressure property of 400 Psi (27.6 bar, 40 MPa), which is more than enough as stated by the requirements section. The total length of the tube will be 40 mm plus an additional 10 mm on both sides to allow space for the other segments to be connected. Furthermore, the tube is flexible enough to allow for a 90 degree over the 40 mm free section of the tube, without causing plastic deformation. Nylon PA12 has very high compression strength (13 MPa till 55 MPa) [62]. Because of this, compression in the axial direction of the tube will be highly unlikely during the experiment. Next to this, expansion of the tube in the radial direction will also not be likely to occur, which is beneficial as radial expansion decreases the efficiency of the transition of the hydraulic pressure wave through the tube [52].

Possible other options of tubing were using braided medical tubes. These tubes have a braided metal wire structure running through the tube wall. This would increase the burst resistance even more. However, this seemed unnecessary, as the current tube already has qualities sufficient enough for the experiment to be performed. It was also unknown if the braided structure would form micro variations in wall thickness, which would lead to a more uneven inner wall surface. This could lead to more friction, resulting into a less efficient transition of the hydraulic pressure wave.

The choice of liquid medium, that will allow for the transmission of the hydraulic pressure wave through the tube, will be a saline solution. The reason for this, is that the instrument will most likely leak, due to the high pressures that are created inside the instrument. For this reason, a saline solution would be the only safe solution, as to not harm the tissue it comes into contact with in the case of leakage.

Working head

Figure 4.10 shows the fabricated prototype of the working head. The piston is constructed from a RVS316 beam by milling it down on a milling machine. The larger diameter fits exactly into the tube. The smaller diameter segment has a spring (∅2.5 mm, spring constant k = 1.41 Nmm^1) that fits exactly around it, with the outer diameter smaller than the inner diameter of the tube, so it does not cause friction with the inner tube surface. The stop was also fabricated with a milling machine. The stop is bronze to allow for less friction between the piston and the stop, then if both were to be made of RVS. The outer surface of

Figure 4.10: Fabricated end product of the proof-of-principle prototype working head part with A) an exploded view, with the components disassembled, and B) a view of the pieces assembled.

the smaller diameter segment is glued (Cyanolit®) to the inside of the tube at the distal end. The distal segment of the piston, containing the metric thread, is positioned through the centre hole of the stop. This allows for the working head tip to be screwed onto the piston, securing the working head in place. The tip is fabricated with RVS316 by turning it down on a lathe, whilst the screw thread, in the centre of the tip, was made with a milling machine.

Impact generator

Figure 4.11 shows the fabricated impact generator part. In the first segment, the handle, the stop and the protective housing of the mechanism are all 3D printed with the use of digital light processing (DLP). The machine used to print these parts is a EnvisionTEC's Perfactory 4 Mini XL with ERM. For the handle R5 was used, and for the stop and protective housing EnvisionTEC R5 Gray as material, both from the company Perfactory. In the handle, an extra hole has been drilled, whereafter a helicoil was inserted. This was done so the beam could be attached to the handle, allowing for alteration in the compression distance of the spring which was been previously explained. This beam, made of Aluminum 7075-T6 was made with a lathe. Around the beam, a spring (∅24.4 mm, spring constant k = 0.78 Nmm^1) is fitted. The second segment, the housing is made of RVS316 and milled to its current shape. The stop, that keeps the O-ring in the middle of the part, has also been milled and press fitted into the housing. The Luer-Lock has been fabricated with Aluminum 7075-T6, as well as the front insert. The axis of the piston has been made with *'Tampon staal'* and the other part is made with RVS316. The two pieces are brazed together. Around the piston a spring (∅3.2 mm, spring constant k = 0.62 Nmm^1) is fitted.

Full assembly

The full assembly is presented in Figure 4.12. The tube, at its distal end, has been glued to the working head, as explained above and the proximal end of the tube has been glued (Araldite® 2000) to the front insert module. The front part of the impact generator has been attached to the back part of the impact generator with the use of three M4 screws and Helicoil inserts in the back part of the impact generator. The springs are still interchangable should a different spring force range be required.

Figure 4.11: Fabricated end product of the proof-of-principle prototype impulse generator part with A) an exploded view, with the components disassembled, and B) a view of the pieces assembled.

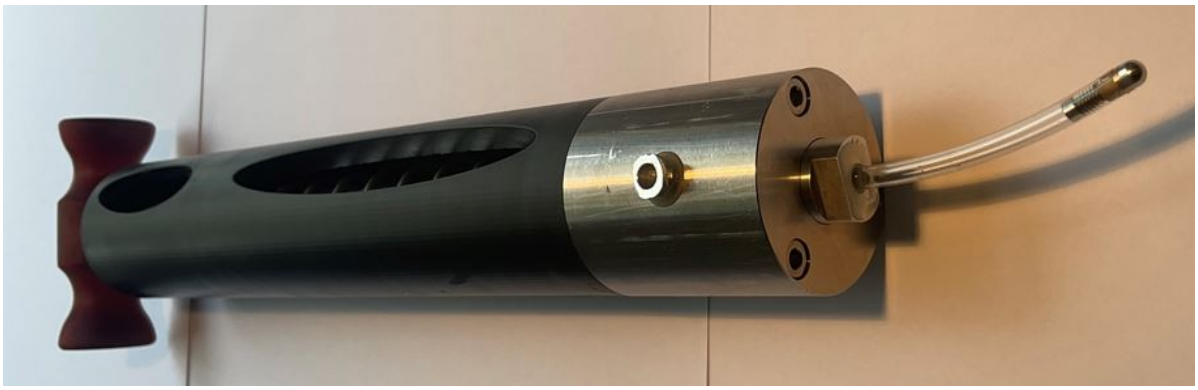

Figure 4.12: Assembled end product of the proof-of-principle prototype, with on the right the working head attached to the transmitting tube, which is connected at its proximal end to the impact generator handle, at the the left.

5

Instrument testing

5.1. Experimental goal

The goal of this experiment with the proof-of-principle instrument is to: 1) evaluate if the instrument actually performs the required impacts, 2) examine the variation and efficiency in the impacts if the input impulses altered, 3) examine the effect of the impacts and potential efficiency alterations when the transmitting tube is at a certain curvature, and 4) observe the effect the impact produces on a sample of the cancellous bone replica. This experiment will determine the feasibility of this method to be used for a potential future instrument that can penetrate the cancellous bone of the thoracic vertebra through repeated impact forming curved holes. An experimental facility was developed for this purpose.

5.2. Research variables

Independent variables

Input impulse

Through the use of a compression spring and compressing the spring over alternate distances, d [mm], a range of impulses, S_{input} [Ns], can be generated. Through altering the input impulses the efficiency can be evaluated, when compared to the output impulse, and a possible optimal impulse can be found. Calculations of the theoretical impulse that will be generated can be found in Section 3.2.2. No loadcell will be placed directly on the strike plane of the strike beam, that is activated by the compression spring, to measure the exact input impulse. The theoretical impulse input can be measured precisely by the magnitude of compression of the compression spring. This theoretical impulse will then be compared with the impulse output to measure the efficiency. The actual input impulse will obviously not be entirely correct, but as every test is measured this way, the measurements can be compared relative to each other in order to find the most efficient impulse range.

Tube curvature

In order to allow for a steerable medical drilling instrument, there needs to be a part that can curve to allow for curved holes. This application is performed by the transmitting tube. To validate that such an application works, the tube needs to be evaluated under certain curvatures to see if it still translates the required impulse from the impact generator, to the working head. In order to determine the effect of curvature on energy losses of the impulse, a range of curvatures over the entire length of the tube have been selected. This range will be from 0 degrees, no curvature in the tube at all, to a curvature of 90 degrees, which is believed to be the maximum curvature need, as explained in the requirements section. Therefore, the tube curvatures chosen will be 0 degrees, 45 degrees and 90 degrees, to allow for a variety of observations.

Dependent variables

Output impulse

The output impulse, S_{output} [Ns], will be measured by a loadcell directly in front of the strike head of the working head. The loadcell will provide the force, F [N], over a period of time, t [s]. With this data, the impulse is calculated by the integral of time over the force, given by the equation in Section 3.2.2. As previously mentioned, theoretically this should be equal to the input impulse, but in reality this will not be the case. There will be several losses that will decrease the magnitude of impulse that will be measured by the loadcell. These losses consist of friction from the linear slider with the setup, air resistance, refraction losses of the hydraulic shockwave in the transition tube and potential heatloss. With the impulse output data, the magnitude of the impulse can be compared to the penetration rate to find the most efficient impulse magnitude.

Penetration rate

The penetration rate, millimetres per strike [mm/strike], will be found by measuring the depth of a hole, that is formed due to a number of repetitive strikes of the working head on a particular spot on the cancellous bone replica sample. The depth of the hole will be divided by the amount of strikes it took to reach that

particular depth, which results in the average penetration depth of that particular working head.

5.3. Experimental facility

For this experiment, an experimental facility is used, illustrated in Figure 5.1. Additional versions of the proof-of-principle experiment are found in Appendix E. With this setup, an impulse can be generated by a compression spring (∅24.4 mm, spring constant k=0.78 N mm^{-1}) over a set distance and then releasing the spring to generate an impulse. The system is designed in such a way, that if one rotates the pullback handle 360 degrees, the pullback distance decreases or increases by 1 millimeter, depending on the direction of rotation. The pullback distance is determined by the difference in distance between the spring in its rest state, and the point were the pullback stop stops any further pullback from occurring. By altering the compression distance different magnitudes of impact can be performed.

The mentioned spring is chosen, as compressing the spring over a distance of 40 millimetres would give more than enough energy, theoretically, to perform relevant impacts with the working head based on all experiments done and insights gathered previously in this thesis (Appendix C). This spring is placed on a linear slider that can be pulled back over a set distance and then be released, in order to propel the linear slider towards a piston that will then generate a hydraulic pressure wave inside the tube. The linear slider could be pulled back accurately, manually by the operator, in order to provide the right amount of impulse. The entire instrument is mounted to a breadboard. This is done to provide stability during experiments and to ensure, the exact distance and point of impact of the working head is guaranteed.

The data analysis and acquisition of the output impulse is done with a data acquisition system (NI USB-6002: 12-Bit, 10kS/s Low-Cost Multifunction DAQ) and an analogue signal conditioner (CPJ RAIL, SCAIME, S.N.: 001436), all connected to a loadcell (PST, S-Type Load Cell) with a capacity of 150 kg. The loadcell was controlled with a software programme (NI LabVIEW 2018). The programme registered a change in force on the loadcell and provided a data sample of the force over time change during a 0.15 second window.

The transmitting tube is secured in place by a module that supports the tube on all sides and bends the tube into the desired curvature. The tube has to be supported on all sides to decrease the refraction rate of the hydraulic pressure wave. At the end of the tube the working head is found. The impact of the working head is delivered upon a loadcell, which is positioned perpendicular to the impact direction. This way, the entire impulse can be measured, as the working head strikes the loadcell. When testing the penetration rate of the working head, a module containing the cancellous bone replica sample is placed in front of the working head.

It is always ensured that the tip of the working head will always strike the target tissue with the same travel distance, allowing for a more accurate impulse result. Saline solution for the transmission tube is supplied by the additional liquid injection instrument that, connected to the Luer-Lock, can fill the entire transmission tube with as little as possible additional air. Additional air would make the transmission very inefficient or disable the application all together. It is expected that the system will leak, so the liquid injection module is constantly attached, ensuring the transmission tube has the same amount of saline solution in it at all times.

5.4. Experimental protocol

Out of previous experiments with the same loadcell with a maximum load of 150 kg, it has been established that the loadcell can capture all the required data and force spikes produced by the working head. As it is not expected that higher force spikes will be measured for this experiment, than the ones before, no initial test on the loadcell will be performed to analyse if all extreme data can be captured with the loadcell. A few different tests will be performed to evaluate if this method is viable and could potentially be used to create a new instrument for steerable drilling in the vertebra.

The first test, will test the efficiency of the output impacts compared to the input. This is done by securing the transmitting tube into a module that will hold the tube straight. The loadcell will be perpendicular to the strike direction of the working head. Different compression distances of the compression spring will be evaluated by steps of 5 mm, and with the captured data from the loadcell, the optimal input/output ratio will be found. For this test, it is desired to at least reach an output impulse of 0.077 Ns. This will validate that the method does have enough impulse to penetrate a replica cancellous bone sample, as is found in Appendix C.

Having found the optimal input, the next test can be performed. This test will test if the instrument functions when the transmitting tube has a curvature. This is done by using different modules that hold the transmitting tube in different curvatures. Two curvatures, apart from the straight one, will be tested. These are 45 and 90 degrees. This will prove that the method works in curved circumstances as well, indicating further validation of the proof of principle. During these tests the loss in efficiency will be registered as well, to see how much energy is lost when performing the impacts in different curvatures.

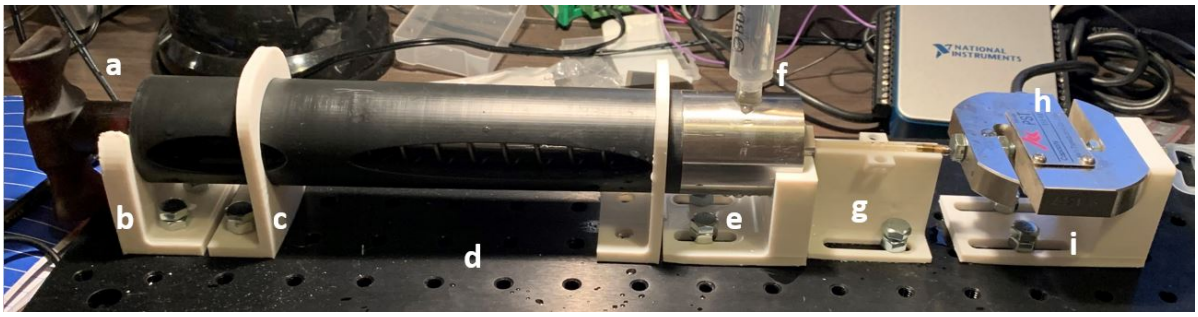

Figure 5.1: Full proof of principle experiment setup with a) the handle used to pullback and compress the compression spring, with additional application by rotating the handle, the pullback distance can be adjusted, b) the back support of the experiment holding the instrument in place in the horizontal plane whilst impacts are performed, c) the vertical supports, fixing the instrument in the vertical plan whilst impacts are performed, d) the breadboard used to fix the entire experiment in place, e) the front support of the experiment holding the instrument in place in the horizontal plane whilst impacts are performed, f) the saline input module attached to the Luerlock to provide the saline solution to the tube, g) the tube holder module, fixating the tube in a certain curvature (the Figure showcases the 0 degree curvature module, but different curvature modules were used as well, as seen in Appendix E, h) the loadcell module that will capture the impact from the tip at the distal end of the tube, and i) the loadcell support module, which fixates the loadcell in place and allows for adjustable distance of the loadcell module to the tip.

For the last test a sample of cancellous bone replica material from Sawbones will be utilised. This sample will be positioned between the working head and the loadcell. Different impact magnitudes will be performed upon the sample to analyse the penetration rate. This will be done with the transmitting tube in the straight position, as well as, in the 90 degrees position to prove that it still works when the tube is in curvature. For each impact magnitude, 10 strikes will be performed. The depth of the penetration will be measured and averaged, so the average penetration rate for that magnitude is found. Each individual test over a certain compression distance will be performed 3 times, in order to, provide a more accurate penetration distance by taking the average of the three. The working head will have the same travel distance each time before impacting the sample.

5.5. Data analysis

For each test, the penetration depth after 10 strikes is registered in an Excel table. The depth of the hole will be measured with the help of a caliper with an accuracy of 0.1 mm. For each test the mean penetration depth is taken and from that, the average penetration rate, millimetre per strike [mm/strike], is calculated. The data of the output of the loadcell, captured with the help of LabVIEW, are processed with MATLAB R2020a, to generate force over time graphs. These force over time graphs are used to find the impulse generated for every single impact of the working head on the target tissue.

5.6. Results: Instrument testing

The goal of this experiment was to determine the feasibility of the proof-of-principle hydraulic pressure wave drilling method designed in this thesis. This was done by 1) evaluating if the instrument actually performed the required impacts, 2) examining the variation and efficiency in the impacts if the input impulses altered, 3) examining the effect of the impacts and potential efficiency alterations when the transmitting tube was at a certain curvature, and 4) observing the effect the impact produces on a sample of the cancellous bone replica material. All steps have been performed with the proof-of-principle instrument.

For the first step, the entire instrument was setup to see if the instrument would work as intended. The saline solution injection module was added and the tube was filled. Getting the tube filled, without air left in it, required many attempts to perfect. Air bubbles remained in the tube, no matter the shaking, tapping or adding of more liquid. Eventually, it was observed that at a certain rotation of the part at the proximal part of the tube, which would compress an O-ring, inside the handle part of the instrument, would allow for liquid to be fully transported to the tube, where it would remain without leaking, till impact occurred. Furthermore, it was found that the tube needed to be dismantled and manually drained of liquid before it could be filled again. If this was not done, the tube would not fill entirely, but would have residue gas bubbles left inside. Refilling of the tube was required, as after impact the tube lost some liquid, due to the sudden high pressure in the tube, forcing some of the liquid through the minuscule spacing between the tip part and the tube.

The loadcell needed to be placed directly touching the tip, as if it was further away, it would show really low force output levels which were unusable. It was confirmed at the start of every impact test, whilst the tip was touching the loadcell, no actual force was being applied on the loadcell by the tip prior to the impact test. All in all, the mechanisms in the instrument

all worked as intended, and a force over time output was measured after every strike.

Having confirmed that the instrument worked, the next step was to examine the variation in the compression distance of the spring as input compared to the output given by the loadcell. The tests started with a 10 mm compression distance of the spring, which was increased with incremental steps of 5 mm till the maximum compression distance of 40 mm was achieved. From 10 mm till 25 mm, no reliable output was observed. In the graphs it was barely observed that a impact had occurred between the tip and the loadcell. From 30 mm onward, usable output data was observed. For every step, 10 impacts tests were performed. This was done, as there seemed to be some variance in the output of every test. Figure 5.2 gives a representation of 3 single output impacts from the 3 measured compression distances chosen at the writers own discretion. This figure shows only a single strike instead of the averaged fitted line of the total of 10 strikes for that particular compression distance. This was done, because there was a lot of noise and fluctuations which would result in an unusable graph were it an averaged fitted line.

For the next step it was decided to continue with the 40 mm compression distance. This was done because the impact, most often, succeeded with this input compared to the others. Furthermore, it was hypothesized that a bigger input would lead to a more reliable output, as small outputs would be distorted by the noise of the loadcell. In this step, curvature of the tube was analysed. Two test experiments were done and compared to each other and the initial no curvature position. The first experiment had a curvature of 45 degrees and the second one had a curvature of 90 degrees. Both curvatures ran across the entire

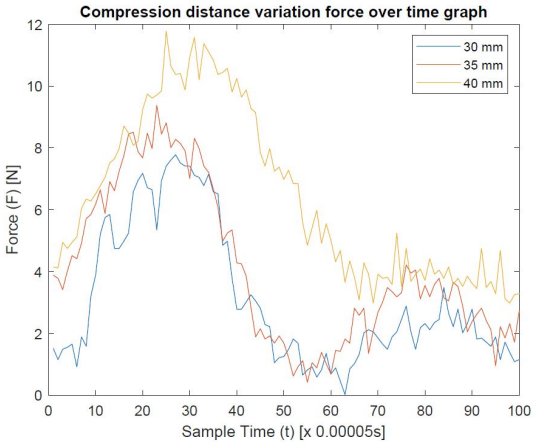

Figure 5.2: Loadcell output of three single strikes with blue) having a compression distance of the spring of 30 mm, red) having a compression distance of 35 mm, and yellow) having a compression distance of 40 mm.

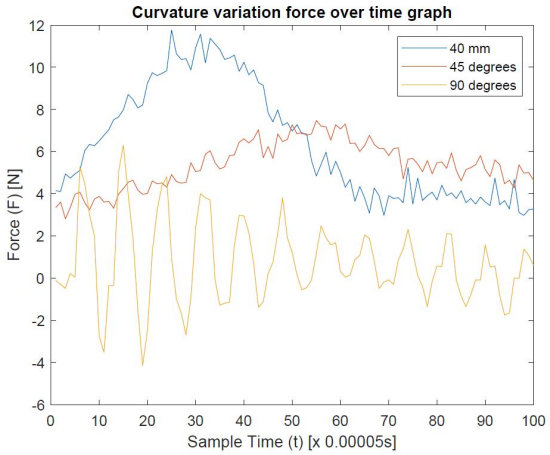

Figure 5.3: Loadcell output of three single strikes with blue) having a compression distance of the spring of 40 mm, as a reference for the curvature variations, red) having a compression distance of 40 mm and a curvature of 45 degrees, and yellow) having a compression distance of 40 mm and a curvature of 90 degrees.

length of the tube excluding the tip mechanism, as that needed to be straight in order to perform the impact and not get stuck. Figure 5.3 presents 3 different single impacts of the two curvature variations and the initial straight variation, all having the 40 mm compression distance of the spring. Again no averaged fitted line was presented for the same reasoning as the previous figure. In the figure, it is observed that the 90 degrees curve presents the fluctuating curve, as happened numerous times at the smaller output levels of the impacts.

As all graphs had a same general triangle shape, with an impact lasting 25 ms to 30 ms. The impulse was approximated by calculating the impact duration time by the peak force and dividing it by half, as using the Matlab function to calculate the area beneath the curve let to unusable data. This let to Figure 5.4, which shows the impulse variation of the impulse outputs for every experiment variation.

As a last experiment, a use case was performed. Although the highest impulse output found was below the required impulse output of 0.077 Ns that was needed to show visible drilling of the cancellous bone, as was previously stated at the start of this chapter as a requirement, the experiment was still performed to see if some interesting findings would be observed. This experiment tested the impact of the tip on a block of the cancellous bone sample. The cancellous bone was held in place and positioned against the tip, whilst making sure no initial force already occurred. 30 strikes were performed on the cancellous bone. It was hypothesized that potentially a lot of strikes would still amount to drilling of the cancellous bone sample. After 30 strikes, a small indentation of 1 mm to 2 mm was observed, as seen in Figure 5.5.

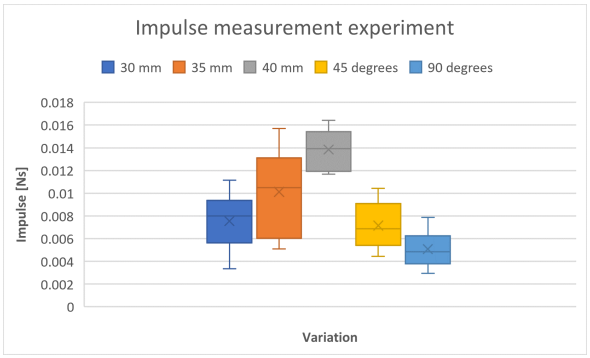

Figure 5.4: Impulse output of the different experiment variations with blue) impulse output variation of the spring compression distance of 30 mm, orange) impulse output variation of the spring compression distance of 35 mm, grey) impulse output variation of the spring compression distance of 40 mm, yellow) impulse output variation of the spring compression distance of 40 mm and curvature of the tube of 45 degrees, and light blue) impulse output variation of the spring compression distance of 40 mm and curvature of the tube of 90 degrees.

Figure 5.5: Small indentation observed after striking the same spot for 30 repetitive strikes with a compression distance of the spring of 40 mm. (Tube is removed in order to see the indentation better from an angle)

6

Discussion

6.1. Main findings

The final experiment has proven successful.The experiments performed in this thesis have provided proof for the overall validity of the steerable drilling method suggested in this thesis. During previous experiments it has been observed that during penetration of the sample low impulses were needed, no heat was produced, which could lead to necrosis, and resected material was compacted against the side walls of the generated hole, which could potentially increase the holding strength of pedicle screws that would be placed there. The last experiment has proven that the method is able to perform as intended in curved conditions. Through this, the application of steerable drilling could be achieved. Furthermore, the repetitive mechanism has proven to work. After every strike, all mechanisms returned to their initial position. Through this, the repetitive impact drilling could be achieved. The mean impulse of the largest compression distance of the spring measured achieved almost 20% of the required 0.077 Ns impulse that was required to allow for visible fast drilling in the cancellous bone with a penetration rate of 0.3 mm per strike.

Although, the required impulse of 0.077 Ns was not achieved with the current setup, the method worked and the potential is there to create a fully operable new steerable drilling method. Numerous reasons can be stated that the final impulse magnitude was not fully achieved. First, it was observed that the tip had to be positioned against the loadcell in order to capture the output. Where the tip and loadcell further away from the tip, between 1 mm to 2 mm, a large decrease in output was observed. A reason for this could be the friction that occurred in the tip part of the tube. Whilst receiving the hydraulic impulse the tip would shoot forward. But displacement of the tip forward induced friction with the sides of the tube, and energy losses due to the spring attached to the tip, that insured that the tip would return to its initial position after impact. During the many experiments and constant exposure of liquid, this friction became more as the spring in the tip started to show signs of corrosion.

Further reason of lower efficiency was caused by potential air still being in the tube. The tube needed constant draining, and refilling to make sure no gas bubbles remained in the tube itself. Through visual observation by eye of the tube after every refill it was confirmed if the next impact test could be performed if no gas bubbles were present. However, micro bubbles could not be observed this way, whilst they could still decrease the efficiency of the hydraulic pressure wave. This could be the biggest reason of the variation in impulse output during the different tests. Furthermore, at the proximal end of the tube, which had the part which allowed the tube to be coupled to the impact generation part of the instrument, there was a part of the tube not visible. It was unsure if gas bubbles were present in this part. If bubbles were present, these would be of the micro kind, as bubbles with a diameter of around 1 mm would cause detrimental decrease in the impact output, which would be noted with the loadcell output.

The instrument hosted more unavoidable efficiency losses. One being the piston that would generate the hydraulic pressure wave at the proximal end of the tube. This piston needed to fit exactly in the tube. The less space between the piston and the tube, the better the formation of the hydraulic pressure wave. However, theoretically they could fit exactly against each other, but in reality this of course is impossible. By decreasing the gap between the tube and the piston to generate a more efficient hydraulic pressure wave, would also increase the friction between the tube and the piston, which would in turn decrease the efficiency of the instrument. Finding a balance is very difficult, because of unevenness in the surface of both parts. This piston had an O-ring around it as well, to circumvent flow of liquid in the opposite direction of the tube, as well as, a spring that would return the piston to its initial position. Both these parts caused efficiency losses as well.

All these previously mentioned efficiency losses, together with the general friction and heat generation between moving parts, caused a large drop in

efficiency of the instrument. In Table 6.1, the theoretical impulse is compared to the actual impulse output of every experiment variation and calculated in a similar fashion as was done in Chapter 3. As is clearly observed in the Table, there was a low efficiency in the transition of the input to the output. In Table 6.1, it can be seen that there is a positive correlation between the increase in impulse and the increase in efficiency. This is most likely caused by the larger impulse inputs showing a more clear output graph than the lower input impulses, as at lower impulse noise in the loadcell played a larger part. Furthermore, it can be observed that the efficiency decreases, as the curvature increases in the tube. This makes sense, as the hydraulic pressure wave is more easily refracted in a more curved tube.

It must be noted that to calculate the output impulse general calculations were used, instead of measuring the exact impulse output. This was done, as the loadcell did not provide extremely precise output, due to the minor fluctuations. Still, the figures and the table provide an averaged impulse, which shows a clear positive correlation with the compression distance of the spring and the impulse output, next to a clear negative correlation with the magnitude of curvature and the impulse output, which confirm the expectations of the experiment. Furthermore, it can be noted that there is an almost linear increase in impulse output suggesting that if the impulse input were to increase, even higher impulse outputs can be achieved.

Examining Figure 5.2, it can be noted that the curves when returning back to the rest state, tend to go up again or remain constant at a point above zero Newton. This is most likely caused by the tip still applying some pressure to the loadcell after the initial impact has occurred, as in the starting position, the tip was already in contact with the loadcell. Furthermore, the curves, before they capture the impact, already start not at zero Newton. This is because before the curve starts to rise due to the impact of the tip, some fluctuations are measured. These fluctuations before the actual impact output are disregarded, as it does not contribute to the impulse output of the instrument. These fluctuations are mostly caused by the entire experiment experiencing some initial shock and vibration caused by the input impulse generated in the impulse generation part. For this reason, it was decided to only examine the actual impact output caused by the tip itself.

Figure 5.3 presents the same characteristics as the characteristics previously mentioned for Figure 5.2. Furthermore, the 90 degrees curve, presented an interesting fluctuating curve. This loadcell output tended to happen at the lower impulse magnitude levels. A possible reason for this phenomena could be that the impulse magnitude was not strong enough to induce a continues line, but instead it would cause hitches whilst performing the impact, causing the loadcell to display a rising and declining fluctuating curve.

The use case experiment presented a small indentation after 30 repetitive strikes with a compression distance of the spring of 40 mm. The depth of the indentation was around 1 mm to 2 mm. If this would be achieved purely through the impulses of the tip, this would mean that with a high frequency repetitive strikes, the impulse magnitude level would already be enough to be used for drilling in the cancellous bone. With impacts only lasting around 25 ms, potentially 400 strikes per second can be achieved. However, it is hard to say, if this was caused by the repetitive strikes or could have occurred over time during the dismantling, draining, reattaching, and refilling of the tube, which could have caused some minor contact indentation as well. Furthermore, the indentation was only on the surface of the cancellous bone replica sample. From previous experiments, it has been found that the deeper the instrument would penetrate the sample, the higher the impulses are needed to penetrate further. No loadcell was attached during this experiment, due to time constraints as the belief no promising results would occur during the use case, as from previous experiments it was validated that theoretically the maximum impulse measured was below the required impulse that was needed to create visible indentations after a few strikes.

6.2. Limitations

Partially addressed already in the previous section, certain limitations were found. These consisted of large amounts of efficiency losses mostly caused by friction and leakage. Corrosion development in the tip mechanism, also generated a decrease in efficiency. Furthermore, the experiments proved to be really time consuming, as after every impact test, the tube had to be manually removed, drained, reattached and refilled, whilst ensuring no gas was left in the tube. If gas bubbles occurred during the refilling process, the entire process needed to be repeated. Whilst modelling the final experiment, a lot of parts were required that exactly had to fit. This was all needed to circumvent leakage of the system. However, every self fabricated or ordered part, of course came with certain size tolerances, which generated extra friction between parts, as they were not exactly the same size as the modelled part.

Due to the high speed of impact collisions and the small scale of the instrument, it was hard to visibly confirm that a strike occurred. Next to that, it was impossible to guess at the magnitude of the impulse that was produced by observing the tests, in order to verify the validity of the data that was shown as the output of

Experiment variation	**Theoretical**	**Measured**	**Efficiency**
No curvature & 30 mm compression distance of spring	0.2998	0.0075 ± 0.0024	2.5% ± 0.8%
No curvature & 35 mm compression distance of spring	0.3497	0.0101 ± 0.0038	2.8% ± 1.1%
No curvature & 40 mm compression distance of spring	0.3997	0.0139 ± 0.0017	3.5% ± 0.2%
40 mm compression & 45 degrees curvature	0.3997	0.0072 ± 0.0020	1.7% ± 0.5%
40 mm compression & 90 degrees curvature	0.3997	0.0051 ± 0.0016	1.3% ± 0.4%

Table 6.1: Theoretical impulse input [Ns], compared to the measured impulse output [Ns], of the five different experiment variations. The most left column indicates the achieved efficiency.

the loadcell. The method proposed in this thesis is also intended to function with high frequency repetitive impact. Due to time, costs and high complications in design constrains, a manual single input impulse was tested, with the assumption that if it worked for single strikes, it would also work for high frequency repetitive strikes. This ensured, however, that no tests could be performed with this higher frequency, which could have let to interesting findings that would be missed by just observing individual impacts. Furthermore, all experiments in this thesis are performed on replica cancellous bone samples, which is not to say that the findings will be same if they are to be performed on actual cancellous bone of the vertebra.

6.3. Recommendations

To address the limitations mentioned in the previous section, a number of recommendations will be mentioned. If follow-up experiments are to be done and a new instrument is to be made for testing the method, a high focus must be on the efficiency of the instrument. Alternate applications must be utilized in order to minimize leakage, keep the tube filled with a constant water reservoir eliminating gas formation, or eliminate leakage altogether by designing an enclosed system that can transmit the hydraulic pressure wave through a medium without leakage. Having exact fitting parts works theoretically, but during fabrication, you will always encounter parts being slightly larger or smaller than the model. For this reason, designing a new instrument that allows for minor size tolerances of parts whilst operating as needed is important. Furthermore, extra care must be taken to design with materials that are resistant to corrosion, as was the case eventually with one of the springs in the final experiment.

Having an automatic impulse generator, like a solenoid, would also decrease the manual labour of doing every test by hand. If combining this with removing the leakage, a lot more tests can be performed, as every single test would also be performed much quicker. Furthermore, with these applications, the high-frequency repetitive impacts can be tested as a solenoid allows for continuous repetitive impulse inputs. Not having to refill the tube would mean the instrument can run continuously, delivering a continuous frequency impulse output, which is the goal of this method. Having a solenoid would also remove the intermediate step that was used in the final experiment where the impulse generation part would first strike a piston that would then generate the hydraulic pressure wave. A solenoid could be immediately attached to the tube to generate the hydraulic pressure wave. Alternate ways to generate impact could also be examined, as mentioned in the preliminary research of this thesis, like the electrohydraulic shockwave or utilizing ultrasonics.

6.4. Future vision

With the recommendations in mind and the previous findings found throughout the research on this thesis, a theoretical instrument can be designed that could potentially work as a real-life instrument used for steerable drilling through repetitive impact in the cancellous bone of the vertebra. A visualisation of this theoretical instrument can be seen in Figure 6.1. For the impulse generation part, a solenoid will be utilized. Many solenoids are available on the market that can easily reach the impulse input needed to penetrate the cancellous bone, as well as operate at a high frequency and possess the correct travel distance. This solenoid would generate a hydraulic pressure wave in a bendable tube holding an enclosed liquid medium to prevent leakage. This high-speed displacement of the liquid without leakage generated by the solenoid will generate a hydraulic pressure wave through the tube and activate a tip at the distal end of the tube. The liquid will be enclosed by highly elastic membranes, which circumvent leakage but can be deformed elastically if the membrane is struck by the solenoid. At the proximal end of the tube, a tip will be situated, attached to a membrane as well. This will be activated

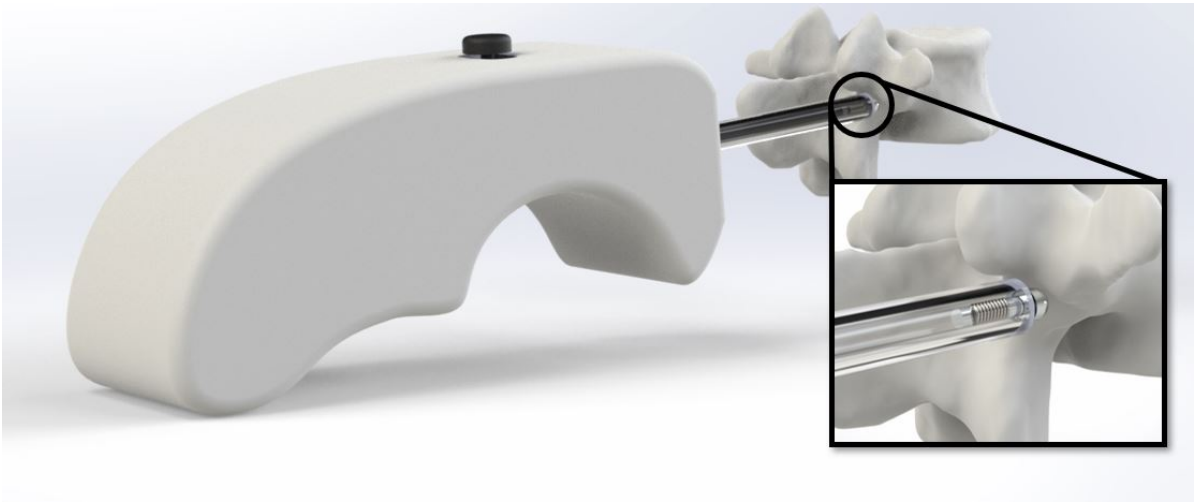

Figure 6.1: Visualisation of a theoretical instrument applying the method of drilling discussed in this thesis. It consists of the main handle, which the operator holds while operating. This handle has a steering mechanism on top, allowing the surgeon to manipulate the working head either to the left or to the right to allow for trajectory control during drilling. Pressing this mechanism downwards activates the drill. Protruding from the front of the instrument is a shaft that functions as a retractable telescope used to support the part of the tube that has not yet entered the vertebra. The tube inside the telescope holds a liquid medium through which hydraulic pressure waves can travel from the handle part to the working head of the instrument. These hydraulic pressure waves are generated by a solenoid inside the main handle. The hydraulic pressure waves activate the working head, making it shoot forwards, enabling it to penetrate the vertebra.

by the hydraulic pressure wave and shoot forward, forming an impact on the target tissue.

Whilst the tube is still fully or partially operating outside the cancellous bone, unwanted bending of the tube can occur. For this reason, the tube will be surrounded by a telescope that will retract the further the tube penetrates the tissue. With this application, the tube will be supported on all sides, removing unwanted refraction of the hydraulic pressure wave leading to efficiency losses. When the tube is fully inside the tissue, the surrounding walls will act as the support. At this stage, the telescope will be fully retracted. To make the device steerable, cables run through the tube to allow for course alteration at the tip. As the formed hole provides support on all sides of the tube, only the tip needs to alter in direction. The rest of the tube will follow automatically. The steering mechanism will be activated by moving a mechanism, represented by the black protrusion on top of the handle in Figure 6.1, either to the left or to the right. Pushing it to the right will make the tip curve to the right and vice versa. Pressing this mechanism downwards will initiate the drilling. By combining these applications into one mechanism simplifies the procedure of drilling for the surgeon operating the instrument.

With this instrument, a new method for steerable drilling in the vertebra is possible, which can aid in drilling holes for pedicle screw placement. Errors can be corrected easily if a wrong drilling trajectory is chosen, which was previously not the case with straight drilling. Furthermore, it could create curved holes, which would allow for a whole new range of pedicle screw designs that might possess higher holding strength. This future vision has been made at the discretion of the author of this thesis. Its workings are based on an educated guess combined with the knowledge gained through the research in this thesis that penetration through the use of repetitive strikes and the bendable medium that can transmit the impulses has been proven to work.

7

Conclusion

This thesis presents the successful development of an innovative drilling method that would allow for trajectory control during drilling through the vertebra, particularly the cancellous bone of the vertebra. This research was undertaken to combat complications that occur during drilling of the vertebra, like ill-placed trajectories of standard straight drilling equipment, which could lead to detrimental results if no course correction is applied. Forming alternate curved holes could lead to new innovative pedicle screws with higher holding strength as well. Initial research was done to find a promising drilling method out of numerous known drilling methods. Following this research, experiments were performed to validate the effectiveness of the chosen drilling method on cancellous bone using the cancellous bone replica material from Sawbones. Positive results were found, which led to the continuation of the drilling method. This method consisted of drilling with the use of repetitive strikes.

Impulse magnitude relations with penetration rates were found for various tip variations, and an optimal tip was selected that would be used to perform the strikes. Following this, the most viable method for the application of curved drilling was selected. The final method selected used impulse, generated in a handle, which would generate a hydraulic pressure wave at the proximal end of a tube containing a liquid medium. This hydraulic pressure wave would be translated through the tube and activate a mechanism displacing the working head forward at high velocity to perform an impact on the cancellous bone. The tube is bendable, which would grant the application of non-straight drilling. After every strike, the instrument returns to its initial state, which allows for repetitive strikes.

A proof-of-principle instrument was designed to identify if the method could be adapted to allow for the application of steerable drilling, and further research was performed with positive results. Although the instrument showed inefficiency, the method has proven to be viable. The instrument proved that it is possible to use repetitive impact drilling, presented in this thesis, in curved states up to at least the desired 90 degrees. The curvature of the tube led to a decrease in impulse output. The method reached almost 20% of the target impulse, which would allow for high-speed drilling of the cancellous bone. An increase in impulse input led to an almost linear increase in impulse output, potentially indicating higher outputs could be reached in the range of the target impulse magnitude. Experiments found that during the repetitive strikes, no heat development occurred, repressing some necrosis, and resected bone was compacted to the sides of the formed hole, potentially increasing the holding strength for screw placement.

In the future, the problem of leakage should be removed to increase efficiency, and an automatic impulse generator, like a solenoid, should be utilized. With the method validated in this thesis combined with a mechanism that could alter the trajectory of the working head, an innovative trajectory controlled drilling instrument can be designed, which will have great benefits in spinal surgery and possibly other fields.

A

Polyurethane foam compression strength test

Overview

Synthetic bone is often used as a replacement for cadaveric specimens. This is because they have a low variance in mechanical properties and are more commonly available, than real bone specimens. Furthermore they are uncontaminated and can be fabricated in easy to work with geometries [55]. Polyurethane foam is a widely used standard for mimicking human cancellous bone [55]. Therefore a test is done to validate and find the exact mechanical properties of store bought two component polyurethane foam, which will be utilized in this thesis for experiments.

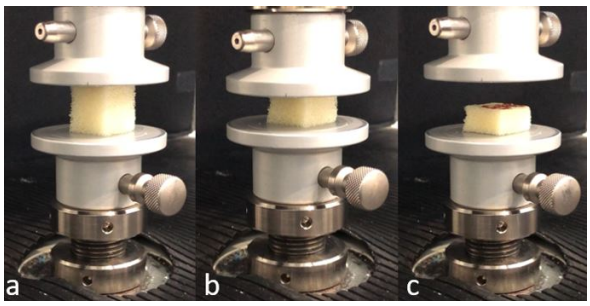

Figure A.1: The compression machine performing the compression test shown in three stages: a) the start of the compression, b) halfway during the compression test, c) the end of the compression test, showing the plastic deformation of the test sample.

Method

To validate if the use of polyurethane foam, made from a ratio of 1:1 from the substances Polyol and Iso, is a valid substitute for cancellous bone as the literature proclaims it to be, a compression test is performed. For this test the NEN-ISO 13314:2012 [63] was used as a guideline. This is the international standard for compression test for porous and cellular metals, which was used as a guidance for the compression test, as it gives the general steps ,which could also be applied to a polyurethane foam. The test machine was conforming to ISO 7500-1 and could compress the material, at a constant crosshead speed, up to 5 kN. The test specimen was placed between two parallel plates, that would compress it, as seen in Figure A.1.

For this test five cubes of polyurethane foam were compressed (Figure A.2). The density of the material is 0.53 g/cm^3, which is in the range of what the literature prescribes as relevant density of polyurethane foam for mimicking human cancellous bone [55]. The specimens were tested at room temperature, around 20 degrees, under normal conditions. The dimensions of each test specimen are found in Table A1. For the compression speed, a speed of 0.1 mm/s was chosen. This velocity resulted out of the length of the test specimen times the $5 * 10^{-3}$, as was stated in part 7.3 of the ISO-Norm [63]. When the machine performs a test, it generates six different curves with on the x-axis the sample steps and on the y the time, the load, the extension of the compressor head, the stress, the percentage strain and the deflection from preload.

Specimen code	Length [mm]	Width [mm]	Depth [mm]
G1	20.2	19.6	20.0
G2	20.5	20.0	19.5
G3	21.3	19.6	20.0
G4	20.5	19.3	19.8
G5	20.6	20.1	20.1

Table A.1: Length, width and depth of each test specimen tested. Orientation of the length, width and depth is found in Figure A.2.

Results

From the results of the tests, stress strain curves can be made, as seen in Figure A.3. There numerous outcomes to the material properties of the polyurethane foam test specimens can be found. The results show the first maximum compressive stress and from the graphs with the Equation A.1, the Young's modules can be calculated. This is calculated to see the elasticity of

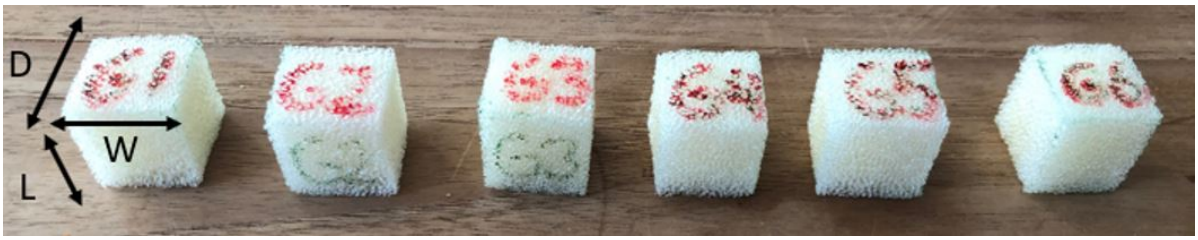

Figure A.2: Six test samples. The first five are used for the compression test with the last as backup.

Specimen code	Maximum compressive stress (σ) [MPa]	Young's Modules (E) [MPa]
G1	0.20	16.8
G2	0.23	19.8
G3	0.34	10.3
G4	0.22	28.7
G5	0.23	27.0
Mean + SD	0.24 ± 0.06	20.5 ± 7.54

Table A.2: Maximum compressive stress and Young's modules for each test specimen, read out of the graphs. Lastly the mean ± standard deviation is given from all the test (n=5).

the polyurethane foam.

$$E = \frac{\sigma}{e} \tag{A.1}$$

The Young's Modules shows a wide range of results. This is most likely because of the inhomogeneous material structure of the polyurethane foam, which causes for a wide scale of elasticity. The results for each test are found in Table A.2, with the average result at the end.

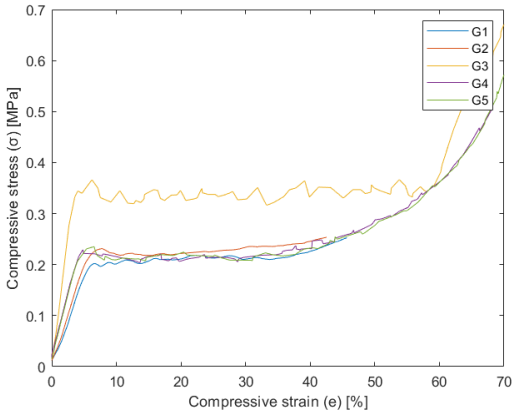

Figure A.3: The stress/strain curve of the five different tests with the polyurethane specimens.

Discussion

One test specimen, G3, had a stress/strain curve that lay much higher than the rest of the tests. The exact reason for this outlier is unknown, but it could have been caused by a local increased density of the polyurethane foam in that particular specimen piece. The mean maximum compressive stress of the tested polyurethane foam material is lower than that of the compressive strength of cancellous bone in the vertebra found in the literature. Banse *et al* [64] finds, for human cancellous bone in the vertebra, a maximum compressive stress range from 0.60 MPa to 6.17 MPa with a mean of 2.37 MPa. This is higher than the range found in this compression test.

Conclusion

There are companies that specialize in human bone replica material, like Sawbones and Synbone, that offer polyurethane foam blocks in the range of the compressive strengths. However, for the initial experiments that will be performed to examine the effect of impact on polyurethane foam, the current polyurethane foam, examined in this experiment, is deemed acceptable, as it is relatively cheap and easier to acquire than the materials offered by the previous mentioned companies. This will be advantageous for the initial experiments as they require large quantities of material in order for testing. For the post experiments that will decide the official parameters of the instrument that will perform the penetration of the cancellous bone, polyurethane foam blocks from the previously mentioned companies, that are in the range of the measured compressive strength range of human cancellous bone of the vertebra, will be utilized.

B

Linear stage working head compression experiment

Overview

In order to understand the amount of kinetic energy the impact, from the polyurethane foam impact test, has to provide to the target tissue in order to penetrate it, a test has to be done. Force, penetration rate and work needed to penetrate the cancellous bone substitute with the range of different working head variations, will be tested. Due to lack of papers with accurate data on penetration rates, forces, amount of work or pressure to penetrate cancellous bone or polyurethane foam, it was decided to test this for the purpose of this paper. To test the magnitude of the impact that is needed to penetrate the target tissue at a certain rate, clear data has to be obtained for the amount of work it takes to penetrate the target material for certain depths. This test will provide answers to the amount of work needed to penetrate the target tissue to a certain depth with each variation of the working heads. This will be done by penetrating the target tissue with a constant velocity and measuring the amount of force it takes to penetrate the target tissue. The force integrated over displacement will results in the total work, in joule [J], needed to move from point x1 to x2, as seen in Equation B.1.

$$W = \int_{x1}^{x2} F dx \tag{B.1}$$

Because only the maximum force needed to penetrate the material over a small distance will be examined, the work equation can be generalised to a more simple equation, shown in Equation B.2, where a constant force, F in newton, is assumed over a certain distance, s in meters.

$$W = F * s \tag{B.2}$$

The work is the amount of energy needed to penetrate the target tissue. This, will than give insight into the amount of kinetic energy that is needed to penetrate the target tissue through impact. In order to generate this kinetic energy, compression springs are utilized in the experiment following the current experiment. The spring constant, k in Newton per millimetre, needed, can be calculated by assuming conservation of energy, which proclaims that the work (Equation B.2) is equal to the spring potential energy, shown by Equation B.3 with x, the compression distance in meters, which allows for the Equation B.4.

$$P = \frac{1}{2} k * x^2 \tag{B.3}$$

$$W = P, F * s = \frac{1}{2} k * x^2 \tag{B.4}$$

Of course, total conservation of energy is not possible. There will be various energy losses, but it will provide an approximation of the range of springs that will be needed, in order to obtain the right amount of kinetic energy for the impact experiment, that will follow out of this experiment.

Method

The test setup that is used to acquire the results consists of four parts:

- **A linear stage:** That will provide the constant penetration velocity to the working head.
- **A load cell:** That will measure the amount of force that is applied, whilst penetrating the target tissue, over a period of time. The load cell has a capacity of 150 kg. The load cell is connected to a Multifunctional NI-DAQMX and a CPJ Analog Transmitter, that will translate the load cells input to useable data which can be utilized by LabVIEW.
- **The working heads:** That will be used to penetrate the target tissue.
- **Target tissue (polyurethane block):** The sample that will used to perform the penetration onto. The dimensions of the sample block are 100 mm x 100 mm x 30 mm.

The test setup, as seen in Figure B.1, will be able to penetrate, with different working heads shown in Figure 3.2, the target tissue. The linear stage will move

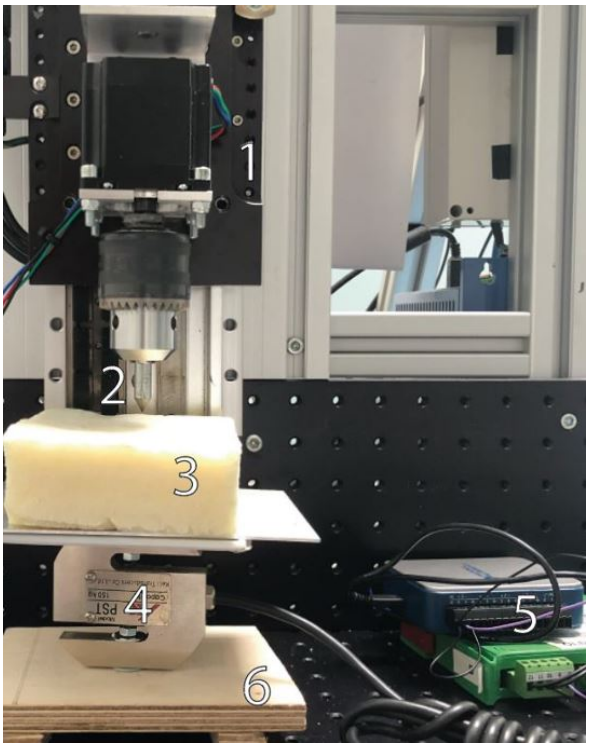

Figure B.1: The setup to test the effect of penetrating a cancellous bone substitute, polyurethane, at constant speed. 1) linear stage, with a chuck attached in order to insert different working heads, 2) the working head that will penetrate the target tissue, 3) the target tissue, consisting of a block of polyurethane, 4) the load cell, 5) A Multifunctional NI-DAQMX and a CPJ Analog Transmitter, 6) the mounting for the load cell and the plateau supporting the block of polyurethane.

downwards at a constant speed of 1.0 mm/s, to allow for accurate measurement of the required work. The linear stage will move the working head over a distance of 25 mm. Over this 25 mm of penetration, 17.5 mm will be examined. For every working head variation the test will be performed four times, to get more accurate results. The chosen penetration range will be of the moment the working head makes contact with the target tissue till the tip of the working head has reached 17.5mm. This distance is chosen, as for every tip variation at this distance, the tip of the working head will be fully inserted into the target tissue, which allows for a more relevant comparison, as some tips have a point while others are blunt. Next to this, the effect of deeper penetration can also be examined, as deeper penetration might require more work, due to friction or accumulation of compressed material in front of the tip. The amount of force exerted by the working head on the target tissue will be measured by a loadcell. This loadcell will measure the force applied over time. The load cell, in combination with a software programme called LabVIEW will measure the required data. Further analysis of this data is done with the help of MATLAB in order to find the required results.

Results

Penetration with the variation of working heads was performed a total of 84 times, 4 times for every single working head of the 21 different working heads. Force over a period of time was measured. From this data, graphs were generated. When examining the graphs (Figure B.2, B.3 and B.4), three variations of lines are found. Of the first two, one has a steep increase in force and then remains constant (Figure B.2), the other has a continuous build-up of pressure till the maximum penetration depth is reached (Figure B.3), in the form of a steep rise in force, followed by a linear and more gradual continuous increase in force. The first variation graph, showing a constant force when an initial depth was reached, only happened for the working head variation 1 and 4, both having a relative sharper tip than the rest. The rest of the working heads showed a continuous increase in force needed to penetrate the target tissue for increasing depth. Some of the more blunt working head variations showed a steep initial increase in force at the start of the penetration, but after that, had a steep drop off of the force, as can be seen in Figure B.4.

Figures B.2, B.3 and B.4 show the standard deviation of the maximum measured forces of each test. The more pointy tip variations show a smaller range of maxima than the other tips. This might indicate that those tips have a more constant penetration force to get to certain depths, which is more beneficial, as it allows for better predictions of the penetration rate of the material with different force inputs. As earlier mentioned, tip variation 1 and 4 displayed a constant pen-

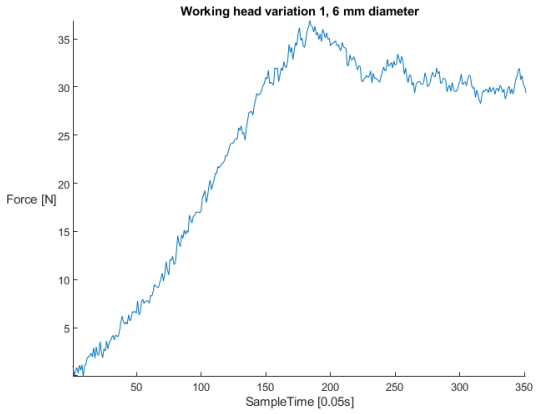

Figure B.2: Force over sample time graph for working head variation 1, with a 6 mm diameter, showing no force increase when a certain depth is reached.

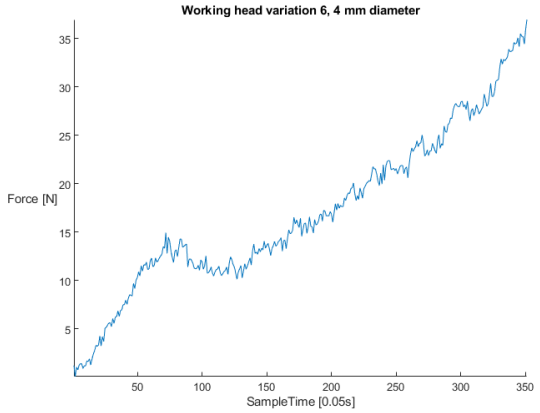

Figure B.3: Force over sample time graph for working head variation 6, with a 4 mm diameter, showing continuous force rise for increasing material depth.

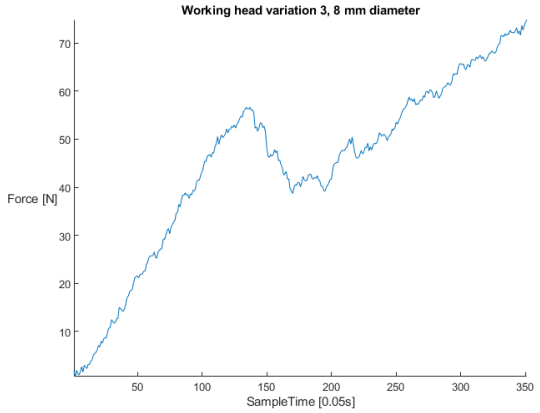

Figure B.4: Force over sample time graph for working head variation 7, with a 8 mm diameter, showing dip after initial force peak is reached.

etration force, when an initial depth was reached. Figure B.5 shows, that tip variation 1 performed slightly better than 4, as it required less force to penetrate the material with the two smallest diameters and had a more constant force needed to penetrate the material, when an initial depth was reached.

Table B.1, shows the average of the 4 individual tests per tip variation. This gives an average of the maximum force that was applied on the target tissue with that particular working head. From this force, the pressure was calculated as well, with the standard force over area equation, where the area was generalised to a flat surface with the relevant diameter. The results can be seen in Table 1 and show, that having a sharper tip decreases the amount of force needed to penetrate the material. Lastly, the flat tip working head, variation 7, needs almost double the force to penetrate the material than the sharpest working head, variation 1, for the smallest two diameters.

Discussion

By examining Figure B.3, it can be noted that it is highly likely that with deeper penetration, the forces might be even higher than measured at the maximum depth of this experiment. This can be seen, as at the end of the measurement, when the maximum depth is reached, the force increase is still slightly linear upwards. This can be explained by possible build-up of material which occurs while penetrating the target tissue at constant velocity, as for the more blunt tips the material accumulates in the direction of penetration. This increases the amount of force needed, as the density of the material increases due to compacting of the material. For the sharper tip variations, it is most likely that they push the material to the side, resulting in a more constant penetration force required, as can be seen in Figure B.2, as there is minimum accumulation of the material in the direction of penetration. For penetrating cancellous bone by using a repeated impact method, this would be a great benefit, as no removal of resected bone material is needed, because the material gets compacted to the sides. This might also increase the holding strength of potential screws being placed in the formed holes. Figure B.4 could be explained by the initial large increase of load, which causes fast accumulation of material in front of the tip. If the load then keeps increasing, the material might succumb to the pressure, causing the tip to shoot forward with little resistance, hence the drop in force. This might be disadvantageous when performing drilling in the vertebra as the operator might slip due to the sudden decrease in resistance of the material, which might have detrimental effects. Furthermore, Table B.1 shows that increasing the working head diameter, decreases the amount of pressure over the penetration area needed to penetrate the material. This might be caused by the slightly elastic properties of polyurethane foam, found in appendix A, of the target material. This might cause more friction to the smaller diameter working heads than to the larger diameter working heads, through clamping the working heads due to elastic pushback of the material. This would have a larger effect on smaller diameters than on larger diameters. All in all, tip variation 1 and 4 were most efficient as they required the least penetration force. Next to this, they showed that they required a relative constant penetration force, to penetrate the material, which is also beneficial.

Conclusion

With the maximum force measured, the amount of work can be calculated, which is needed to penetrate the material at the maximum depth of this experiment. By taking equation B.2 over a distance of 2 mm with the maximum force that was found, by working head

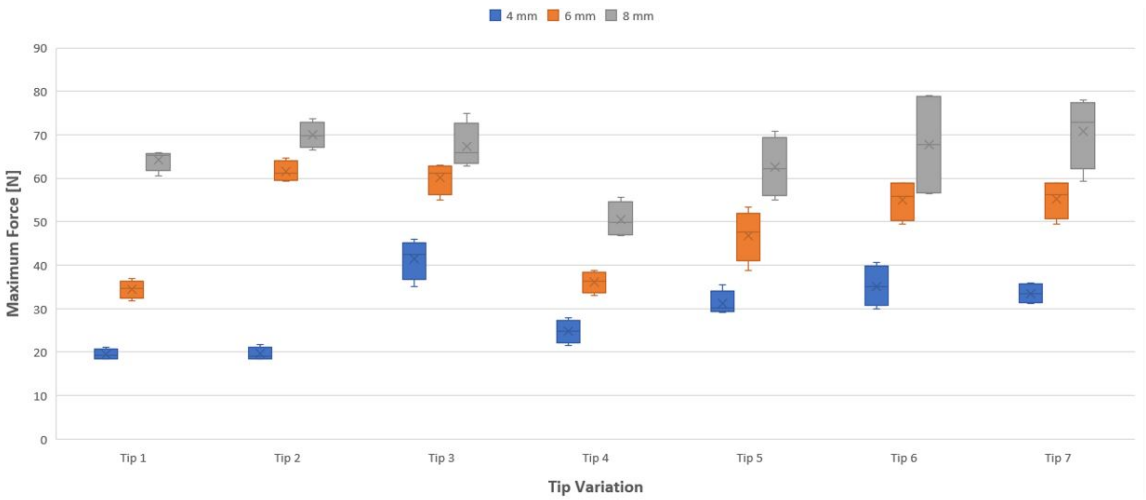

Figure B.5: Standard deviation of the maximum measured forces of each test. The working head (tip) variation number is shown in Figure 3.2.

Compression test: tip variation	**Diameter of the working head**					
	4 mm		**6 mm**		**8 mm**	
Tip variation*	Maximum average Force (N)	Maximum average Pressure (Mpa)	Maximum average Force (N)	Maximum average Pressure (Mpa)	Maximum average Force (N)	Maximum average Pressure (Mpa)
1	19.5	1.55	34.5	1.22	64.3	1.28
2	19.6	1.56	61.6	2.18	69.9	1.39
3	41.5	3.3	60.1	2.13	67.4	1.34
4	24.7	1.97	36.1	1.28	50.5	1
5	31.2	2.48	46.8	1.66	62.6	1.24
6	35.2	2.8	55.1	1.95	67.7	1.35
7	33.5	2.66	55.3	1.95	70.8	1.41

Table B.1: This table presents the average of the maximum forces [N] needed, for each test, to penetrate the target tissue for every single working head to a depth of 17.5 mm for 17.5 seconds, with a penetration speed of 1 mm/s. Next to this, from this maximum force, the maximum pressure [MPa] is calculated and presented table as well. * The working head (tip) variation number is shown in Figure 3.2.

variation 7 with an 8 mm diameter, a work of 0.142 Joule is found. The distance of 2 mm was chosen to also have the ability to see if fast penetration of the working heads was possible. With this result, the range of energy, the compression spring will need, in order to, penetrate the target tissue with 2 mm per strike, is set, as shown by equation B.4. With this range the spring constant of the spring needed can be decided, that will be able to generate the amount of energy needed to penetrate the target tissue, with the various working heads. As there will be losses due to friction, air resistance, thermodynamics and possible recoil of the tip when it strikes the target tissue, the maximum amount of energy needed is doubled, to ensure the losses are accounted for and penetration will still be possible with all tip variations. The maximum energy needed will be set to 0.282 Joule, calculated with the previous set parameters and Equation B.4. To allow for a sufficient variation in different impact magnitudes, that will be delivered by the spring, a minimum compression distance of the spring is set to 30 mm. This distance is chosen, as is believed that this will allow for a sufficient range of different impact magnitudes to be analysed. By inserting the established prerequisites, a minimum compression capability of 30 mm and maximum energy of 0.282 Joule, into Equation B.3, a spring constant of 0.63 newton per millimetre is found. A spring, with a spring constant in the range of the established spring constant, will be utilized in the succeeding impact experiment.

C

Impact test: Sawbones, cancellous bone replica sample

Overview

To establish the right parameters that will be used to penetrate cancellous bone, an impact test of the final tip variant (Tip Variant 4, ∅ 4 mm, Figure 3.2) on a cancellous bone replica sample, with a compression strength and porosity characteristics in the range of actual cancellous bone of the vertebra, must be performed. The goal of this test will establish the impulse required to achieve a certain penetration rate that will be used for the final proof of principle instrument that will be designed. In the previous tests, done in Chapter 3, the store bought polyurethane foam was used, described in Appendix B. For the new test, a new cancellous bone replica sample is utilized from the Company Sawbones. They provide certified professional made and tested bone replica models and samples, with a variety of mechanical characteristics. In this new test, the impact test on the Sawbones sample, comparison to the previous used polyurethane foam will be done, in order to, validate that tip variant has the same desirable tip characteristics when performing the impact, as was seen while testing impact on the polyurethane foam. This is because, the desired tip characteristics, higher penetration rate and no material accumulation, that were found with the use of the polyurethane foam, are also desired for the new sample, in order for, tip variation 4 to still be a viable variant.

Method

The test set up used for this test is exactly the same as the one used for the impact tests in Chapter 3, including the same spring (∅24.4 mm, spring constant k=0.78 N mm^{-1}). The only difference is that instead of the block polyurethane foam, as target tissue, another material is used. For this test a block of Solid Foam, 10 PCF, 130 mm x 180 mm x 40 mm (*Sawbones, USA)* is utilized. The material has a compressive strength of 2.2 MPa, which is in the range of actual cancellous bone of the vertebra (0.60 MPa to 6.17 MPa with a mean of 2.37 MPa [64]). Next to this, it provides consistent properties that are in the range of human cancellous bone. The sample conforms to the ASTM F-1839-08 *"Standard Specification for Rigid Polyurethane Foam for Use as a Standard Material for Testing Orthopaedic Devices and Instruments"*.

The only tip variant used during this experiment will be Tip Variant 4 (Figure 3.2), which will be mounted to the distal end of the linear slider (Figure 3.3.a4). A total of 3 test sets will be performed for each compression distance. A test set consists of ten sequential strikes with the same compression distance of the spring. Compressing the spring and releasing it will form the impulse the tip variant will perform onto the Sawbones sample, the target tissue. After the ten strikes are performed, the depth of the indent in the sample, will be measured. This measurement will result into the penetration rate [mm/strike], calculated simply by dividing the depth by the ten strikes. A total of 5 different compression distances of the spring will be tested. These are 10 mm, 15 mm, 20 mm, 25 mm and 30 mm. This will give a sufficient variety of impulses with their related penetration rates, from were the final instrument can be designed. Next to this, the effect these impulses will have on the target tissue can be examined, as well as, to see if they compare to the previous used polyurethane block in Chapter 3.

Results

The impact test with the tip variant 4, with O.D. 4 mm, was performed a total of fifteen times. The test was done three times for every compression distance, with a test consisting of ten strikes. Force, caused by the impulse of the tip, over a period of time was measured, with the loadcell. From this data, the impulse of each strike could be calculated with the help of Equation 3.4. Next to this, the depth of the hole that was created after the ten strikes was measured with the use of a caliper. This depth measurement averaged over

the ten strikes resulted into the penetration rate. The results of these two measurements are presented in Table C.1.

Discussion

The impact test has proven to still be viable using a cancellous bone replica material with a higher compression strength. This is because it is still possible to create holes using the impact method. Furthermore it is observed that a same sort of hole forms, when the working head strikes the target tissue. The material gets pushed to the side, just as what happened with the initial polyurethane foam. This is beneficial as there will be no need for resected bone removal and the sides of the formed hole will become more compact, which could increase the holding strength of a potential future placed screw. Furthermore, no crackforming was found while striking the target tissue. Next to this, an obvious increase in impulse, needed to achieve the same penetration rate as the previous test in Chapter 3, was found. This was caused by the increase in compression strength of the Sawbones material compared to the initial polyurethane foam material. When comparing Table C.1 with Figure 3.4, a decrease in penetration rate between 5 and 6 is found, whilst the compression strength of the material increased by around a factor of ten. The penetration rate still showed a relative large range between ± 5 % to 10 %, similar to the initial used polyurethane foam, except that there were no real outliers. The two aforementioned points are most likely caused because of the Sawbones material being more consistent throughout the material than the initial polyurethane foam material, which is beneficial for testing, as it results into more consistent measurements. Furthermore, it was found that the new material had less damping than the initial material, as can be seen in Figure C.1, where the impulse of the new material takes about half the time to recede, as the same impulse on the initial material. This means the new material is less elastic, resulting in less friction of the working head with the material, as the new material will contract less around the working head than the initial material. This might result into a relative less impulse magnitude needed to gain the same penetration rate, were it a more elastic material like the initial polyurethane material. This means less impact has to be applied on the patient, were it being actually used on real cancellous bone of the vertebra. Furthermore, less elasticity could be a more beneficial effect, as this means the material returns to its rest state faster. Because of this, the frequency can be increased without having to worry about possible other effects that might occur if the material receives an impact whilst still being effected by the previous impact. Although, this might not be a problem at all, as no tests have been performed where this phenomenon was tested.

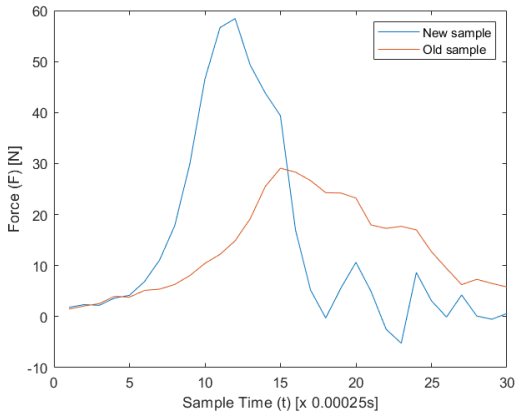

Figure C.1: Two impulses, equal in magnitude and with the same tip variation (tip variation 4, ∅ 4 mm, Figure 3.2), performed on the two cancellous bone replica samples, with blue) the new sample used from Sawbones, and orange) the initial polyurethane foam material used in the initial tests.

Conclusion

A range of different compression distances has been tested with tip variation 4, with O.D. 4 mm, on the new cancellous bone replica material from *Sawbones, USA*. This resulted in a list of different impulse magnitudes with a certain related penetration rate. This data can be used to design the proof of principle instrument. With a spring compression distance of 30 mm a penetration rate of almost 1 mm per strike was achieved. This is believed to be more than sufficient for drilling into a vertebra. Therefore, the aim of the instrument will be to achieve a maximum penetration rate of 1 mm per strike as a benchmark. If the instrument can achieve this, without complications, it has proven its viability as a possible method for possible steerable drilling using the impact method in a future surgical device. Such a penetration rate will be too fast for the delicate surgical procedure, which is drilling into a vertebra. But if it can achieve this penetration rate, it can achieve lower penetration rates. For testing with the proof-of-principle instrument the new material from the company Sawbones will be continued to be utilized. Next to the one used in this test, two other samples, with different compression strengths, will be used, to simulate different bone strengths of different patients.

Compression Distance Spring	**Penetration Depth [mm]**	**Penetration Rate [strike/mm]**	**Impulse [Ns]**
10mm	2.93 ± 0.28	0.293 ± 0.028	0.077 ± 0.005
15mm	4.0 ± 0.46	0.40 ± 0.046	0.100 ± 0.001
20mm	5.97 ± 0.40	0.597 ± 0.040	0.149 ± 0.005
25mm	7.57 ± 0.31	0.757 ± 0.031	0.177 ± 0.009
30mm	9.50 ± 0.70	0.950 ± 0.070	0.198 ± 0.022

Table C.1: Overview of the experimental results from the impact test on the new cancellous bone replica sample from the company Sawbones, USA. The table presents the penetration depth, that was achieved for each test, penetration rate and the impulse that was related to that test. The values are indicated as mean ± standard deviation (n=10). The three values were measured for the five different spring compression distances.

D

Hydraulic pressure wave

Hydraulic pressure wave formation

In order to create a bendable drilling shaft, a method must be utilized that can translate the impulse, generated at the proximal end of the instrument, towards the working head, at the distal end of the instrument. To achieve this, a bendable tube, filled with liquid, is utilized. The impulse generated at the proximal end of the instrument, will be translated through the tube in the form of an hydraulic impulse, also known as a longitudinal hydraulic pressure wave. The hydraulic pressure wave is caused by changing the velocity of a non-compressible liquid suddenly. Pressure energy is changed to kinetic energy in the form of a pressure wave. The hydraulic pressure wave will travel through a medium till it dissipates by either pressure loss over time or if it strikes an obstruction making it bounce back, losing energy in the process. This bouncing back repeats itself, resulting in the wave traveling back and forth through the medium, till the wave is fully dissipated. The hydraulic pressure wave will translate through the tube towards the distal end, where it will activate the working head, which will perform the impulse on the target tissue, as seen in Figure D.1 . This method has been proven to work by Sakes *et al* [52].

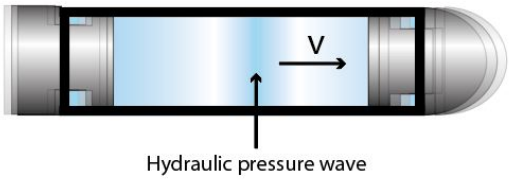

Figure D.1: A longitudinal hydraulic pressure wave, represented by the compressed blue region, travelling to the right with a wave velocity v [m/s]. The pressure wave gets created by the plunger, on the left side, compressing the liquid in the tube in a sudden motion. This creates a compressed region in the liquid, which in turn pushes against the neighboring region, forming a pressure wave through the liquid. Arriving at the distal end, the wave pushes against the working head, accelerating it and making it shoot forward.

Hydraulic pressure wave transfer

The hydraulic pressure wave will travel through the medium with a certain velocity. This velocity can be calculated with equation D.1. The equation, explained in the paper of Sakes *et al* [52], presents a formula to calculate, in a thin-walled cylindrical pipe, the velocity of the hydraulic pressure wave, v [m/s].

$$v = \sqrt{\frac{1}{\rho\left(\frac{1}{K} + \frac{D}{Ee}\right)}} \tag{D.1}$$

The equation takes the Young's modules, E [Pa], and wall thickness, e [m], of the tube into account. Increasing either one, makes the pipe stiffer, hence increases the velocity. Increasing the diameter of the pipe, D [m], has the opposite effect. It decreases the wave velocity. Furthermore, the bulk modules, K [Pa], and the density of the fluid, ρ [kg/m^3] also affect the velocity. The pressure wave causes rarefactions and compressions in the fluid medium. The velocity is, therefore, related to compressibility of the fluid. The bulk modules of the fluid represents this difficulty of fluid compression. Next to this, the inertia of the fluid, which causes the resistance to the return or alteration of the equilibrium state, is represented by the density, due to mass being involved [52].

Hydraulic pressure wave losses

Fluid propagating through a tube, cannot be done without encountering some losses. One of these losses is caused by the no-slip condition for viscous fluids. This condition assumes that fluid will have zero velocity relative to a solid medium. At the fluid-solid boundary, all fluid velocity is equal to that of the solid boundary [65]. The no-slip condition is well explained for conventional pipe-flow. Unfortunately this is not the case for propagating pressure waves. Therefore, in the paper of Sakes *et al* [52], a simulation was done, to establish the effect of a propagating wave in relation with the no-slip condition. It was found that the no-slip condition did have an effect on the decay of the propagating wave. For this reason the volume to

surface area of the tube plays an important role in the efficiency of the transmission of the hydraulic pressure wave through the medium. Furthermore, it was found that, due to surface roughness, a higher magnitude pressure wave loses its energy faster than a lower magnitude pressure wave [52].

Another reason for dissipation of the hydraulic pressure wave is due to partial or total deflection of the wave at the fluid-solid boundaries, which can be caused by having a non-linear tube, a sudden decrease in the inner-diameter of the tube or due to the wave hitting a wall at the end of the tube. Furthermore, the elasticity of the tube wall plays a part in the dissipation speed of the hydraulic pressure wave, as well. Shear stress (explained by the no-slip condition before), axial compression of the wall and movement of the tube, all take energy from the propagating hydraulic pressure wave, hence increasing the decay of the wave. For all these reasons, it is important to select the right tubing, which will allow for the most efficient transmission of the hydraulic pressure wave [52].

Cross-sectional form of the transmitting part

Due to the friction loss, explained in the previous section, the cross-sectional shape plays an important role in the efficiency of the wave transmittance. The best tube cross-sectional shape is found to be the circle. To give an example of why this is, imagine having a circular pipe with a diameter of 0.1 m. If we were to compare it with a square pipe with the same cross-sectional area, we would need a square with 0.1773 m sides. If we calculate the perimeter of both pipes we find that the circular is equal to 0.6286 m and the square pipe is equal to 0.7092 m. Because frictional resistance depends on magnitude of the inner perimeter of the pipe, the resistance, due to the no-slip condition, will be 13% more using a square pipe, than using a circular one.

As explained in the previous section, the elasticity of the wall of the tube, which is related to the Young's modules and the wall thickness, also effect the efficiency of the transmission of the hydraulic pressure wave. However, finding and choosing an optimal wall thickness and material to use for the tubing will be a very difficult task, as the tube must abide to certain criteria. For this reason, it is best to choose a tube with a high enough burst pressure, that will barely expand if a pressure is introduced within the tube, but can still make a bend of 90 degrees over the entire length of the tube.

E

Proof of principle experiment setup variations

This Appendix presents the different variations of the proof of principle experiment, presented in Chapter 5, that was utilized to prove the application of drilling in cancellous bone with the use of hydraulic shockwaves through a bendable medium, as seen in Figures E.1, E.2, E.3, E.4, E.5, E.6, E.7, and E.8. Explanation of the fabrication and workings of the proof of principle experiment are also given in Chapter 5.

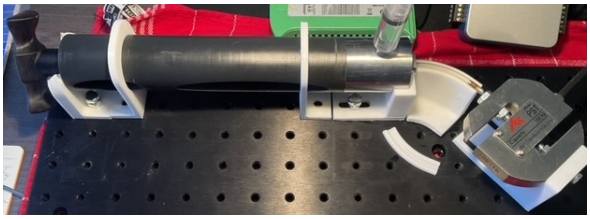

Figure E.1: Proof of principle experiment with the 45 degrees curvature tube holder module. This setup was utilized in order to proof that the instrument would still have an impact output if the tube was bend at a 45 degrees angle over the entire length of the tube excluding the tip part.

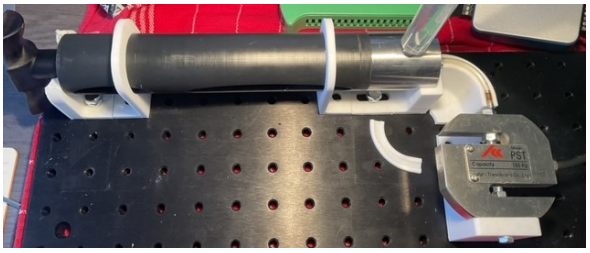

Figure E.2: Proof of principle experiment with the 90 degrees curvature tube holder module. This setup was utilized in order to proof that the instrument would still have an impact output if the tube was bend at a 90 degrees angle over the entire length of the tube excluding the tip part.

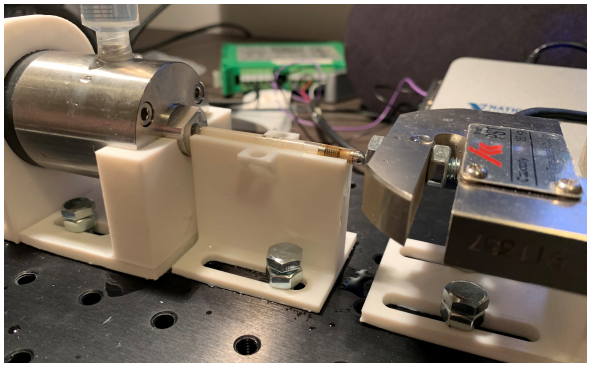

Figure E.3: Close up showing the 0 degrees curvature tube holder module.

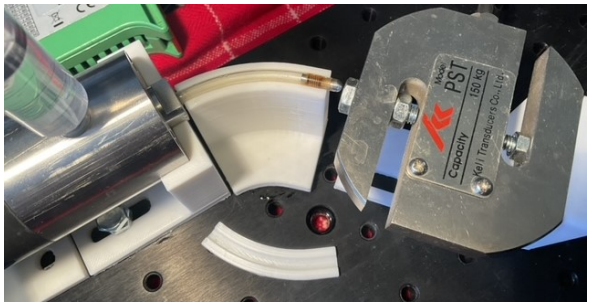

Figure E.4: Close up showing the 45 degrees curvature tube holder module. The white part next to the tube holder module is the top part of the tube holder module, used for securing the tube in place so no movement occurs from the tube itself. This is used so the wave can travel through the tube without losing additional energy to unwanted movement of the tube.

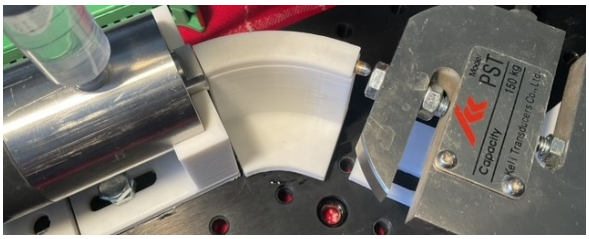

Figure E.5: Close up showing the 45 degrees curvature tube holder module with the additional white part secured on top of the tube to fixate the tube in the correct curvature and withholding it from additional movement of the tube when the impact tests are performed.

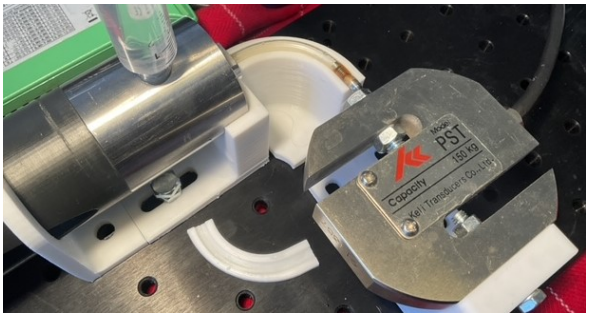

Figure E.6: Close up showing the 90 degrees curvature tube holder module. The white part next to the tube holder module is the top part of the tube holder module, used for securing the tube in place so no movement occurs from the tube itself. This is used so the wave can travel through the tube without losing additional energy to unwanted movement of the tube.

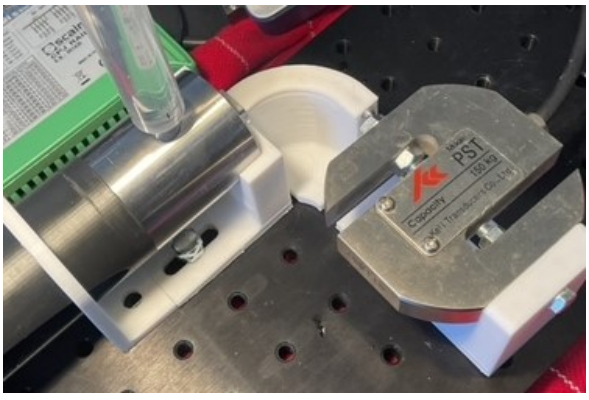

Figure E.7: Close up showing the 90 degrees curvature tube holder module with the additional white part secured on top of the tube to fixate the tube in the correct curvature and withholding it from additional movement of the tube when the impact tests are performed.

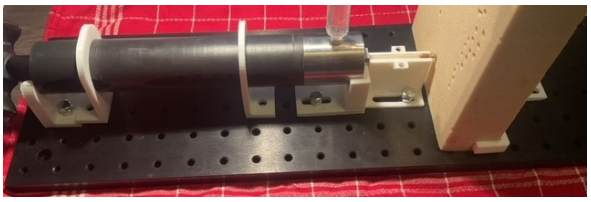

Figure E.8: Use case experiment of the proof of principle instrument. In this setup, the impact output of the tip is used to examine if it is strong enough to cause indentation in the cancellous bone sample. The sample is secured in a 3D printed clamp. This clamp allows for the sample to be moved forwards and backwards, in relation to the instrument, where after when the right position is found in relation to the tip, the sample is secured.

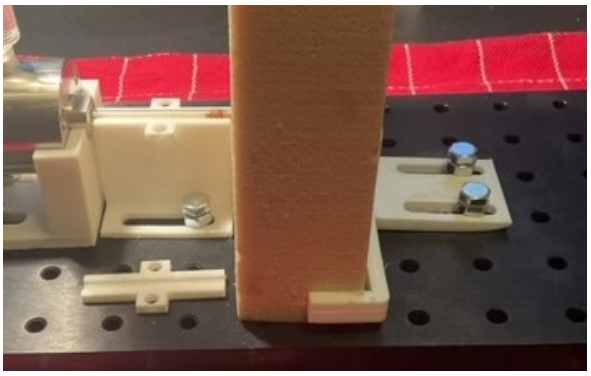

Figure E.9: Side view of the use case experiment of the proof of principle instrument. On the left is the tube holder module supporting the tube with the tip that will perform the impact upon the cancellous bone sample, which is located in the middle of the Figure. To the right is the clamp module, holding the cancellous bone sample in place. The clamp module can be moved forwards and backwards with the use of the grooves and after the right location is obtained, the clamp module is secured fastly to fixate the cancellous bone sample in place.

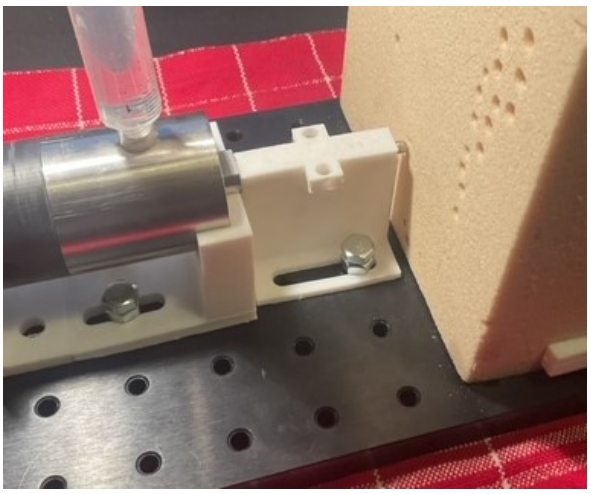

Figure E.10: Close up of the tube holder module with the distal end of the tip in contact with the cancellous bone sample. This was the starting position of every impact test of the use case experiment. The additional holes located in the sample are from previous experiments not related to this experiment.

Bibliography

[1] D. Krogh. *Biology: A Guide to the Natural World*. Benjamin Cummings, 2011. ISBN: 9780321616555. URL: https://books.google.nl/books?id=Ph7NSAAACAAJ.

[2] Bahaa Kornah et al. "Review of Spinal Pedicle Screws". In: (July 2019).

[3] *Anatomy of the spine*. June 2019. URL: https://www.sci-info-pages.com/anatomy-of-the-spine/.

[4] Michael W. Devereaux. "Anatomy and Examination of the Spine". In: *Neurologic Clinics* 25.2 (2007), pp. 331–351. ISSN: 0733-8619. DOI: 10.1016/j.ncl.2007.02.003.

[5] *Spine anatomy*. Feb. 2021. URL: https://www.goodmancampbell.com/conditions/spine/spine-anatomy/.

[6] Vincent J. Miele, Manohar M. Panjabi, and Edward C. Benzel. "Anatomy and biomechanics of the spinal column and cord". In: *The Human Hypothalamus - Neuroendocrine Disorders*. The Human Hypothalamus - Neuroendocrine Disorders, 2012, pp. 31–43. DOI: 10.1016/b978-0-444-52137-8.00002-4.

[7] Max Aebi. "The adult scoliosis". In: *European Spine Journal* 14.10 (2005), pp. 925–948. ISSN: 0940-6719. DOI: 10.1007/s00586-005-1053-9.

[8] Lawrence G. Lenke et al. "Rationale Behind the Current State-of-the-Art Treatment of Scoliosis (in the Pedicle Screw Era)". In: *Spine* 33.10 (2008). ISSN: 0362-2436. URL: https://journals.lww.com/spinejournal/Fulltext/2008/05010/Rationale_Behind_the_Current_State_of_the_Art.2.aspx.

[9] Deepak Awasthi and Najeeb Thomas. "Pedicle screw placement". In: (). URL: https://www.medschool.lsuhsc.edu/neurosurgery/nervecenter/tlscrew.html.

[10] Thomas M. Shea et al. "Designs and Techniques That Improve the Pullout Strength of Pedicle Screws in Osteoporotic Vertebrae: Current Status". In: *BioMed Research International* 2014 (2014), pp. 1–15. ISSN: 2314-6133. DOI: 10.1155/2014/748393. URL: https://dx.doi.org/10.1155/2014/748393.

[11] Amir Manbachi, Richard S.C. Cobbold, and Howard J. Ginsberg. "Guided pedicle screw insertion: techniques and training". In: *The Spine Journal* 14.1 (2014), pp. 165–179. ISSN: 1529-9430. DOI: 10.1016/j.spinee.2013.03.029.

[12] John M. Hicks et al. "Complications of Pedicle Screw Fixation in Scoliosis Surgery: A Systematic Review". In: *Spine* 35.11 (2010). ISSN: 0362-2436. URL: https://journals.lww.com/spinejournal/Fulltext/2010/05150/Complications_of_Pedicle_Screw_Fixation_in.19.aspx.

[13] Boucher H. H. "A method of spinal fusion". In: *J Bone Joint Surg Br* 41-b (1959), pp. 248–59. ISSN: 0301-620X.

[14] Harrington P. R. and Tullos H. S. "Reduction of severe spondylolisthesis in children". In: *South Med J* 62 (1969), pp. 1–7. ISSN: 0038-4348.

[15] JAMES N. WEINSTEIN, BJORN L. RYDEVIK, and WOLFGANG RAUSCHNING. "Anatomic and Technical Considerations of Pedicle Screw Fixation". In: *Clinical Orthopaedics and Related Research*® 284 (1992). ISSN: 0009-921X. URL: https://journals.lww.com/clinorthop/Fulltext/1992/11000/Anatomic_and_Technical_Considerations_of_Pedicle.6.aspx.

[16] Tsung-Jen Huang et al. "The State of the Art in Minimally Invasive Spine Surgery". In: *BioMed Research International* 2017 (2017), pp. 1–4. ISSN: 2314-6133. DOI: 10.1155/2017/6194016. URL: https://dx.doi.org/10.1155/2017/6194016.

[17] Gianluca Vadalà et al. "Robotic Spine Surgery and Augmented Reality Systems: A State of the Art". In: *Neurospine* 17.1 (2020), pp. 88–100. ISSN: 2586-6583. DOI: 10.14245/ns.2040060.030.

[18] Frank Phillips et al. “Breaking Through the "Glass Ceiling" of Minimally Invasive Spine Surgery”. In: *Spine* 41 Suppl 8 (Feb. 2016). DOI: 10.1097/BRS.0000000000001482.

[19] Alexander J. Butler et al. “Endoscopic Lumbar Surgery: The State of the Art in 2019”. In: *Neurospine* 16.1 (2019), pp. 15–23. ISSN: 2586-6583. DOI: 10.14245/ns.1938040.020. URL: https://dx.doi.org/10.14245/ns.1938040.020.

[20] Thorsten Tjardes et al. “Image-guided spine surgery: state of the art and future directions”. In: *European Spine Journal* 19.1 (2010), pp. 25–45. ISSN: 0940-6719. DOI: 10.1007/s00586-009-1091-9. URL: https://dx.doi.org/10.1007/s00586-009-1091-9.

[21] Amir Manbachi, Richard S.C. Cobbold, and Howard J. Ginsberg. “Guided pedicle screw insertion: techniques and training”. In: *The Spine Journal* 14.1 (2014), pp. 165–179. ISSN: 1529-9430. DOI: 10.1016/j.spinee.2013.03.029.

[22] Faris Shweikeh et al. “Robotics and the spine: a review of current and ongoing applications”. In: *Neurosurgical Focus* 36.3 (2014), E10. ISSN: 1092-0684. DOI: 10.3171/2014.1.focus13526.

[23] Adrian Elmi-Terander et al. “Pedicle Screw Placement Using Augmented Reality Surgical Navigation With Intraoperative 3D Imaging”. In: *Spine* 44.7 (2019), pp. 517–525. ISSN: 0362-2436. DOI: 10.1097/brs.0000000000002876.

[24] J -Y Giraud et al. “Bone cutting”. In: *Clinical Physics and Physiological Measurement* 12.1 (Feb. 1991), pp. 1–19. DOI: 10.1088/0143-0815/12/1/001. URL: https://doi.org/10.1088/0143-0815/12/1/001.

[25] Rosario Rullo et al. “Piezoelectric device vs. conventional rotative instruments in impacted third molar surgery: Relationships between surgical difficulty and postoperative pain with histological evaluations”. In: *Journal of Cranio-Maxillofacial Surgery* 41.2 (Mar. 1, 2013), e33–e38. ISSN: 1010-5182. DOI: 10.1016/j.jcms.2012.07.007. URL: https://www.sciencedirect.com/science/article/pii/S1010518212001576.

[26] Guangjun Wang et al. “An inverse method to reconstruct the heat flux produced by bone grinding tools”. In: *International Journal of Thermal Sciences* 101 (2016), pp. 85–92. ISSN: 1290-0729. DOI: 10.1016/j.ijthermalsci.2015.10.021.

[27] Alexander Sendrowicz et al. “Surgical drilling of curved holes in bone – a patent review”. In: *Expert Review of Medical Devices* 16.4 (2019), pp. 287–298. ISSN: 1743-4440. DOI: 10.1080/17434440.2019.1596794.

[28] Vishal Gupta et al. “In vitro comparison of conventional surgical and rotary ultrasonic bone drilling techniques”. In: *Proceedings of the Institution of Mechanical Engineers, Part H: Journal of Engineering in Medicine* 234.4 (2020), pp. 398–411. ISSN: 0954-4119. DOI: 10.1177/0954411919898301.

[29] Ricardo D. Gonzalez, Bryant M. Whiting, and Benjamin K. Canales. “The History of Kidney Stone Dissolution Therapy: 50 Years of Optimism and Frustration With Renacidin”. In: *Journal of Endourology* 26.2 (2012), pp. 110–118. ISSN: 0892-7790. DOI: 10.1089/end.2011.0380. URL: https://dx.doi.org/10.1089/end.2011.0380.

[30] Stefanos Kachrilas et al. “The current role of percutaneous chemolysis in the management of urolithiasis: review and results”. In: *Urolithiasis* 41.4 (2013), pp. 323–326. ISSN: 2194-7228. DOI: 10.1007/s00240-013-0575-6.

[31] Karsten Schwieger et al. “Abrasive water jet cutting as a new procedure for cutting cancellous bone?In vitro testing in comparison with the oscillating saw”. In: *Journal of Biomedical Materials Research* 71B.2 (2004), pp. 223–228. ISSN: 0021-9304. DOI: 10.1002/jbm.b.10078.

[32] Umberto Romeo et al. “Bone damage induced by different cutting instruments: an in vitro study”. In: *Brazilian Dental Journal* 20.2 (2009), pp. 162–168. ISSN: 0103-6440. DOI: 10.1590/s0103-64402009000200013.

[33] Amir Reza Abedi et al. “Pneumatic Lithotripsy Versus Laser Lithotripsy for Ureteral Stones”. In: *Journal of Lasers in Medical Sciences* 9.4 (2018), pp. 233–236. ISSN: 2008-9783. DOI: 10.15171/jlms.2018.42.

[34] Angelo Troedhan et al. “Cutting bone with drills, burs, lasers and piezotomes: A comprehensive systematic review and recommendations for the clinician”. In: *International Journal of Oral and Maxillofacial Research* 3 (Aug. 2017), pp. 20–33. DOI: 10.17352/2455-4634.0000128.

[35] Roland Vorreuther et al. “Investigative Urology: Impact of Shock Wave Pattern and Cavitation Bubble Size on Tissue Damage During Ureteroscopic Electrohydraulic Lithotripsy”. In: *Journal of Urology* 153.3 (1995), pp. 849–853. ISSN: 0022-5347. DOI: 10.1016/s0022-5347(01)67734-6.

[36] John D. Denstedt and Ralph V. Clayman. “Electrohydraulic Lithotripsy of Renal and Ureteral Calculi”. In: *The Journal of Urology* 143.1 (1990), pp. 13–17. ISSN: 0022-5347. DOI: https://doi.org/10.1016/S0022-5347(17)39850-6. URL: https://www.sciencedirect.com/science/article/pii/S0022534717398506.

[37] *Kidney stone Treatment: Shock wave lithotripsy*. May 2021. URL: https://www.kidney.org/atoz/content/kidneystones_shockwave.

[38] Simin Li et al. “Penetration of cutting tool into cortical bone: Experimental and numerical investigation of anisotropic mechanical behaviour”. In: *Journal of Biomechanics* 47.5 (2014), pp. 1117–1126. ISSN: 0021-9290. DOI: 10.1016/j.jbiomech.2013.12.019. URL: https://dx.doi.org/10.1016/j.jbiomech.2013.12.019.

[39] Granta Design Limited. *Granta EduPack 2020*. Version 20.1.1. URL: https://www.ansys.com/products/materials/granta-edupack.

[40] Renae Mulligan et al. “Effect of Penetration Rate on Insertion Force in Trabecular Bone Biopsy”. In: (June 2010).

[41] H. Zaïdi, A. Senouci, and J. Frêne. “Study of Magnetized Sliding Contact Nickel/Stainless Steel.” In: *Thinning Films and Tribological Interfaces*. Ed. by D. Dowson et al. Vol. 38. Tribology Series. Elsevier, 2000, pp. 293–301. DOI: https://doi.org/10.1016/S0167-8922(00)80134-0. URL: https://www.sciencedirect.com/science/article/pii/S0167892200801340.

[42] Edward Ellis and W.J. Gallo. “Use of a pneumatic osteotome to simplify orthognathic surgery”. In: *International Journal of Oral and Maxillofacial Surgery* 16.2 (1987), pp. 245–247. ISSN: 0901-5027. DOI: 10.1016/s0901-5027(87)80141-8.

[43] Yasar Cokkeser et al. “Hammer-Chisel Technique in Endoscopic Dacryocystorhinostomy”. In: *Annals of Otology, Rhinology Laryngology* 112.5 (2003), pp. 444–449. ISSN: 0003-4894. DOI: 10.1177/000348940311200511.

[44] Ibrahim Çukurova et al. “Comparison of Piezosurgery and Hammer-Chisel in Endoscopic Dacryocystorhinostomy”. In: *Journal of Craniofacial Surgery* 29.6 (2018). ISSN: 1049-2275. URL: https://journals.lww.com/jcraniofacialsurgery/Fulltext/2018/09000/Comparison_of_Piezosurgery_and_Hammer_Chisel_in.55.aspx.

[45] İ. Koçak, R. Doğan, and O. Gökler. “A comparison of piezosurgery with conventional techniques for internal osteotomy”. In: *European Archives of Oto-Rhino-Laryngology* 274.6 (2017), pp. 2483–2491. ISSN: 0937-4477. DOI: 10.1007/s00405-017-4514-y.

[46] M.E. Schafer. “Ultrasonic surgical devices and procedures”. In: 2015, pp. 633–660. DOI: 10.1016/b978-1-78242-028-6.00021-1.

[47] Dong Sun et al. “Development and application of ultrasonic surgical instruments”. In: *IEEE Transactions on Biomedical Engineering* 44.6 (1997), pp. 462–467. ISSN: 0018-9294. DOI: 10.1109/10.581934.

[48] Umberto Romeo et al. “Bone damage induced by different cutting instruments: an in vitro study”. In: *Brazilian Dental Journal* 20.2 (2009), pp. 162–168. ISSN: 0103-6440. DOI: 10.1590/s0103-64402009000200013.

[49] Philippe Hennet. “Piezoelectric Bone Surgery: A Review of the Literature and Potential Applications in Veterinary Oromaxillofacial Surgery”. In: *Frontiers in Veterinary Science* 2 (2015). ISSN: 2297-1769. DOI: 10.3389/fvets.2015.00008. URL: https://dx.doi.org/10.3389/fvets.2015.00008.

[50] Sneha Puri. “The Present Status and Current Understanding of Piezosurgery”. In: (2018).

[51] Graham Gavin, M.s.J. Hashmi, and Garrett Mcguinness. “Experimental and Numerical Investigation of Therapeutic Ultrasound Angioplasty”. In: (Jan. 2005).

[52] Aimée Sakes et al. “Crossing Total Occlusions using a hydraulic pressure wave: a feasibility study”. In: *Biomedical Physics & Engineering Express* 4.5 (Aug. 2018), p. 055019. DOI: 10.1088/2057-1976/aad44a. URL: https://doi.org/10.1088/2057-1976/aad44a.

[53] Leen Van Wijngaarden. “Mechanics of collapsing cavitation bubbles”. In: *Ultrasonics Sonochemistry* 29 (2016), pp. 524–527. ISSN: 1350-4177. DOI: 10.1016/j.ultsonch.2015.04.006. URL: https://dx.doi.org/10.1016/j.ultsonch.2015.04.006.

[54] Alan Macbeath. “Ultrasonic Bone cutting”. In: (Mar. 2006).

[55] Purvi Sd Patel, Duncan Et Shepherd, and David Wl Hukins. “Compressive properties of commercially available polyurethane foams as mechanical models for osteoporotic human cancellous bone”. In: *BMC Musculoskeletal Disorders* 9.1 (2008), p. 137. ISSN: 1471-2474. DOI: 10.1186/1471-2474-9-137. URL: https://dx.doi.org/10.1186/1471-2474-9-137.

[56] *Kidney stone Treatment: Shock wave lithotripsy*. May 2021. URL: https://www.kidney.org/atoz/content/kidneystones_shockwave.

[57] Giovanni F. Solitro et al. “Currently Adopted Criteria for Pedicle Screw Diameter Selection”. In: *International Journal of Spine Surgery* 13.2 (2019), pp. 132–145. ISSN: 2211-4599. DOI: 10.14444/6018. URL: https://dx.doi.org/10.14444/6018.

[58] J.-T Hausmann. “Sawbones in Biomechanical Settings - a Review”. In: *Osteosynthesis and Trauma Care* 14 (Nov. 2006), pp. 259–264. DOI: 10.1055/s-2006-942333.

[59] Varun Puvanesarajah. “Techniques and accuracy of thoracolumbar pedicle screw placement”. In: *World Journal of Orthopedics* 5.2 (2014), p. 112. ISSN: 2218-5836. DOI: 10.5312/wjo.v5.i2.112. URL: https://dx.doi.org/10.5312/wjo.v5.i2.112.

[60] Roop Singh et al. “Morphometric Measurements of Cadaveric Thoracic Spine in Indian Population and Its Clinical Applications”. In: *Asian Spine Journal* 5.1 (2011), p. 20. ISSN: 1976-1902. DOI: 10.4184/asj.2011.5.1.20. URL: https://dx.doi.org/10.4184/asj.2011.5.1.20.

[61] S. Richardson. “On the no-slip boundary condition”. In: *Journal of Fluid Mechanics* 59.4 (1973), pp. 707–719. ISSN: 0022-1120. DOI: 10.1017/s0022112073001801.

[62] *PA 12 - Tecamid 12 natural*. URL: https://www.ensingerplastics.com/en/shapes/products/pa12-tecamid-12-natural.

[63] *Mechanical testing of metals - Ductility testing - Compression test for porous and cellular metals*. NEN-ISO 13314:2012. International Organization for Standardization, Jan. 2012.

[64] X. Banse, T. J. Sims, and A. J. Bailey. “Mechanical Properties of Adult Vertebral Cancellous Bone: Correlation With Collagen Intermolecular Cross-Links”. In: *Journal of Bone and Mineral Research* 17.9 (2002), pp. 1621–1628. ISSN: 0884-0431. DOI: 10.1359/jbmr.2002.17.9.1621.

[65] Wikipedia contributors. *No-slip condition — Wikipedia, The Free Encyclopedia*. [Online; accessed 15-September-2021]. 2021. URL: https://en.wikipedia.org/w/index.php?title=No-slip_condition&oldid=1016415614.